Problemy Matematyczne
13 (1992), 53–131

Atlas of extinction curves derived from ultraviolet $TD-1$ spectra of bright stars

Jacek Papaj[1], Walter Wegner[2], Jacek Krełowski[1]

The paper presents a collection of 178 extinction curves derived from the published set of low-resolution spectra acquired with the aid of the spectrometer aboard the $TD-1$ satellite. The bright stars, included in the sample of $TD-1$ material are very likely to be, in many cases, obscured by single interstellar clouds, especially when characterized by low reddening. The latter case requires a very careful selection of unreddened standards for the extinction law determination. The special technique has been applied to get rid of the possible effects of spectral mismatch, making possible the derivation of extinction curves even in cases of very small E_{B-V}'s. The survey of such extinction curves contains thus many "peculiar" cases—strongly differing from a "mean interstellar extinction curve". The observed differences are certainly related to different parameters of interstellar grains contained in these clouds. The curves are presented in the form of plots, normalized to $E_{B-V}=1$.

1. Introduction

Interstellar dust particles are unquestioned source of the continuous extinction of starlight. Their physical andór geometrical properties are evidently responsible for the wavelength dependence of the interstellar extinction. The observed extinction law (extinction curve) is thus the

main source of information concerning the properties of small dust particles such as their chemical composition, crystalline structure, shapes, sizes etc. Unfortunately this curve is typically rather featureless (Savage and Mathis, 1979) and thus the identification of many, possibly different grain parameters is difficult. It is thus of basic importance to try to investigate possible differences between extinction curves originated in different clouds. Only the parameters of single clouds may be considered as physically meaningful. It is now rather well proved that their absorption spectra differ very substantially (see e.g. Krelowski, 1989 for review).

It is to be emphasized, however, that a great majority of observationally determined extinction curves (see Aiello et al. 1988, Fitzpatrick and Massa 1990) concerns relatively distant, heavily reddened objects. Such objects are very likely to be obscured by several interstellar clouds situated along the same line of sight, differing seriously in their physical parameters andór dust content (Krelowski and Wegner, 1989). The extinction curves derived from their spectra are ill-defined averages over all observed clouds and thus useless as a source of information concerning physical parameters of dust particles contained in any of them. The same concerns several "mean extinction curves" (averaged usually over the available samples)—they are not to be used to determine structural details of interstellar grains.

It is thus of basic importance to derive extinction curves from the spectra of slightly reddened stars—they are most likely to be obscured by only single clouds and thus most useful for any physical considerations. This is why we decided to deal with the pretty old, published many years ago, set of low-resolution $TD-1$ spectra (Jamar et al. 1977, Macau-Hercot et al. 1978). These spectra are available in the form of magnetic tape from the Center of Stellar Data in Strasburg. This Atlas is restricted to very bright objects only, because of the low limiting magnitude (~ 6) of the instrument. It includes many bright stars of very low reddenings—almost certainly caused by single interstellar clouds. We must say, however, that low reddening does not prove that a star is obscured by just a single cloud but generally the probability of this situation grows rapidly when reddening lowers.

The extra-atmospheric ultraviolet is the most interesting spectral range as it contains the famous maximum of the curve—the 2200 Å

bump, the only strong feature in the extinction curve. It is important to determine and present the resultant curves in a uniform way allowing direct comparisons. It is also very important to check possible effects of spectral mismatch when the curves are determined using the pair method. This project applies the special procedure of selecting proper standards for any *Sp* (Papaj, Wegner and Krełowski, 1990 — hereafter Paper 1). The standards derived from the $TD-1$ samples of several *Sp* classes allowed to determine extinction curves in cases of 178 bright *O*9–*B*5 dwarf and giant stars. It is the most extensive and homogeneous atlas of extinction curves ever published. We are not going to discuss our results here, but only to show a reliably derived set of extinction curves—many of them certainly originated in single interstellar clouds.

Let us mention also that, despite the low resolution, the $TD-1$ material is sometimes superior to that of IUE. The noisy spectra of the latter instrument allowed Aiello et al. (1988) to determine their extinction curves only in cases of relatively high reddenings. Many low reddening objects or those which are known to be obscured by single clouds (σ *Sco*, ζ *Oph*) are too bright to be observed in low resolution by IUE and thus their extinction curves are not to be determined from the IUE material. On the other hand a great majority of very bright (=nearby) stars are included into the $TD-1$ sample. Thus "peculiarities" (deviations from published mean extinction curves) are much more likely to be observed in $TD-1$ than in IUE spectra.

2. Selection of objects and determination of standards

The sample of stars considered in the present study contains all *O*9–*B*5 stars of luminosity classes *V*–*III* included in the $TD-1$ material. Earlier types have been excluded as their spectral types and luminosity classes are usually rather uncertain. Supergiants are very scarce among so bright stars and thus it is typically very difficult to determine their standard intensity distributions; the same concerns later type stars— only a few of them are reddened which excludes the method of standard determination proposed in Paper 1.

The first step of our procedure consists of the determination of intrinsic flux distributions in the above mentioned spectral types. The method of using two-color diagrams is described in Paper 1. That paper presents the results in the form of "artificial standards" derived as means from the whole samples of given *Sp* classes. Our spectra have

been normalized to the 2740 Å band and the "artificial standards" are given in the same normalization. The "artificial standards" are very useful, being more certain than real, unreddened stars as in the latter case both stars may be classified erroneously. When using an "artificial standard" only the star under consideration may suffer an incorrect Sp determination.

Let us add the fact of basic importance: our procedure of extinction curve determination (using pair method with "artificial standards") described in Paper 1, allows a check of the match between the spectral and luminosity class of the star and the chosen standard after the curve is derived. Let us consider the typical extinction curve presented in Fig. 1. The high quality spectrum of HD 144217 was divided by "artificial standards" of $B0V$ and $B1V$ spectral types. The strong spectral feature of CIV (between $1/\lambda = 6.0$ and $1/\lambda = 7.0$) is apparently observed either in absorption or in emission in the two curves. The mean curve does not contain any remnant of this feature and, in fact, the star β^1 Sco, is classified as $B0.5V$. Let us mention also that, when the spectral type of the standard is later, a small depression between the normalization point (2740 Å) and the next one (2540 Å) may be created. This feature, when present, may be considered as the result of mismatch because it is evidently hard to find any physical reason for the "blueing" of the star under consideration right after the point of normalization. In several cases, determining our extinction curves, we proposed slightly different spectral types of the considered stars to get rid of the above mentioned characteristic features that may be created by the mismatch (see Tables 1 and 2). The special difficulty concerning the $TD-1$ spectra is the fact the data have been acquired in 3 segments and thus points around 1740 Å (5.75 μm^{-1}) and 2140 Å (4.67 μm^{-1}) may be considered as uncertain. Sometimes whole segments are calibrated in quite different ways, producing misfits as shown in Paper 1. Thus a shift of a whole segment of extinction curve (also marked in Fig. 1) may be simply caused by an instrumental effect or just by some error in data acquiring procedure. This is also why we have not used real stars as standards — an error of this kind could be then repeated in all curves derived using such erroneous standard.

Another reason for using our artificial standards is the fact that

$E_{B-V} = 0$ does not guarantee that a stellar spectrum is really free of any obscuration. Very small dust particles do not contribute to the visual extinction (not affecting the color excess) but they can produce some far-UV (shortward of 2200 Å) extinction. Choosing a standard we should be quite sure that it is not reddened neither in visual nor in the far-UV spectral ranges. Our "artificial standards" seem to obey this requirement being thus superior to the real stars of $E_{B-V} = 0$. Moreover their varying spectral gradients behave as should be expected in the case of varying temperatures. Using these standards we may be quite safe that we don't introduce any unexpected effects of non-stellar origin. Not all spectra, recorded aboard the $TD - 1$ satellite are, unfortunately, of good signal-to-noise ratio. The noisy spectra, especially in cases of low E_{B-V} values, are completely useless as sources of reliable extinction curves. We had to eliminate thus many slightly reddened objects from our sample. The noise in spectra is not so much a nuisance in cases of higher reddenings but these cases are less interesting as possible candidates for being obscured by single clouds.

It is to be emphasized we may conclude reliably that a star is obscured by a single cloud only when high resolution profiles of some interstellar atomic or molecular lines do not show any Doppler splitting but these data are usually hardly available. It may be rather interesting now to check whether the most "peculiar" objects of our sample are really single cloud cases.

3. Results

The stars included into our program are listed in Table 1 and Table 2. They give the HD number, spectrum and luminosity classes: these given in the "Bright Star Catalogue" (Hoffleit and Jaschek 1982) — MK and those, following the best match in our resultant extinction curves (Sp), the observed colour index and the E_{B-V} following our best match (Paper 1 includes also our recommended intrinsic colours). The stars in both Tables are ordered as their HD numbers grow. The reason to divide the data into two sets was following: several stars show the extinctions varying in exceptionally wide range; they are included into Table 2 and also in another Figure to make the plots of the majority of curves much more clear. The colour excesses range from few hundredths to few tenths of magnitude; in majority of cases our sample stars are much less reddened than those of Aiello et al. (1988) or Fitzpatrick and

Massa (1990).

The resultant extinction curves are shown as plots presenting extinction curves in the form of the ratios of colour excesses $E(\lambda - 2740)_{B-V}$ plotted vs. $1/\lambda$ (in μm^{-1}). The vertical bars represent the photometric errors calculated from the following formulae:

$$\sigma_\lambda = \frac{1}{(B-V)_\star - (B-V)_0} \times \sqrt{S_{AS}^2 + \frac{2.5^2 S_\lambda^2}{(\ln 10)^2 F_\lambda} + \frac{2.5^2 S_{2740}^2}{(\ln 10)^2 F_{2740}^2}}$$

where

$$S_\lambda = \frac{F_\lambda S_\lambda^{\%}}{100\sqrt{n}}$$

$$S_{2740} = \frac{F_{2740} S_{2740}^{\%}}{100\sqrt{n}}$$

$(B-V)_\star$ — photoelectric $B-V$ colour,

$(B-V)_0$ — intrinsic $B-V$ color from Paper 1,

F_λ — flux in erg cm^{-2} s^{-1} $Å^{-1}$ at wavelength λ,

$S_\lambda^{\%}$ - root-mean-square deviation of the observations used to compute the mean flux at wavelength λ given in per cent,

F_{2740} — flux in erg cm^{-2} s^{-1} $Å^{-1}$ at wavelength 2740 Å,

$S_{2740}^{\%}$ — root-mean-square deviation of the observations used to compute the mean flux at wavelength 2740 Å given in per cent,

n — the number of averaged observations,

S_{AS} — "artificial" standard error from Paper 1.

We have not produced the extinction curves adding data from different spectral ranges (optical or IR) in order to show a very homogeneous set of results. Let's emphasize that the standards have been derived from the same samples of spectra as the resultant curves. We have not used data from another instrument to play the role of standards (as done by Aiello et al. 1988) which makes our low reddening extinction curves more reliable.

The plots show a great variety of the shapes of extinction curves. In spite of curves identical with the "mean" of Savage and Mathis (1979)

(*HD* 170740) we observe steep far-*UV* rise (e.g. *HD* 48434) as well as the lack of any rise (e.g. *HD* 147165). Some of the curves contain very strong extinction bump (e.g. *HD* 180968 or 23180) — some of them do not contain it at all (e.g. *HD* 202904 or 200120). In certain cases a kind of "bump" seems to be present shortward of 2000 Å (*HD* 41335). Let's emphasize that the latter case must not be a result of mismatch. An improper standard may change the gradient of the curve (especially far-*UV*—see Fig. 1) but not the position of a spectral feature. If the observed feature is the displaced bump—our result contradicts the Massa and Savage (1989) statement that the bump wavelength varies in the range ±17 Å around the typical location: 2175 Å. The "mean extinction curve" given already by Savage and Mathis (1979) is plotted as the broken line in all our plots—for comparison. We may see that just a few of real extinction curves resemble this "mean".

Our results seem to be quite different from those of Aiello et al. (1988) and Fitzpatrick and Massa (1990)—their extinction curves do not deviate so much from the "mean galactic". However, the comparison of our Table 1 and the Table VII of Aiello et al. shows 6 stars common in the two samples. They are *HD*'s: 37367, 48434, 53974, 147933, 154445 and 209339. We present also 5 targets common with the sample of Fitzpatrick and Massa (1990), *HD*'s: 37367, 147933, 149757, 154445 and 193322. The extinction curves from all three sources are evidently very similar when compared to the "mean" extinction curve which proves the results are not method-dependent.

Let's emphasize once again that these stars are their "slightly reddened" objects whereas in our sample they are situated in the range of "high reddenings". The three sets are thus practically complementary. Let's mention once again that strong effects suffer usually much less the noise contained in the spectra which makes the results much less sensitive to any of the possible errors. It is rather clear that high reddenings are usually "composite cases"—the extinction is originated in several clouds and thus the extinction curves deviate much less from what is determined as "average galactic extinction curve". The idea of the latter is, in fact, incorrect, as in practically every case the published extinction curves are averaged not in the Galaxy but in the sample of rather randomly chosen stars. Such a sample may be not representative for the Galaxy as a whole. An "average galactic interstellar extinction

curve" should be derived from spectra of distant objects only—distant enough to be obscured by representative samples of all possible kinds of interstellar clouds.

It is to be emphasized that spectra of many slightly reddened stars have not been observed using the $TD-1$ satellite or are recorded with low S ratio. Thus quite a lot of single cloud extinction curves remains unknown. Their derivation would be of basic importance for any analysis of the physical properties of interstellar dust particles. The material presented in this Atlas allows at least one important conclusion: different IS clouds are populated by grains of different properties—how far their chemical composition, crystalline structure,sizes and shapes may differ, depends on the assumed models. A model, applied to a "mean interstellar extinction curve" must produce non-physical results as the "mean" involves many, very different contributions.

The main reason to build up such a set of data was to make a kind of sky survey of the interstellar extinction. As already shown (Krelowski, 1989) the shape of single-cloud extinction curve changes together with ratios of certain diffuse interstellar bands, column densities of interstellar molecules and, may be, also with polarization properties and depletion patterns in the intervening clouds. It is now most easy to spot the most interesting objects for observing programs, analyzing a survey of extinction curves which are available from the extensive, published material. Thus our results are very useful for planning future observations of diffuse bands andór molecular lines as well as atomic resonance lines and polarization properties of IS clouds.

The computer-readable version of this Atlas is available from Stellar Data Center in Strasburg.

Acknowledgements. This project has been supported partially by the Nicolaus Copernicus University of Sciences under the grant 264A.

References

[1] Aiello S., Barsella B., Chlewicki G., Greenberg J.M., Patriarchi P., Perinotto M., *Astron. Astrophys. Suppl. Ser.* 73, 1988, 195

[2] Blanco V.M., Demers S., Douglass G.G., FitzGerald M.P., *Pub-*

lications U.S. Naval Observatory, Second Series, Vol. 21, 1970

[3] Fitzpatrick E.L., Massa D., *Astrophys. J. Suppl. Ser.* 72, 1990, 163

[4] Hoffleit D., Jaschek C., *The Bright Star Catalogue*, 1982 — distributed by the CDS Strasbourg

[5] Jamar C., Macau-Hercot D., Monfils A., Thompson G.I., Houziaux L., Wilson R., *Ultraviolet Bright — Star Spectrophotometric Catalogue*, ESA SR-27, 1976

[6] Jaschek C., Hernandez E., Sierra A., Gerhardt A., *Catalogue of Stars Observed Photoelectrically, Astronomical Observatory La Plata, Serie Astronomica*, Tome XXXVIII, 1972 Kennedy P.M., Buscombe W., *MK Spectral Classifications Evanston 1974*

[7] Krelowski J., in *Interstellar Dust*, L.J. Allamandola and A.G.G.M. Tielens (eds), Kluwer Academic Publishers, Dordrecht, IAU 135, 1989, p.67

[8] Krełowski J., Wegner W., *Astron. Nachr.* 310, 1990, 281

[9] Macau-Hercot D., Jamar C., Monfils A., Thompson G.I., Houziaux L., Wilson R., *Supplement to the Ultraviolet Bright Star Spectrophotometric Catalogue*, ESA SR-28, 1978

[10] Massa D., Savage B.D., in *Interstellar Dust*, L.J. Allamandola and A.G.G.M. Tielens (eds), Kluwer Academic Publishers, Dordrecht, IAU 135, 1989, p. 3

[11] Mermilliod J.C., *Catalogue of UBV photoelectric photometry*, 1974

[12] Papaj J., Wegner W., Krełowski J., *Mon. Not. R. Astron. Soc.* (264, 408), 1990 — Paper 1.

[13] Savage B.D., Mathis J.S., *Ann. Rev. Astron. Astrophys.*, **17**, 1979, 73.

[1]INSTYTUT ASTROMONII
Uniwersytet M. Kopernika
Chopina 12
87-100 Toruń, Poland

[2]INSTYTUT MATEMATYKI
Wyższa Szkoła Pedagogiczna
Chodkiewicza 30
85-064 Bydgoszcz, Poland

Figure captions

Fig. 1.

a) The extinction curves derived from the $TD-1$ spectrum of HD 144217 (β^1 Sco) with the aid of $B0V$ artificial standard (dotted line) and $B1V$ artificial standard (solid line). Note the presence of the remnants of the strong CIV spectral feature in the form of emission or absorption "spectral lines" absent in the mean curve (open circles). The borders of spectral segments (see text) are marked with arrows.

b) The extinction curve of β^1 Sco calculated with the aid of $B3V$ standard. Open circles—the same as in a). Note the "blueing" between 2740 Å and 2540 Å, the change of 2200 bump depth and the growing intensity of remnant CIV feature—the results of spectral mismatch. The bump position remains unchanged.

c) The mean ($B0.5V$) extinction curve of β^1 Sco (crosses—their vertical sizes represent errors) plotted together with the "mean galactic" (broken line) in the same frame as all resultant curves shown in Figs. 2 and 3. The label "extinction" stands for the color excesses ratio: $E_{\lambda-2740B-V}$, $1/\lambda$ denotes the reciprocal wavelength in micrometers.

Fig. 2. The resultant extinction curves ordered with growing HD numbers of the considered stars. All frames as in Fig. 1c), stellar data in Table 1.

Fig. 3 The resultant extinction curves covering much wider range than those in Fig. 2, stellar data in Table 2.

Table 1. Primary data for the target stars.

HD number	*Sp/L*	*MK*	$B-V$	$E(B-V)$	Ref.
593	*B*1 *V*	*B*1 *V*	0.03	0.260	2
2083	*B*1 *V*	*B*1 *V*	0.03	0.260	2
3901	*B*2 *V*	*B*2 *V*	−0.11	0.100	1
10516	*B*1 *V*	*B*2 *Vep*	−0.04	0.170	1
21428	*B*4 *V*	*B*3 *V*	−0.09	0.090	1
21856	*B*2 *V*	*B*1 *V*	−0.06	0.170	1
22192	*B*5 *V*	*B*5 *Ve*	−0.06	0.090	1
22951	*B*0.5 *V*	*B*0.5 *V*	−0.01	0.230	1
23180	*B*1 *III*	*B*1 *III*	0.05	0.260	1
23478	*B*3 *V*	*B*3 *IV*	0.09	0.270	2
23625	*B*2.5 *V*	*B*2.5 *V*	0.08	0.275	1
24131	*B*1 *V*	*B*1 *V*	0.00	0.230	1
24263	*B*5 *V*	*B*5 *V*	0.06	0.210	1
24534	*O*9.5 *V*	*O*9.5 *Vep*	0.29	0.560	1
24640	*B*1.5 *V*	*B*1.5 *V*	−0.03	0.190	1
25204	*B*2 *V*	*B*3 *V* + *A*4 *IV*	−0.12	0.060	1
25539	*B*2.5 *V*	*B*3 *V*	0.06	0.240	2
25940	*B*3 *V*	*B*3 *Ve*	−0.03	0.150	1
26912	*B*2.5 *V*	*B*3 *IV*	−0.06	0.120	1
27192	*B*2 *V*	*B*1.5 *IV*	−0.01	0.210	1
27396	*B*4 *V*	*B*4 *IV*	−0.03	0.130	1
28446	*B*1 *III*	*B*0 *III*	0.18	0.410	1
30076	*B*2 *V*	*B*2 *Ve*	−0.11	0.100	1
30870	*B*5 *V*	*B*5 *V*	0.08	0.230	1
32990	*B*2 *V*	*B*2 *V*	0.06	0.270	1
32991	*B*2 *V*	*B*2 *Ve*	0.19	0.400	1
34748	*B*1.5 *V*	*B*1.5 *Vn*	−0.11	0.110	1
34989	*B*0.5 *V*	*B*1 *V*	−0.13	0.100	1
35149	*B*1 *V*	*B*1 *V*	−0.15	0.080	1
35411	*B*0.5 *V*	*B*1 *V* + *B*2 *Ve*	−0.17	0.060	1
35532	*B*2 *V*	*B*2 *Vn*	−0.08	0.130	1
36576	*B*2 *V*	*B*2 *IV–Ve*	0.01	0.220	1
36819	*B*2.5 *V*	*B*2.5 *IV*	−0.09	0.105	1
37367	*B*2 *V*	*B*2 *IV–V*	0.16	0.370	1

Table 1. — *continued*

HD number	*Sp/L*	*MK*	$B-V$	$E(B-V)$	Ref.
37490	*B2 III*	*B3 IIIe*	−0.11	0.050	1
37711	*B2 V*	*B3 IV*	−0.13	0.050	1
37967	*B2.5 V*	*B2.5 Ve*	−0.06	0.135	1
40111	*B0 III*	*B0.5 II*	−0.06	0.160	1
41335	*B2 V*	*B2 Ven*	−0.06	0.150	1
44458	*B1 V*	*B1 Vpe*	−0.02	0.210	1
45314	*O9.5 V*	*O9 pe*	0.15	0.450	2
45725	*B2 V*	*B3 Ve*	−0.10	0.080	1
45726	*B2 V*	*B3 ne*	−0.07	0.110	1
45995	*B2 V*	*B2 V : nne*	−0.08	0.130	1
46064	*B1.5 V*	*B1.5 V*	−0.15	0.070	1
47417	*B0 V*	*B0 IV*	0.01	0.265	2
48434	*B0.5 III*	*B0 III*	−0.02	0.210	1
48917	*B1.5 III*	*B2 IIIe*	−0.12	0.070	1
50083	*B2 V*	*B2 e*	0.06	0.270	2
51756	*B0.5 V*	*B0.5 IV*	−0.07	0.170	2
52266	*O9.5 V*	*O9.5 V*	−0.01	0.260	2
52721	*B1 V*	*B2 e*	0.06	0.270	2
53755	*B0.5 V*	*B0.5 V + F5 III*	−0.05	0.190	1
53974	*B0 V*	*B0.5 IV*	0.05	0.290	1
54764	*B1 III*	*B1 II*	0.06	0.270	1
57150	*B2 V*	*B2 V + B3 IVne*	−0.10	0.110	1
58343	*B2 V*	*B2.5 IVe*	−0.05	0.145	1
58978	*B0 V*	*B0 IV : pe*	−0.13	0.125	1
60325	*B1 V*	*B1 V*	−0.04	0.190	1
60606	*B2 V*	*B3 Vne*	−0.06	0.120	1
63462	*B0 V*	*B0 V : pe :*	−0.05	0.200	1
63578	*B1 V*	*B1.5 IV*	−0.14	0.080	1
63949	*B1 V*	*B1.5 IV*	−0.14	0.080	1
65875	*B2 V*	*B2.5 Ve*	−0.07	0.125	1
66546	*B2 V*	*B2 IV–V*	−0.04	0.170	1
68761	*B0.5 III*	*B0.5 III–IV*	−0.07	0.150	3
68980	*B1 III*	*B1.5 IIIe*	−0.11	0.090	1

Table 1. — *continued*

HD number	*Sp/L*	*MK*	$B-V$	$E(B-V)$	Ref.
69144	*B2 V*	*B2.5 IV*	−0.14	0.055	1
70930	*B1 V*	*B1 V*	−0.15	0.080	1
78764	*B1.5 V*	*B2 IVe*	−0.15	0.060	1
83183	*B5 III*	*B5 II*	0.01	0.160	1
88661	*B2 V*	*B2 IVpne*	−0.08	0.130	1
91465	*B2 V*	*B4 Vne*	−0.09	0.070	1
124471	*B1 III*	*B1.5 III*	−0.06	0.140	1
128293	*B1 V*	*B3 Vne*	−0.01	0.170	3
131492	*B2 V*	*B4 Vnpe*	0.00	0.160	1
135160	*B0.5 V*	*B0.5 Ve*	−0.08	0.160	1
138485	*B2 V*	*B2 Vn*	−0.14	0.070	1
141318	*B2 III*	*B2 II*	0.06	0.250	1
141637	*B2 V*	*B3 V*	−0.05	0.130	1
142096	*B2 V*	*B2.5 V*	−0.01	0.185	1
142114	*B2 V*	*B2.5 Vn*	−0.07	0.125	1
142184	*B2.5 V*	*B2.5 Vne*	−0.04	0.155	1
142378	*B5 V*	*B5 V*	−0.01	0.140	1
142883	*B3 V*	*B3 V*	0.02	0.200	1
142990	*B3 V*	*B5 IV*	−0.09	0.060	1
143018	*B0 V*	*B1 V + B2 V*	−0.19	0.040	1
143275	*B0.5 V*	*B0.3 IV*	−0.12	0.120	1
144217	*B0.5 V*	*B1 V*	−0.07	0.160	1
144470	*B1 V*	*B1 V*	−0.04	0.190	1
145502	*B2 V*	*B3 V*	0.04	0.220	1
147165	*B1 III*	*B2 III + O9.5 V*	0.13	0.340	1
147933	*B2 V*	*B2 IV*	0.24	0.450	1
147934	*B2 V*	*B2 V*	0.24	0.450	1
148184	*B2 V*	*B2 IV : pe*	0.28	0.490	1
149711	*B2.5 V*	*B2.5 IV*	−0.02	0.175	1
149757	*O9.5 V*	*O9.5 Vn*	0.02	0.290	1
150745	*B1 V*	*B2 IV–V*	−0.09	0.120	1
154445	*B1 V*	*B1 V*	0.16	0.390	1
155450	*B1 III*	*B1 II*	0.07	0.280	1

Table 1. — *continued*

HD number	*Sp/L*	*MK*	$B-V$	$E(B-V)$	Ref.
155889	*B*0 *V*	*B*0 *V*	−0.02	0.235	3
163472	*B*2 *V*	*B*2 *IV–V*	0.09	0.300	1
163685	*B*3 *V*	*B*3 *IV*	−0.08	0.100	1
164284	*B*2 *V*	*B*2 *Ve*	−0.03	0.180	1
164432	*B*2 *V*	*B*2 *IV*	−0.08	0.130	1
164581	*B*1 *V*	*B*1 *V*	0.12	0.350	4, 5
164852	*B*2.5 *V*	*B*3 *IV*	−0.09	0.090	1
164900	*B*3 *V*	*B*3 *Vn*	−0.10	0.080	1
165174	*B*0 *III*	*B*0 *IIIn*	0.00	0.230	1
165793	*B*1 *III*	*B*1 *II*	−0.03	0.180	1
166182	*B*2 *V*	*B*2 *IV*	−0.16	0.050	1
168797	*B*3 *V*	*B*3 *Ve*	−0.04	0.140	1
170235	*B*2 *V*	*B*2 *IVpe*	0.07	0.280	1
170740	*B*2 *V*	*B*2 *V*	0.24	0.450	1
170978	*B*3 *V*	*B*3 *IV*	0.04	0.220	3
171034	*B*2 *V*	*B*2 *IV–V*	−0.11	0.100	1
173117	*B*5 *V*	*B*5 *V*	0.05	0.200	1
175156	*B*5 *III*	*B*5 *II*	0.17	0.320	1
176819	*B*2 *V*	*B*2 *IV–V*	0.02	0.230	1
176871	*B*3 *V*	*B*5 *V*	−0.08	0.070	1
179406	*B*3 *V*	*B*3 *V*	0.13	0.310	1
180554	*B*4 *V*	*B*4 *IV*	−0.05	0.110	1
180968	*B*0.5 *V*	*B*0.5 *IV*	0.02	0.260	1
181858	*B*2 *V*	*B*3 *IVp*	−0.03	0.150	1
182568	*B*3 *V*	*B*3 *IV*	−0.10	0.080	1
183144	*B*4 *III*	*B*4 *III*	−0.06	0.095	1
184915	*B*0.5 *III*	*B*0.5 *III*	0.00	0.220	1
185423	*B*3 *III*	*B*3 *III*	0.04	0.200	1
185507	*B*2 *V*	*B*3 *V* + *B*3 *V*	0.03	0.210	1
187879	*B*1 *III*	*B*1 *III* + *B*3 *V*	−0.04	0.170	1
188892	*B*5 *V*	*B*5 *IV*	−0.08	0.070	1
191610	*B*2 *V*	*B*2.5 *Ve*	−0.13	0.065	1
193237	*B*2 *III*	*B*2 *pe*	0.42	0.610	3

Table 1. — *continued*

HD number	*Sp/L*	*MK*	$B-V$	$E(B-V)$	Ref.
193322	*O*9.5 *V*	*O*9 *V*	0.10	0.400	1
193536	*B*2 *V*	*B*2 *V*	−0.13	0.080	1
195556	*B*2.5 *V*	*B*2.5 *IV*	−0.09	0.105	1
197511	*B*1 *V*	*B*2 *V*	−0.10	0.110	1
198781	*B*0.5 *V*	*B*0.5 *V*	0.07	0.310	1
200120	*B*1 *V*	*B*1.5 *Venn*	−0.05	0.180	3
202214	*B*0 *V*	*B*0 *V*	0.11	0.365	3
202904	*B*2 *V*	*B*2 *Vne*	−0.11	0.100	1
203374	*B*0 *V*	*B*0 *IVpe*	0.31	0.565	2
203467	*B*3 *V*	*B*3 *IVe*	−0.04	0.140	1
203532	*B*3 *V*	*B*3 *IV*	0.13	0.310	1
205139	*B*2 *III*	*B*1 *II*	0.12	0.330	1
206672	*B*3 *V*	*B*3 *IV*	−0.12	0.060	1
206773	*B*0 *V*	*B*0 *Vpe*	0.21	0.465	2
208682	*B*2.5 *V*	*B*2.5 *Ve*	−0.06	0.135	1
208905	*B*1 *V*	*B*1 *Vp*	0.09	0.320	2
208947	*B*2 *V*	*B*2 *V*	−0.05	0.160	1
209339	*B*0 *V*	*B*0 *IV*	0.06	0.315	1
209481	*O*9.5 *V*	*O*9 *V*	0.06	0.360	1
209744	*B*1 *V*	*B*1 *V*	0.22	0.450	2
209961	*B*1.5 *V*	*B*2 *V*	−0.06	0.150	1
212076	*B*2 *V*	*B*2 *IV–Ve*	−0.13	0.080	1
213420	*B*2 *V*	*B*2 *IV*	−0.09	0.120	1
214168	*B*1 *V*	*B*2 *Ve*	−0.15	0.060	1
215191	*B*1 *V*	*B*1 *V*	−0.09	0.140	1
216916	*B*1 *V*	*B*2 *IV*	−0.14	0.070	1
218376	*B*0.5 *V*	*B*0.5 *IV*	−0.03	0.210	1
218440	*B*1 *V*	*B*2 *V*	−0.01	0.200	1
218537	*B*3 *V*	*B*3 *V*	−0.02	0.160	1
223128	*B*2 *V*	*B*2 *IV*	−0.04	0.170	1
224572	*B*1 *V*	*B*1 *V*	−0.07	0.160	1

References:

(1) **Hoffleit & Jaschek** (1982),

(2) Blanco et al. (1970),

(3) Kennedy & Buscombe (1974),

(4) Jaschek et al. (1972),

(5) Mermilliod (1974).

Table 2. Primary data for the additional target stars.

HD number	*Sp/L*	*MK*	$B-V$	$E(B-V)$	Ref.
19268	*B*5 *V*	*B*5 *V*	−0.01	0.140	1
23466	*B*3 *V*	*B*3 *V*	−0.12	0.060	1
35708	*B*2 *V*	*B*2.5 *IV*	−0.15	0.045	1
51309	*B*2 *III*	*B*3 *II*	−0.07	0.090	1
52559	*B*2 *V*	*B*2 *IV–V*	−0.02	0.190	1
56139	*B*2 *V*	*B*2 *IV–Ve*	−0.17	0.040	1
129557	*B*2 *III*	*B*2 *III*	−0.06	0.130	1
158427	*B*2 *V*	*B*2 *Vne*	−0.17	0.040	1
176162	*B*5 *V*	*B*5 *IV*	−0.04	0.110	1
178175	*B*2 *V*	*B*2 *Ve*	−0.11	0.100	1
183133	*B*4 *V*	*B*5 *V*	−0.02	0.140	2
185936	*B*5 *V*	*B*5 *V*	−0.08	0.070	1
187567	*B*2 *V*	*B*2.5 *IVe*	−0.10	0.095	1
188439	*B*0.5 *III*	*B*0.5 *IIIn*	−0.11	0.110	1

References:

(1) Hoffleit & Jaschek (1982),

(2) Kennedy & Buscombe (1974).

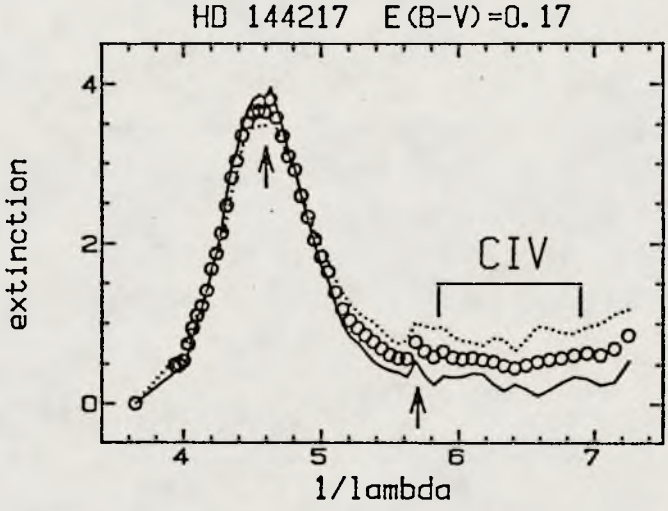
HD 144217 E(B-V)=0.17
extinction
CIV
1/lambda

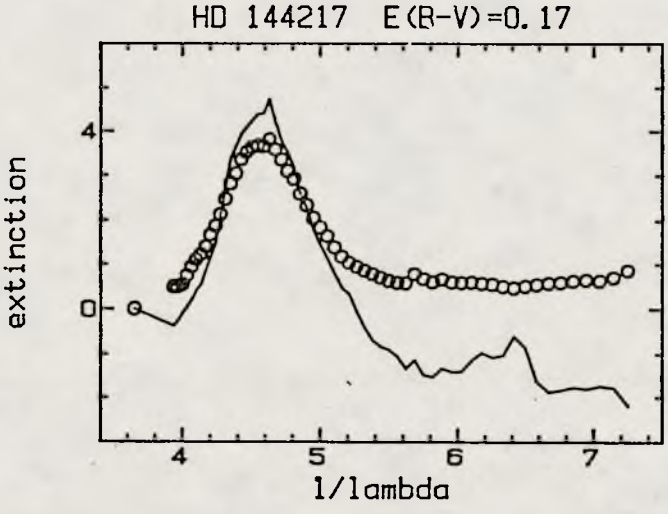
HD 144217 E(B-V)=0.17
extinction
1/lambda

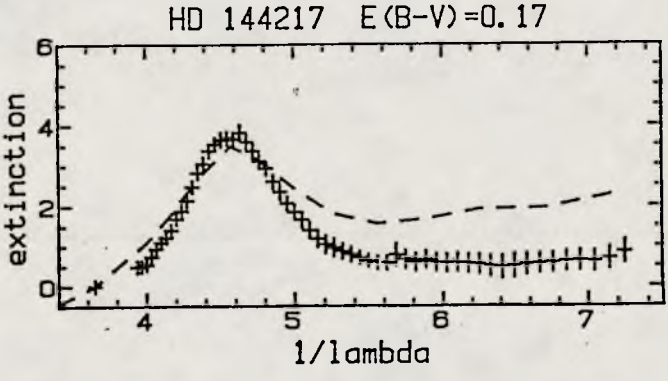
HD 144217 E(B-V)=0.17
extinction
1/lambda

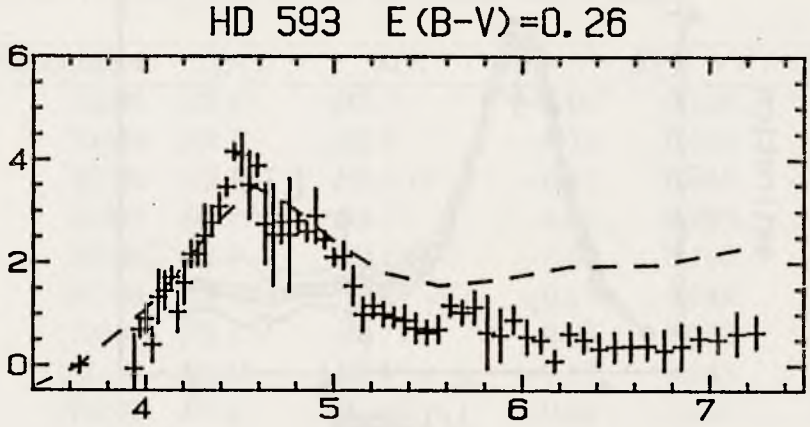
HD 593 E(B-V)=0.26
6
4
2
0
4
5
6
7

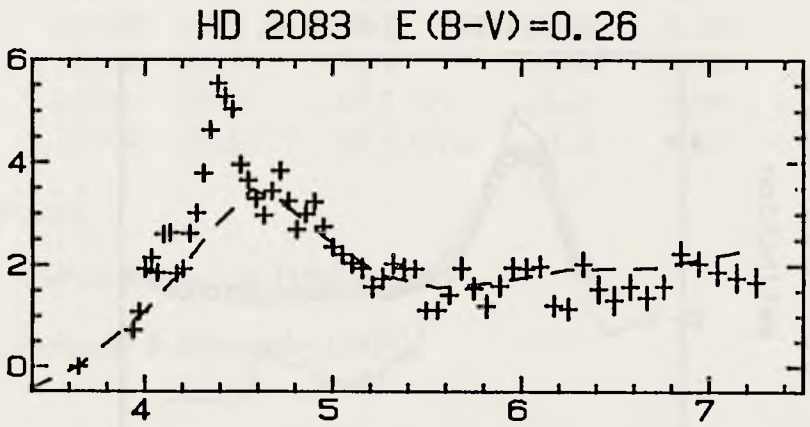
HD 2083 E(B-V)=0.26
6
4
2
0
4
5
6
7

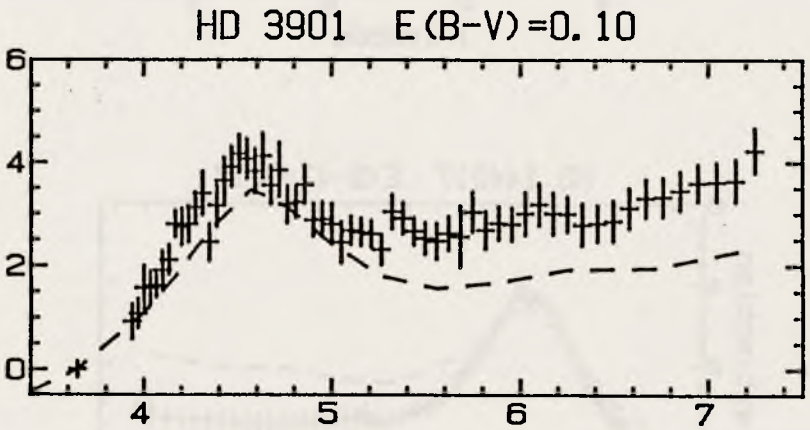
HD 3901 E(B-V)=0.10
6
4
2
0
4
5
6
7

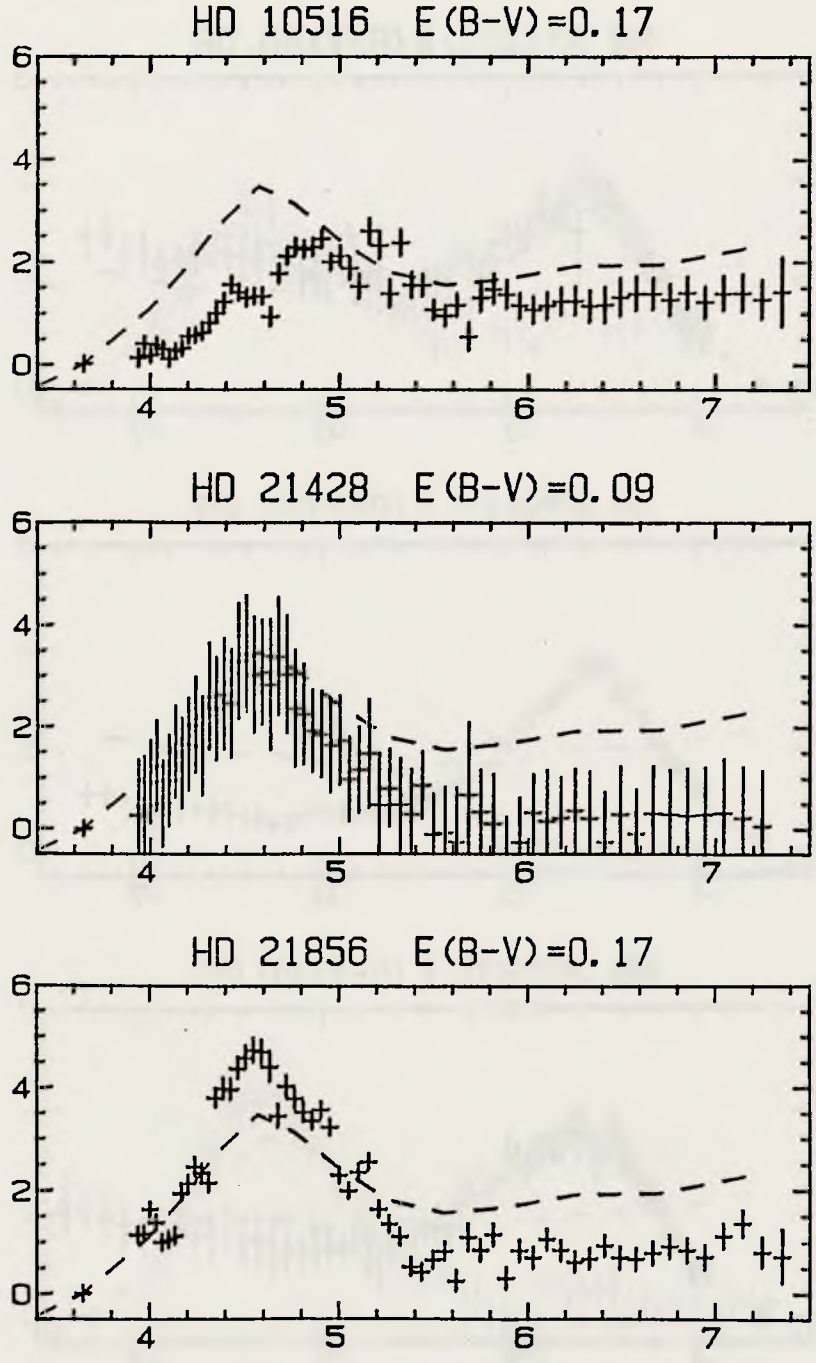
HD 10516 E(B-V)=0.17
HD 21428 E(B-V)=0.09
HD 21856 E(B-V)=0.17
6
4
2
0
4
5
6
7

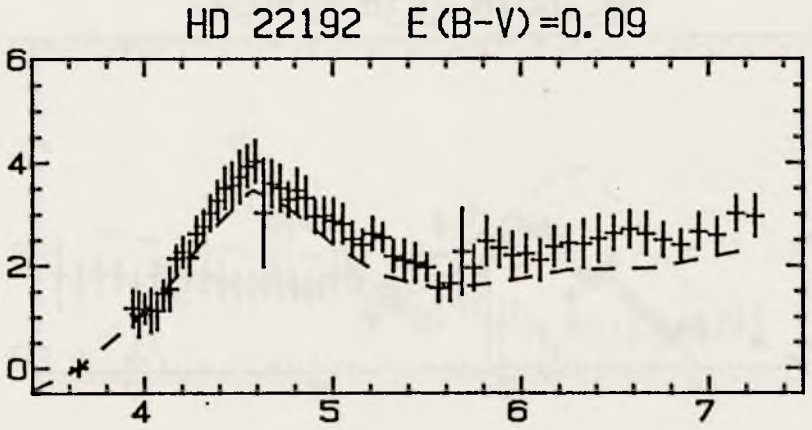
HD 22192 E(B-V)=0.09
6
4
2
0
4
5
6
7

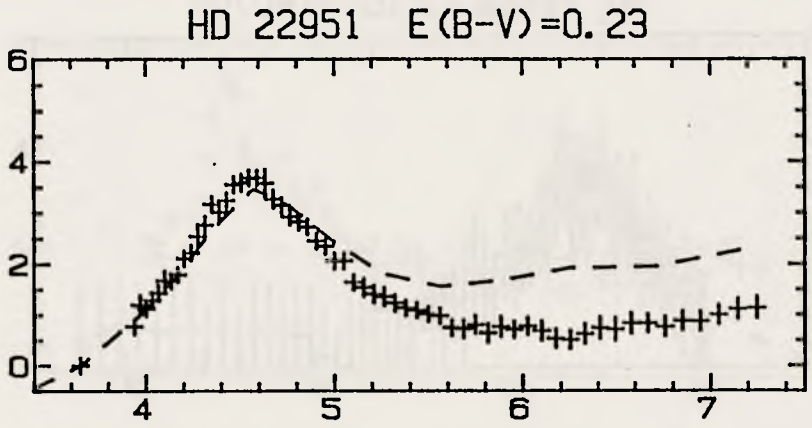
HD 22951 E(B-V)=0.23
6
4
2
0
4
5
6
7

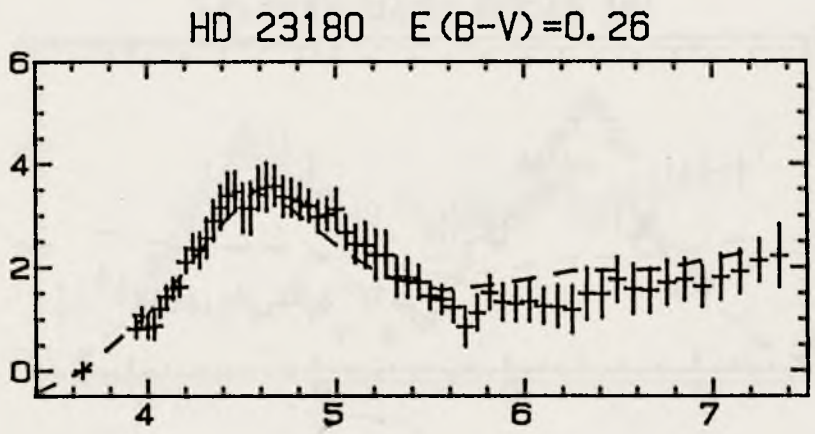
HD 23180 E(B-V)=0.26
6
4
2
0
4
5
6
7

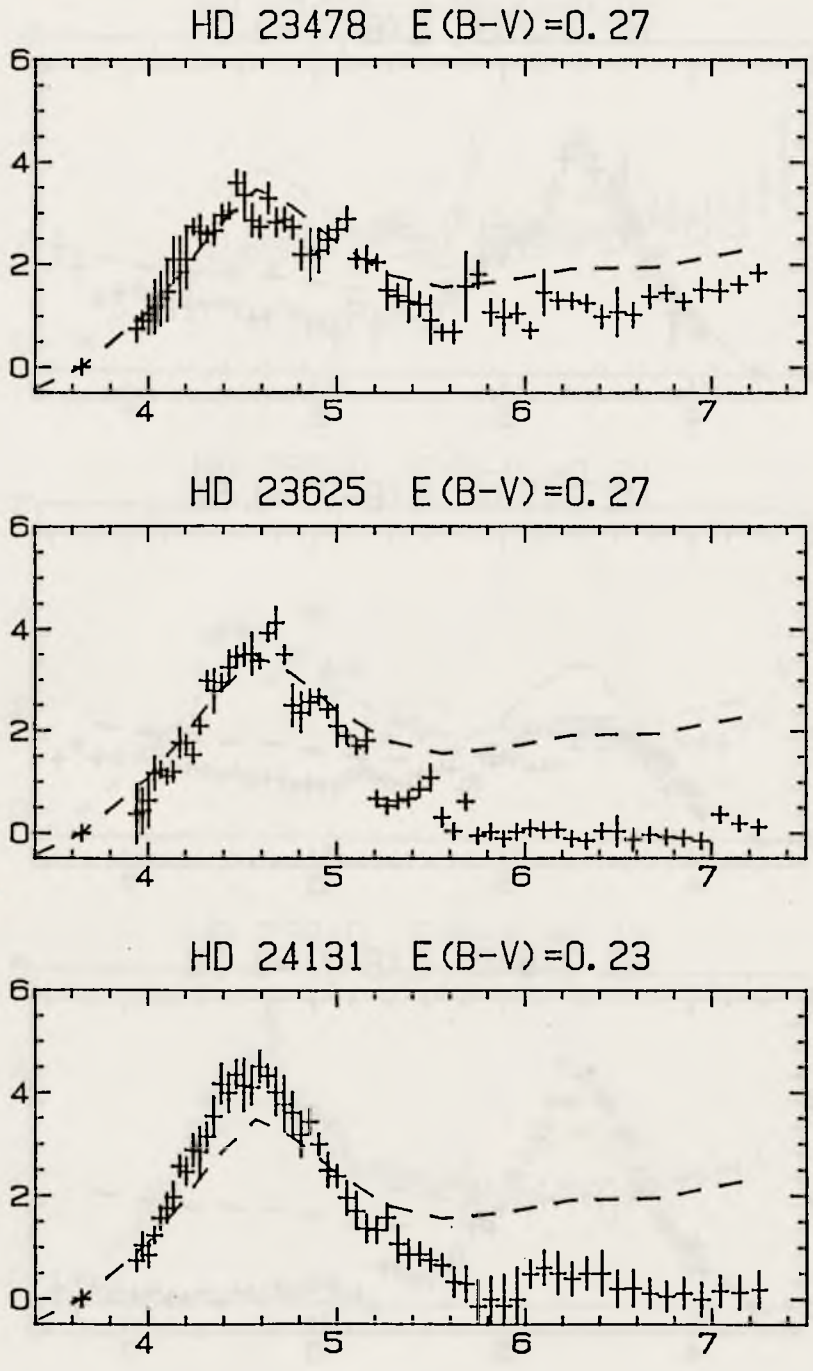
HD 23478 E(B-V)=0.27
HD 23625 E(B-V)=0.27
HD 24131 E(B-V)=0.23
6
4
2
0
4
5
6
7

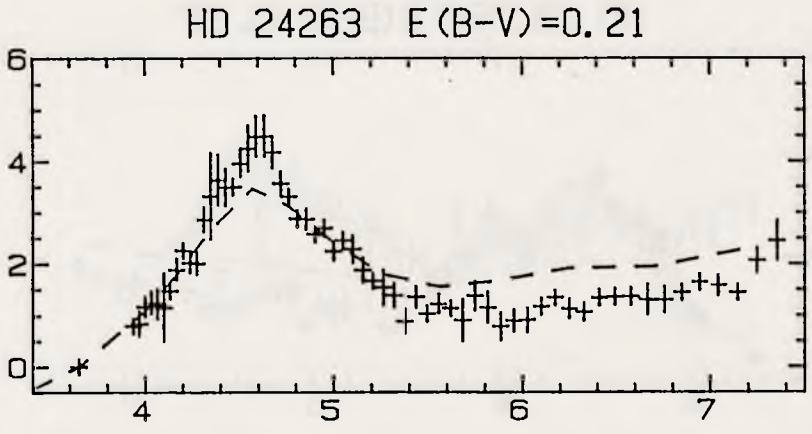
HD 24263 E(B-V)=0.21
6
4
2
0
4
5
6
7

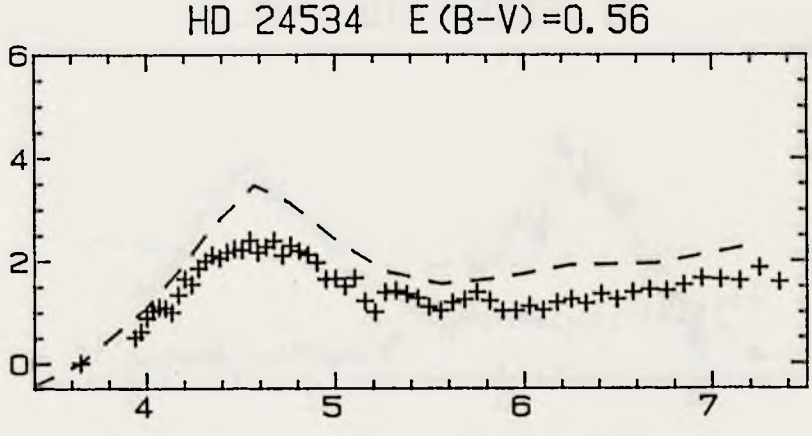
HD 24534 E(B-V)=0.56
6
4
2
0
4
5
6
7

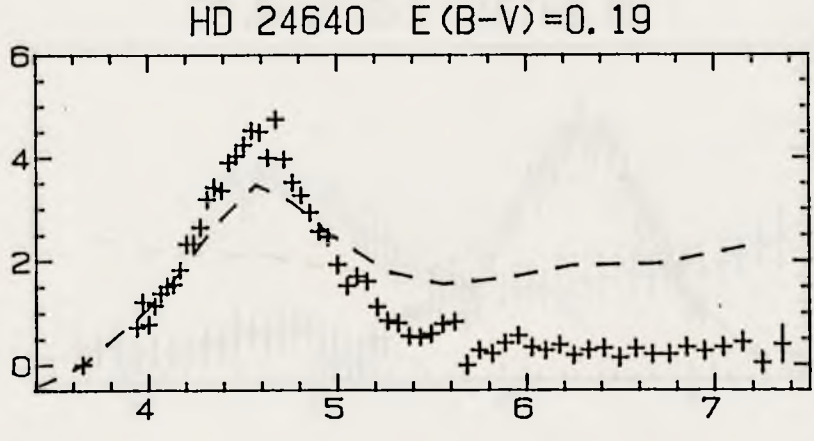
HD 24640 E(B-V)=0.19
6
4
2
0
4
5
6
7

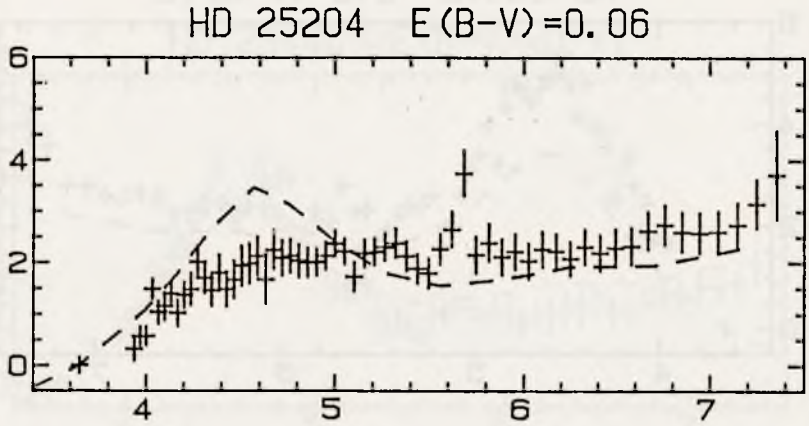
HD 25204 E(B-V)=0.06
6
4
2
0
4
5
6
7

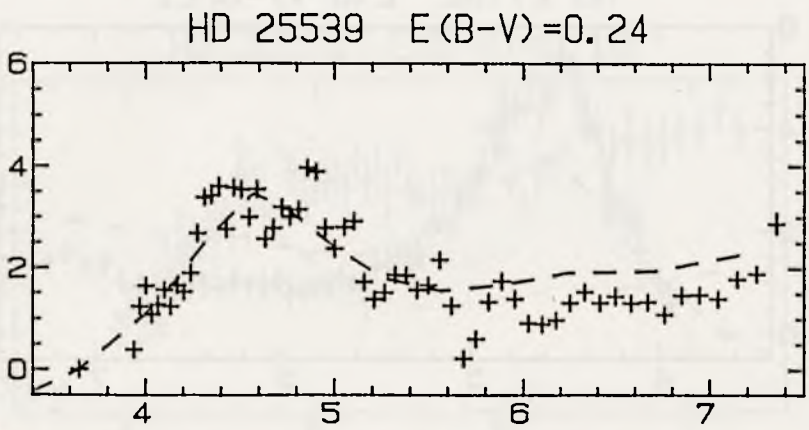
HD 25539 E(B-V)=0.24
6
4
2
0
4
5
6
7

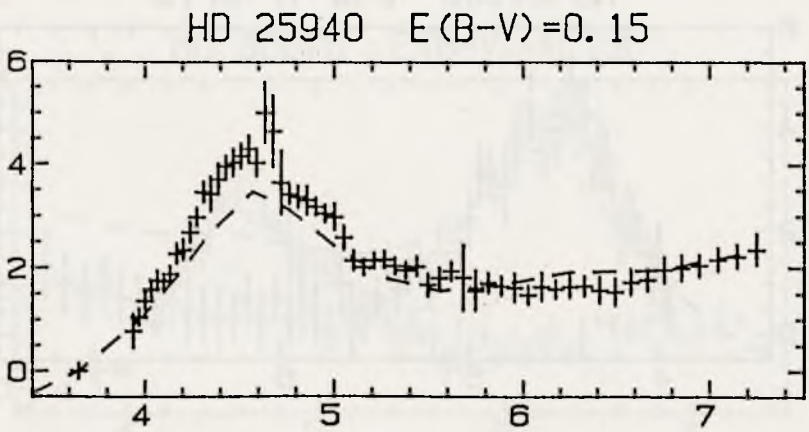
HD 25940 E(B-V)=0.15
6
4
2
0
4
5
6
7

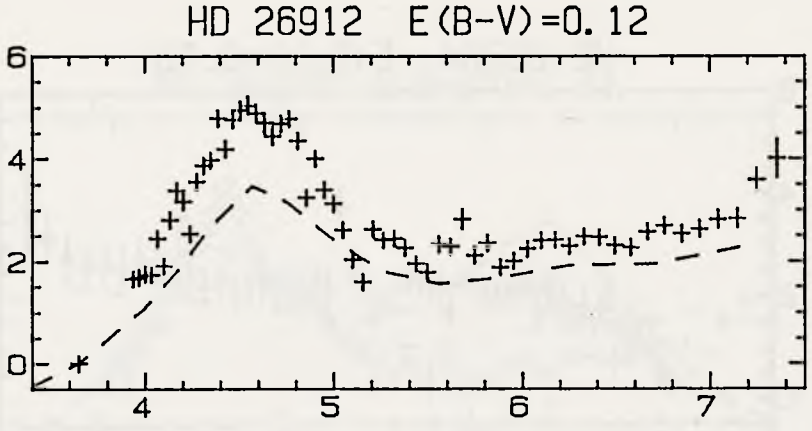
HD 26912 E(B-V)=0.12
6
4
2
0
4
5
6
7

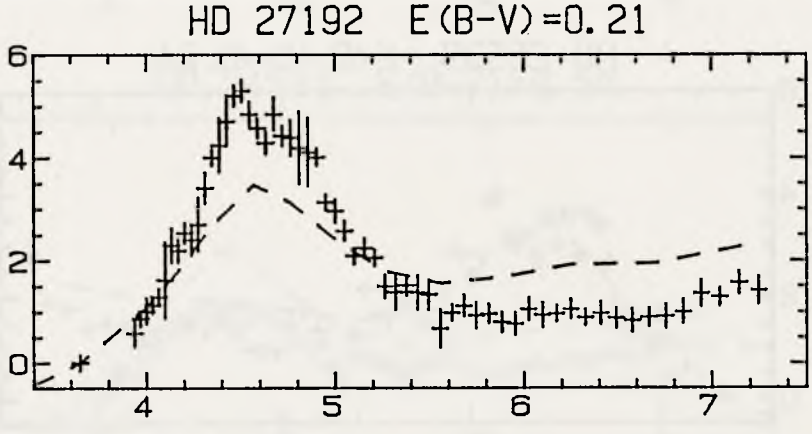
HD 27192 E(B-V)=0.21
6
4
2
0
4
5
6
7

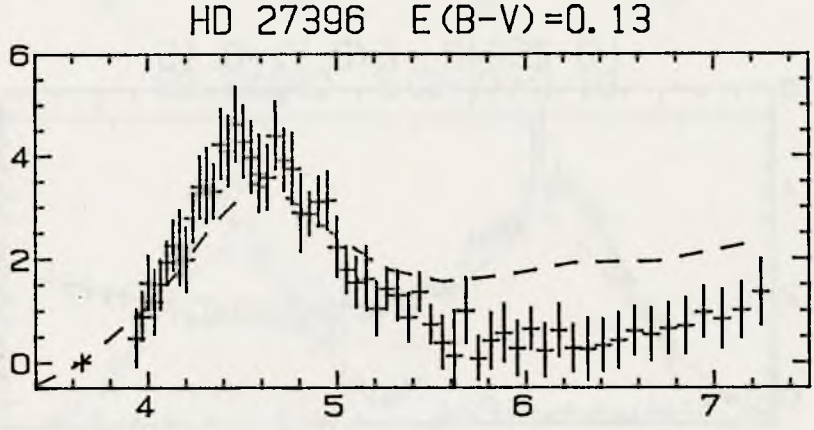
HD 27396 E(B-V)=0.13
6
4
2
0
4
5
6
7

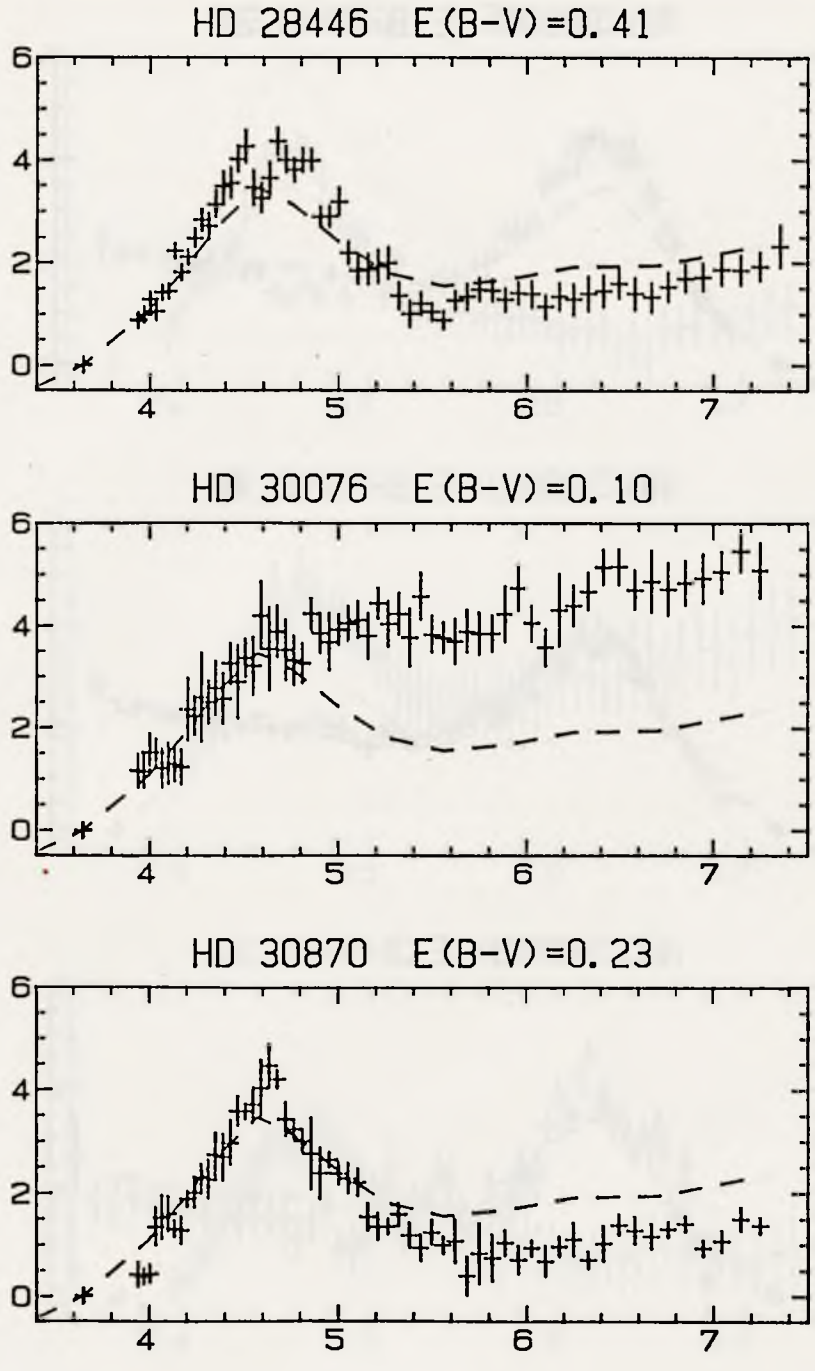
HD 28446 E(B-V)=0.41
HD 30076 E(B-V)=0.10
HD 30870 E(B-V)=0.23
0
2
4
6
4
5
6
7

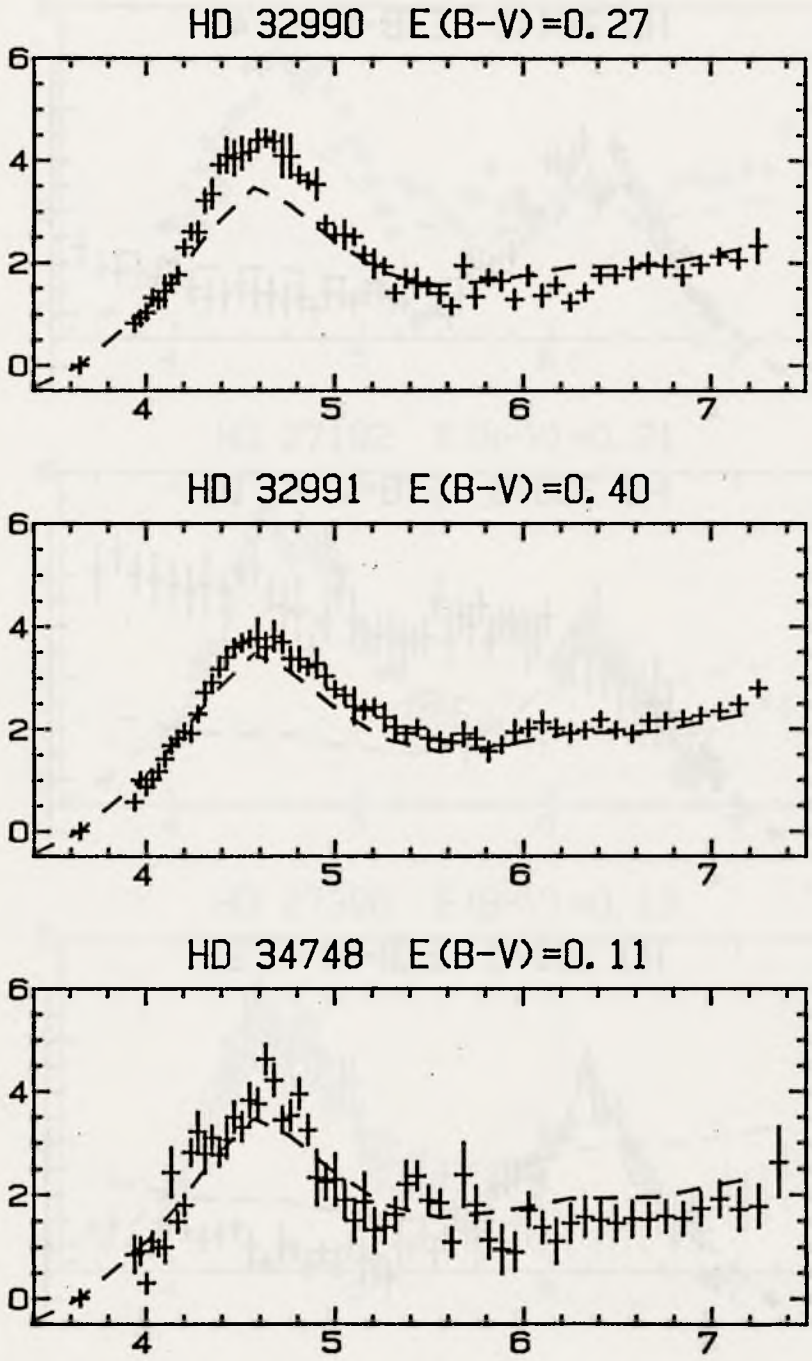
HD 32990 E(B-V)=0.27
HD 32991 E(B-V)=0.40
HD 34748 E(B-V)=0.11
0
2
4
6
4
5
6
7

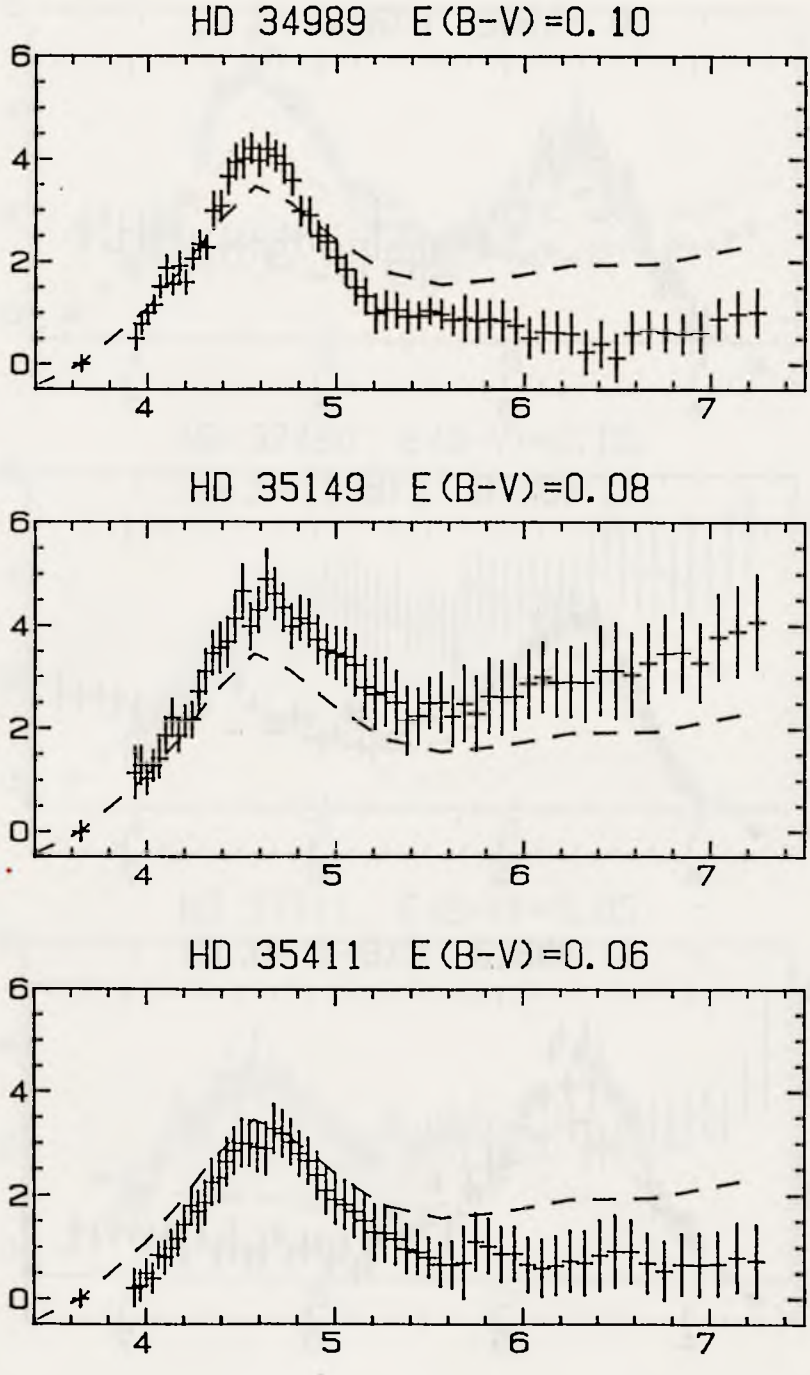
HD 34989 E(B-V)=0.10
HD 35149 E(B-V)=0.08
HD 35411 E(B-V)=0.06
6
4
2
0
4
5
6
7

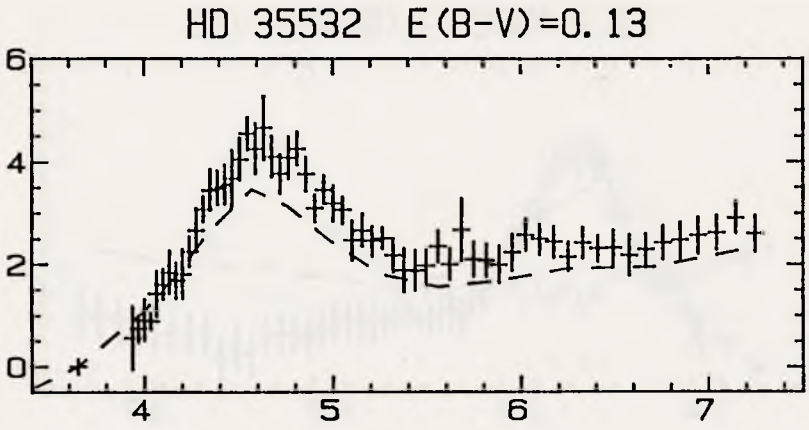
HD 35532 E(B-V)=0.13
6
4
2
0
4
5
6
7

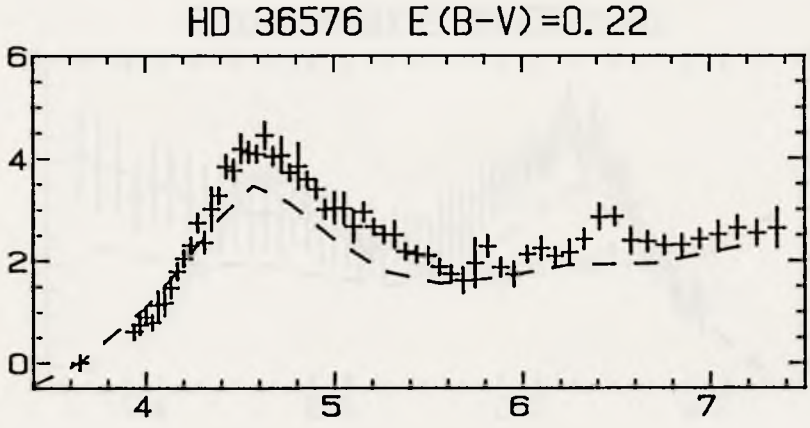
HD 36576 E(B-V)=0.22
6
4
2
0
4
5
6
7

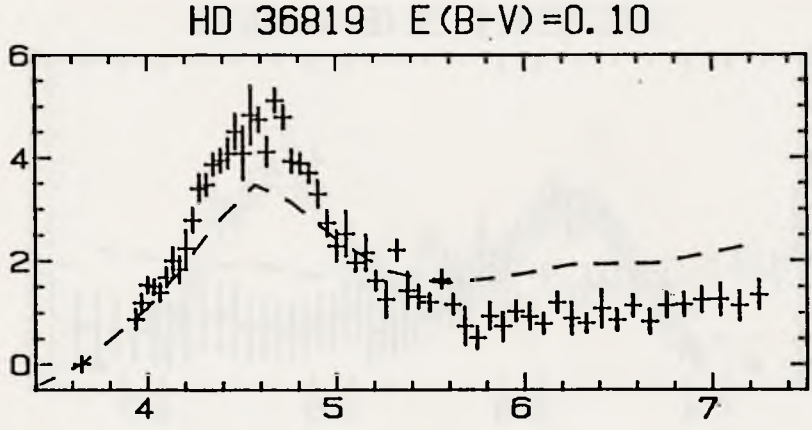
HD 36819 E(B-V)=0.10
6
4
2
0
4
5
6
7

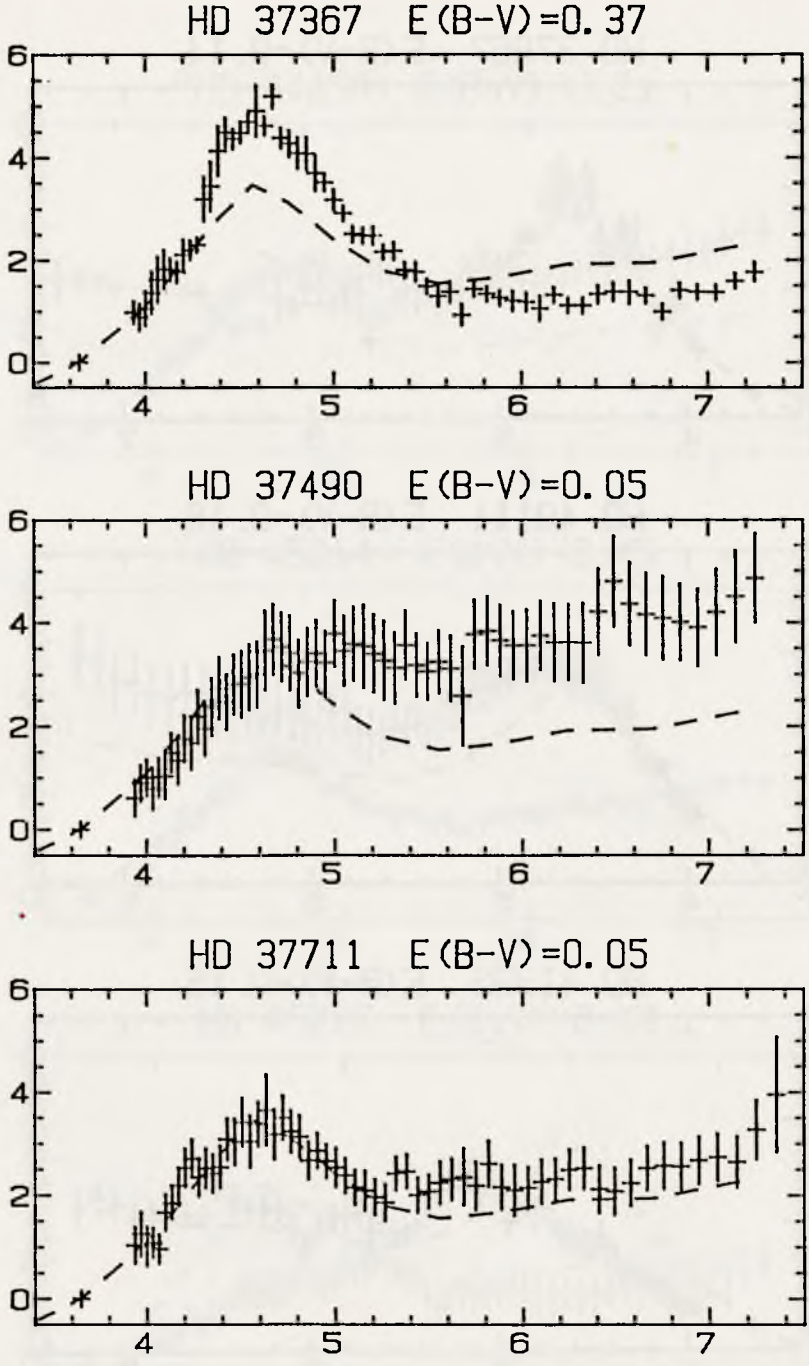
HD 37367 E(B-V)=0.37
HD 37490 E(B-V)=0.05
HD 37711 E(B-V)=0.05
0
2
4
6
4
5
6
7

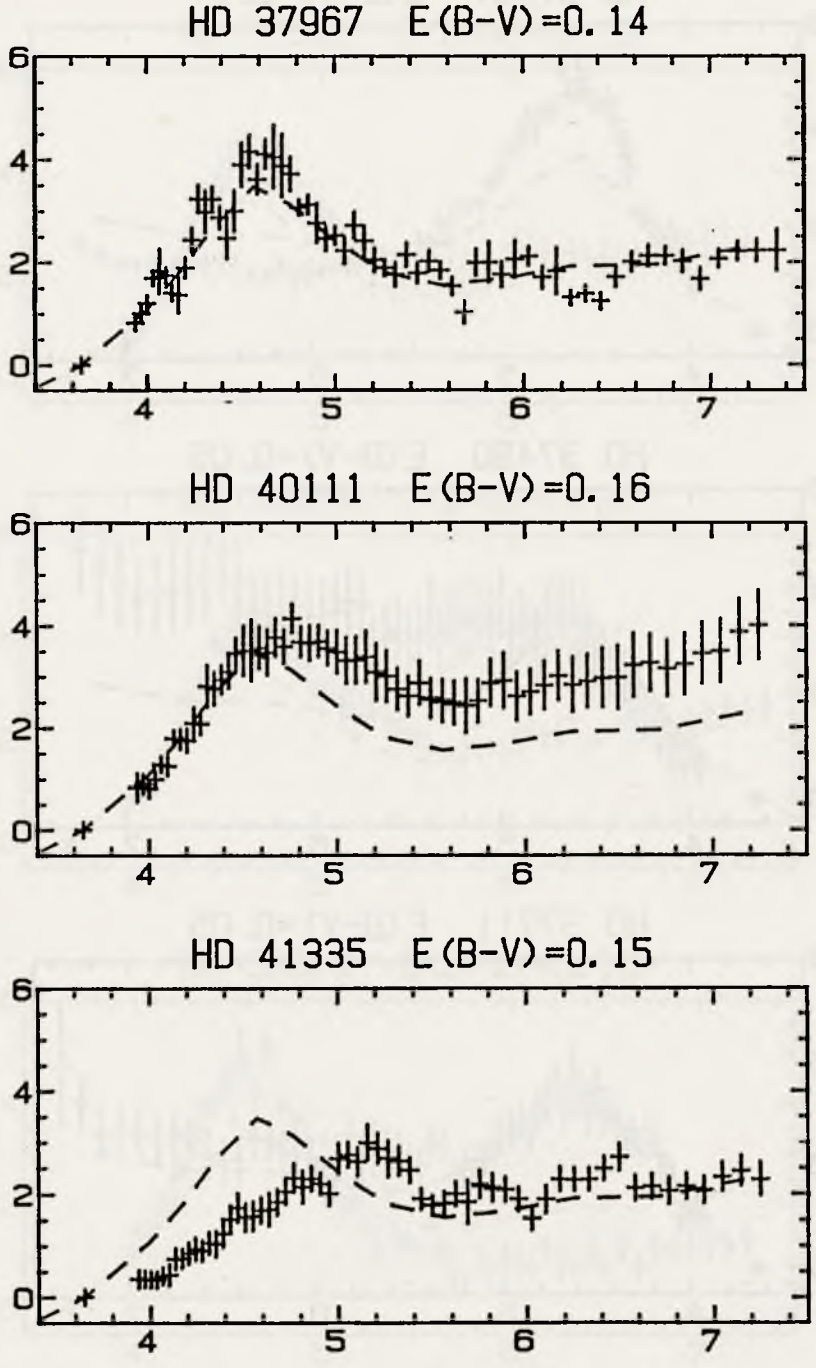
HD 37967 E(B-V)=0.14
HD 40111 E(B-V)=0.16
HD 41335 E(B-V)=0.15
0
2
4
6
4
5
6
7

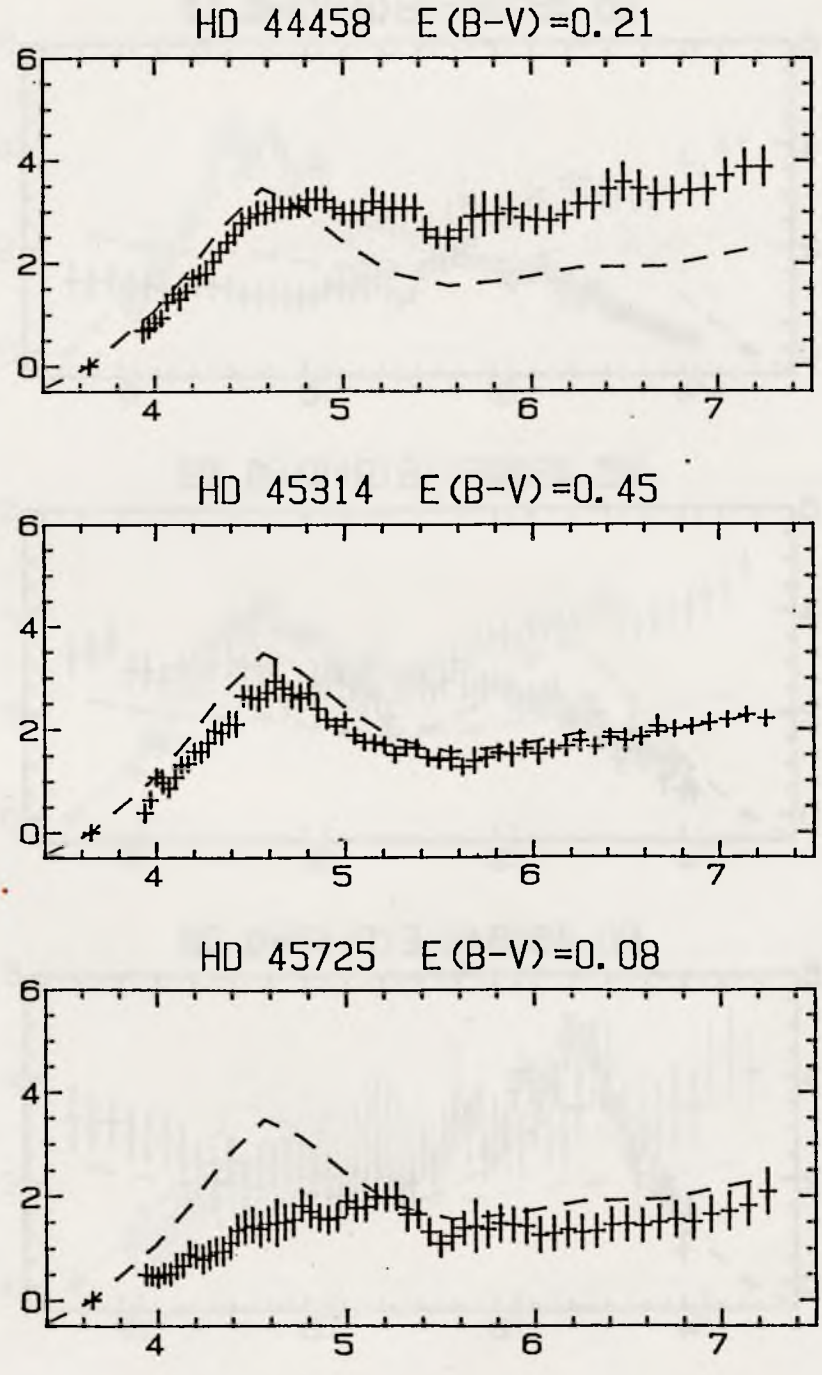
HD 44458 E(B-V)=0.21
HD 45314 E(B-V)=0.45
HD 45725 E(B-V)=0.08
0
2
4
6
4
5
6
7

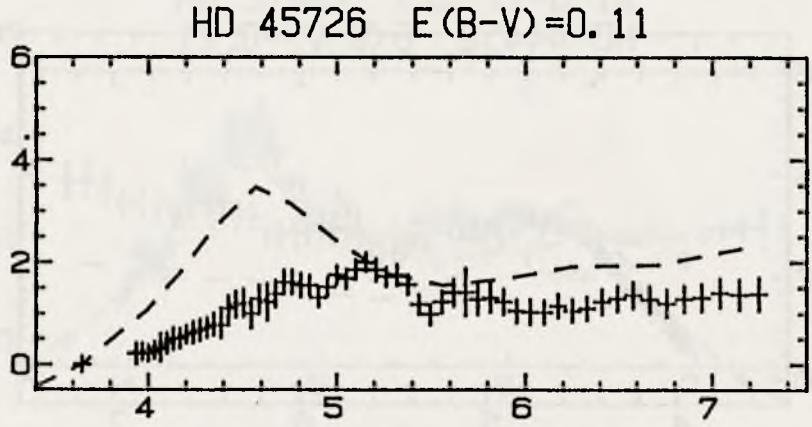
HD 45726 E(B-V)=0.11
6
4
2
0
4
5
6
7

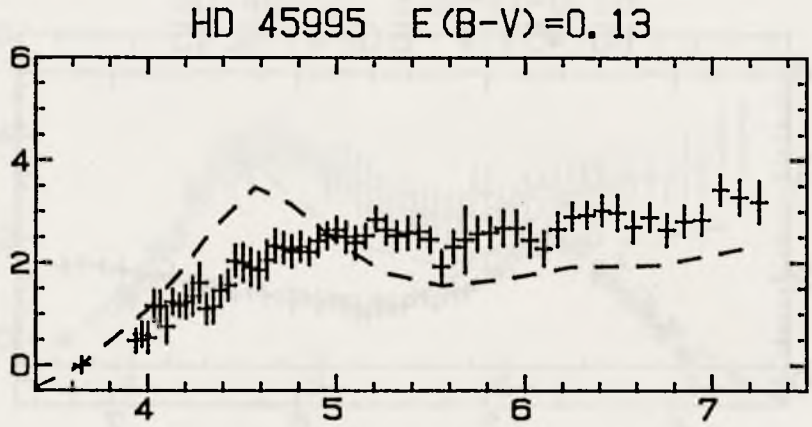
HD 45995 E(B-V)=0.13
6
4
2
0
4
5
6
7

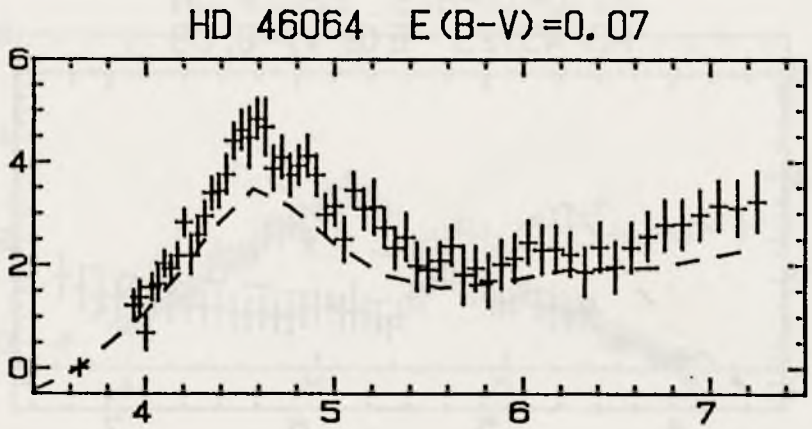
HD 46064 E(B-V)=0.07
6
4
2
0
4
5
6
7

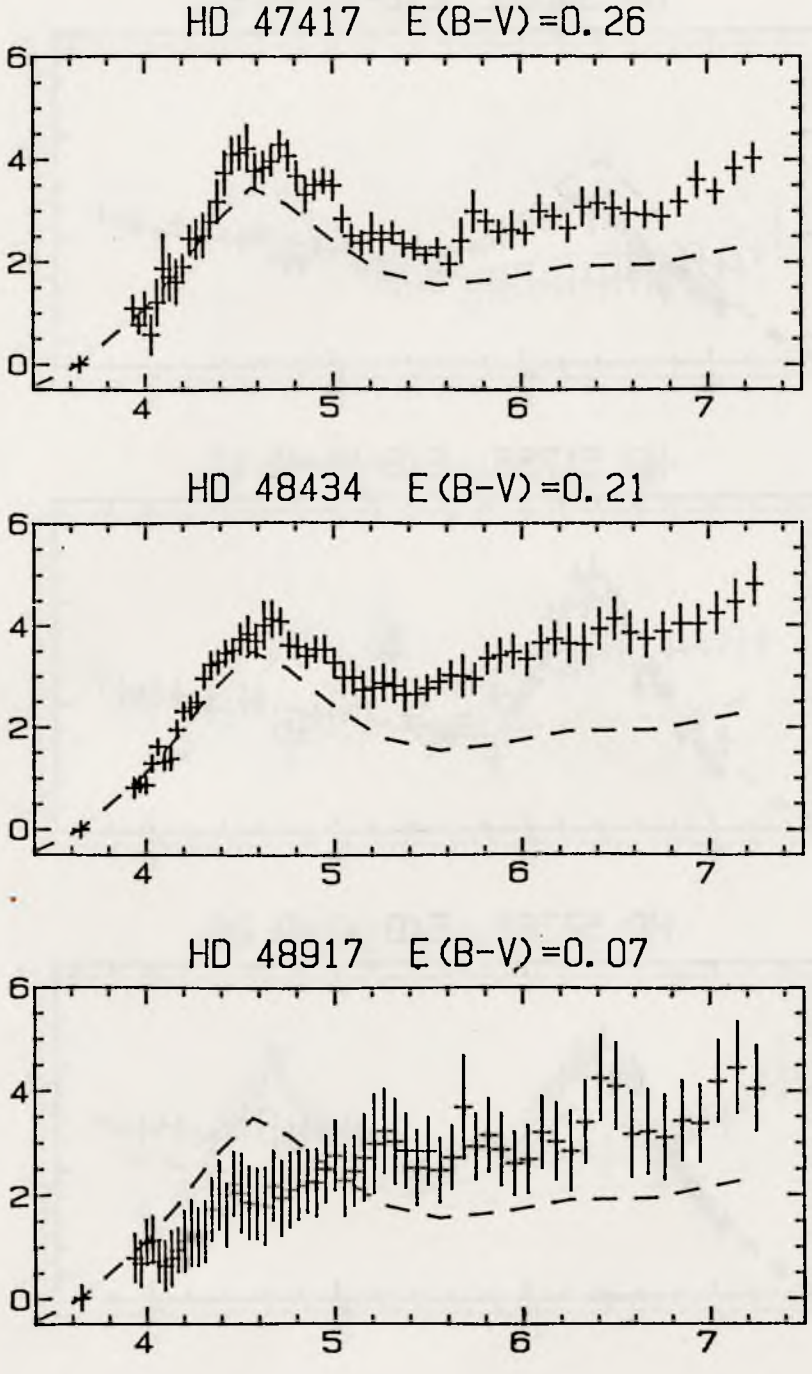
HD 47417 E(B-V)=0.26
HD 48434 E(B-V)=0.21
HD 48917 E(B-V)=0.07
0
2
4
6
4
5
6
7

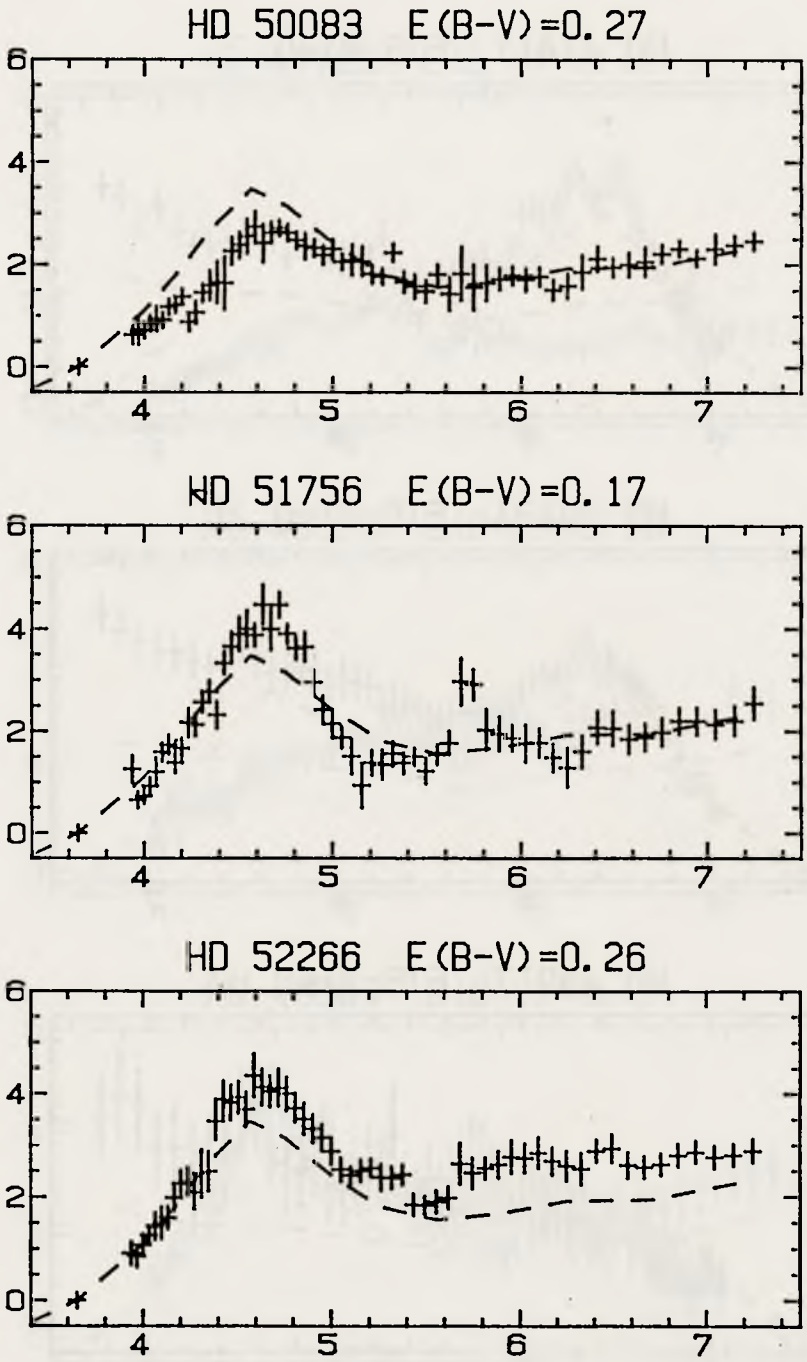
HD 50083 E(B-V)=0.27
HD 51756 E(B-V)=0.17
HD 52266 E(B-V)=0.26
0
2
4
6
4
5
6
7

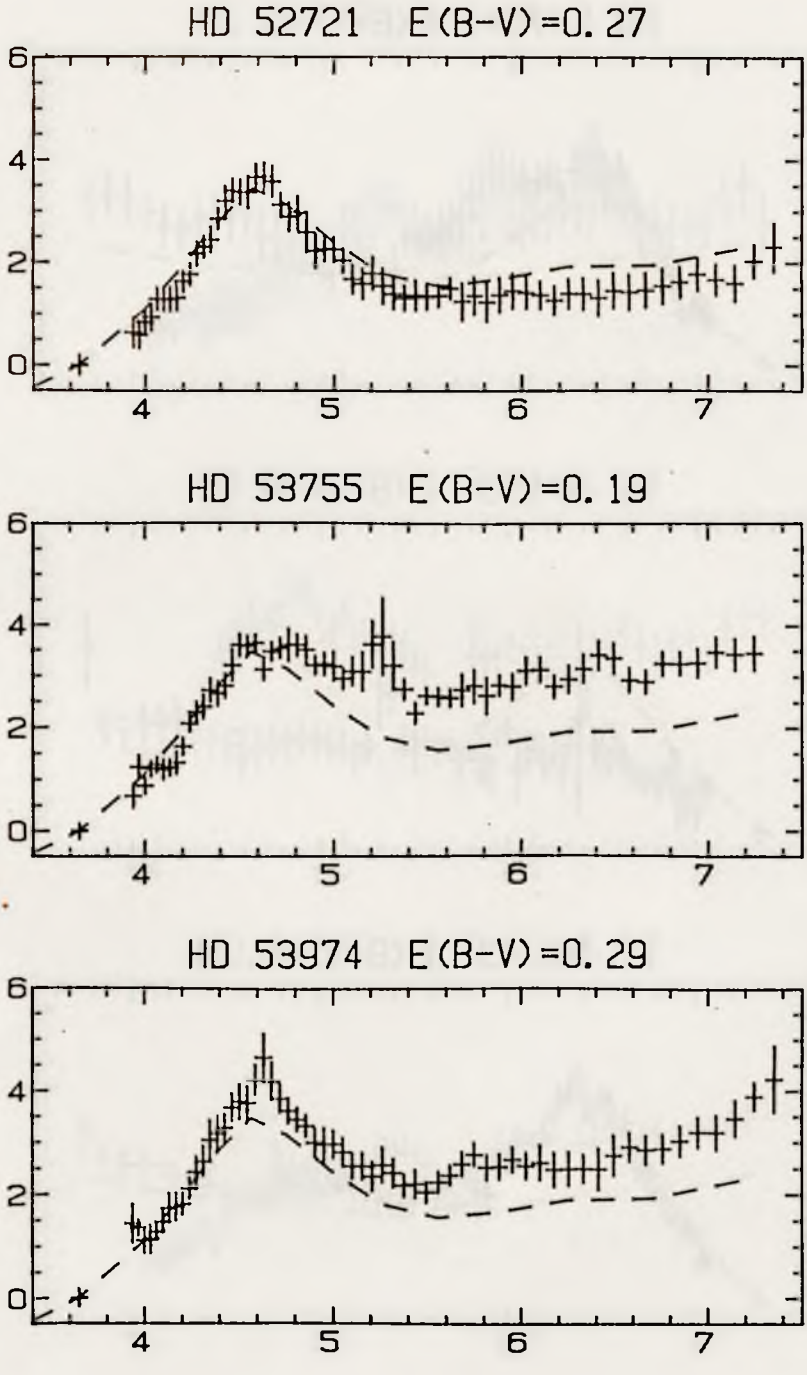
HD 52721 E(B-V)=0.27
HD 53755 E(B-V)=0.19
HD 53974 E(B-V)=0.29
0
2
4
6
4
5
6
7

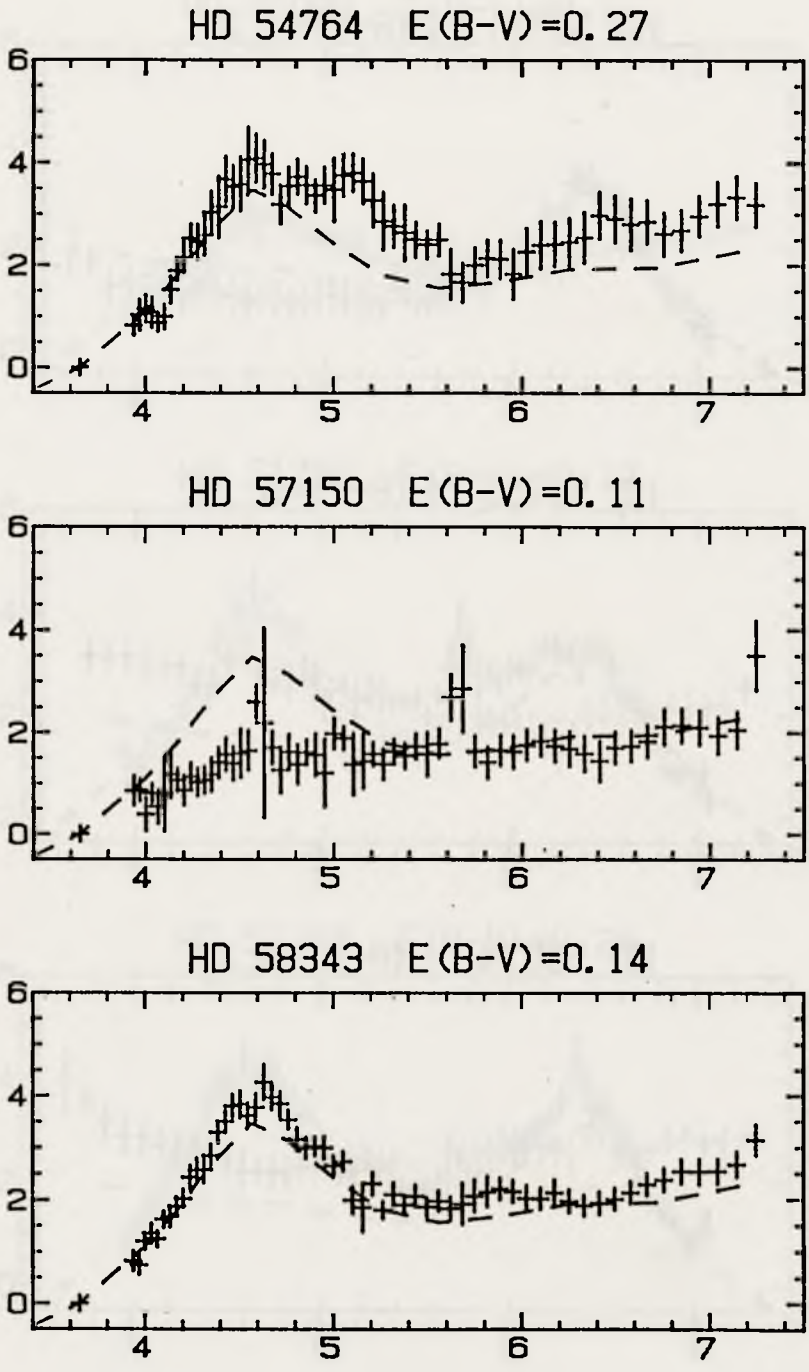
HD 54764 E(B-V)=0.27
HD 57150 E(B-V)=0.11
HD 58343 E(B-V)=0.14
0
2
4
6
4
5
6
7

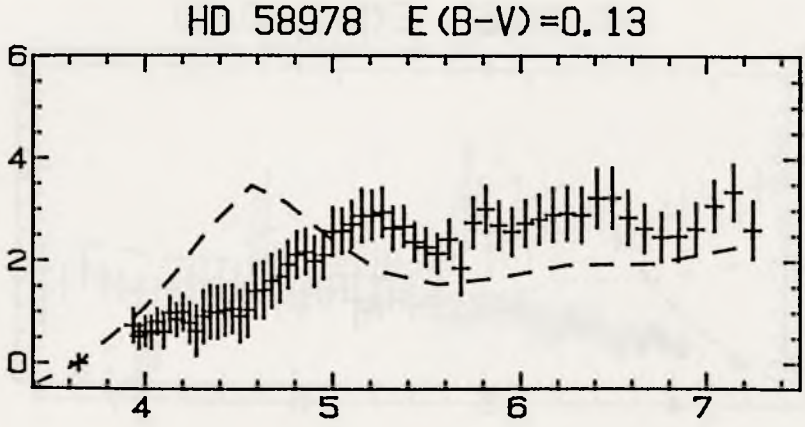
HD 58978 E(B-V)=0.13
6
4
2
0
4
5
6
7

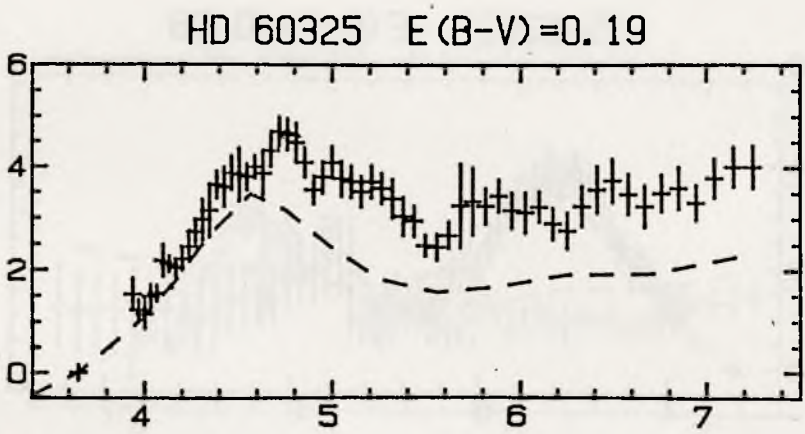
HD 60325 E(B-V)=0.19
6
4
2
0
4
5
6
7

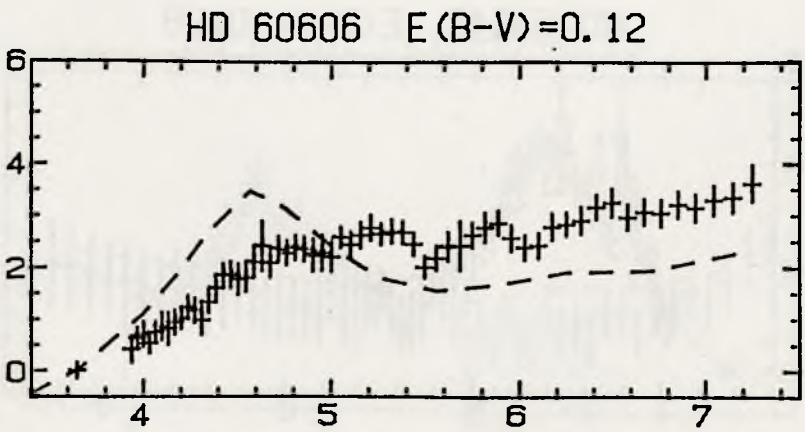
HD 60606 E(B-V)=0.12
6
4
2
0
4
5
6
7

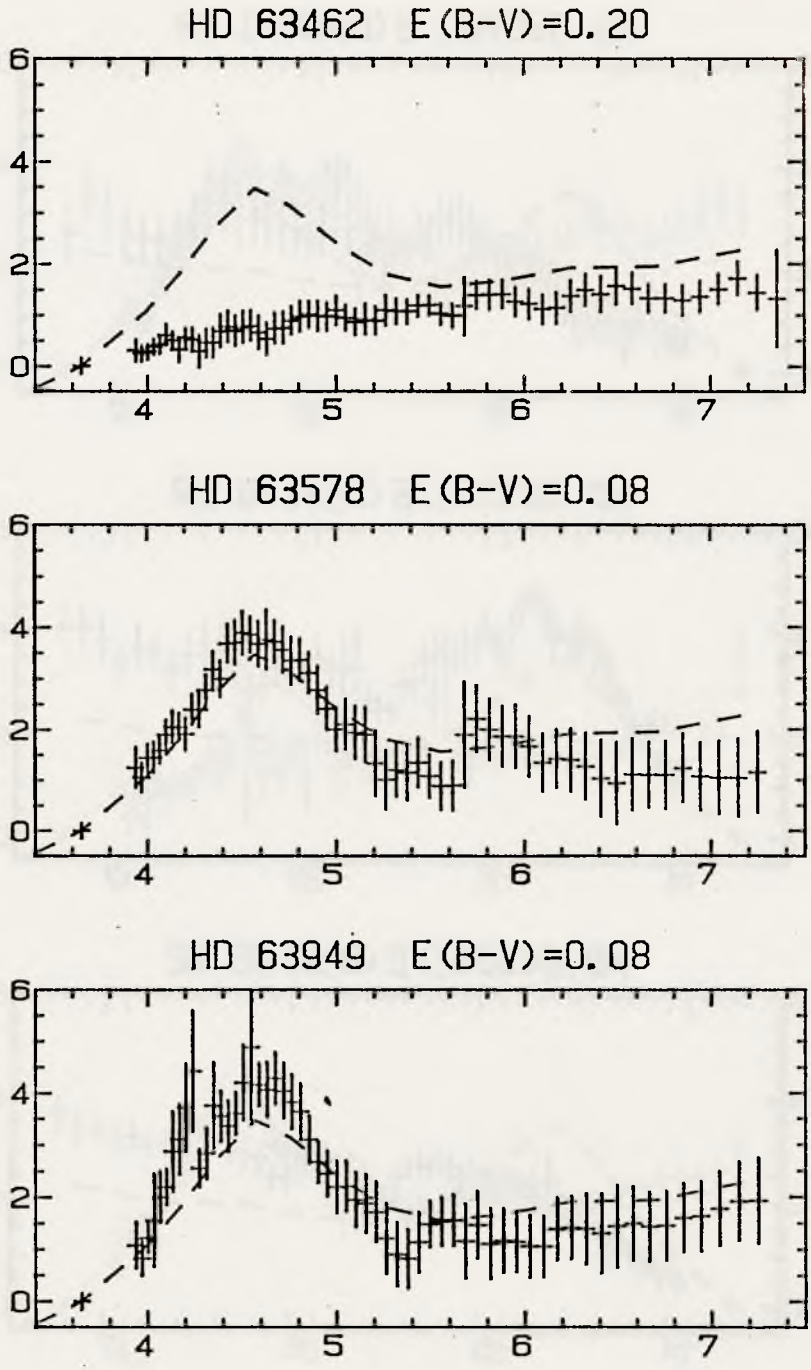
HD 63462 E(B-V)=0.20
HD 63578 E(B-V)=0.08
HD 63949 E(B-V)=0.08
0
2
4
6
4
5
6
7

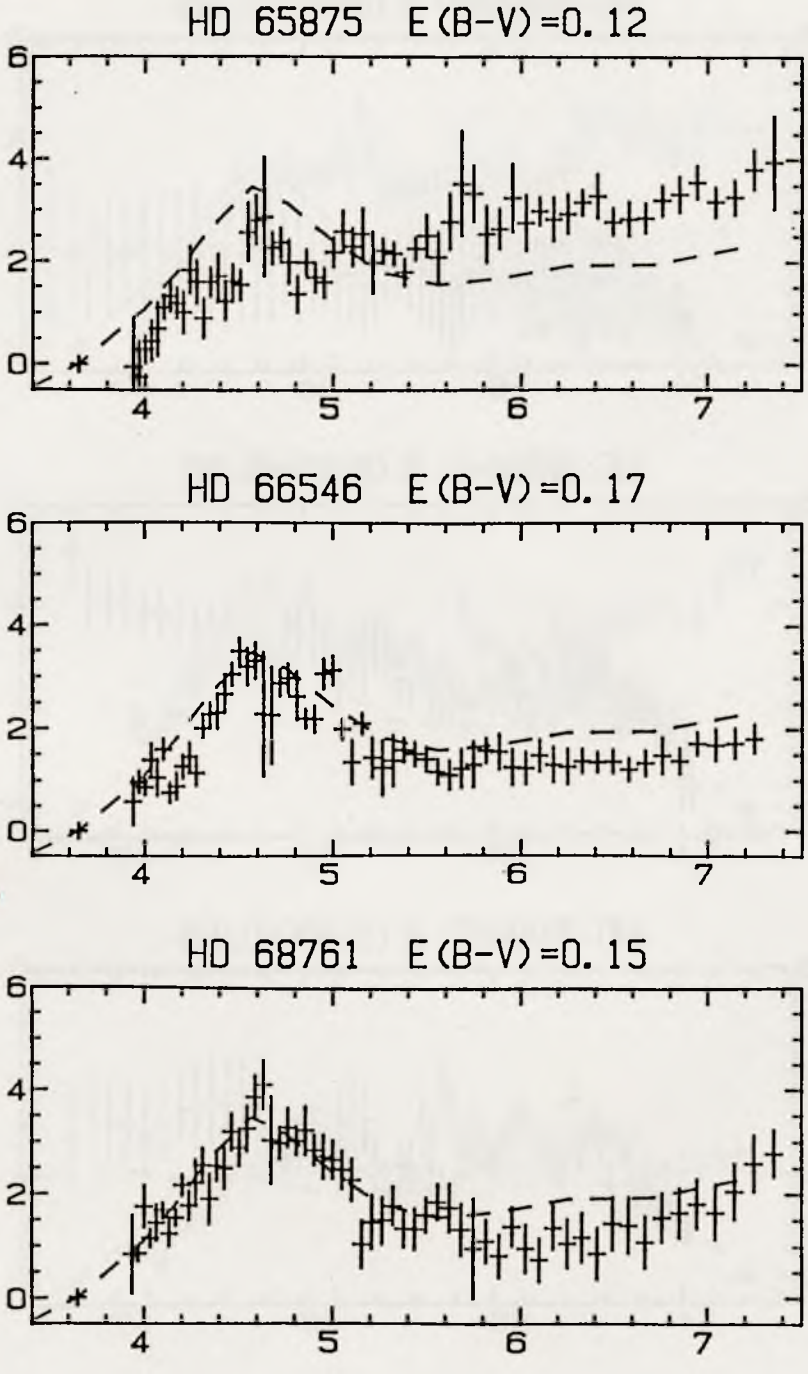
HD 65875 E(B-V)=0.12
HD 66546 E(B-V)=0.17
HD 68761 E(B-V)=0.15
0
2
4
6
4
5
6
7

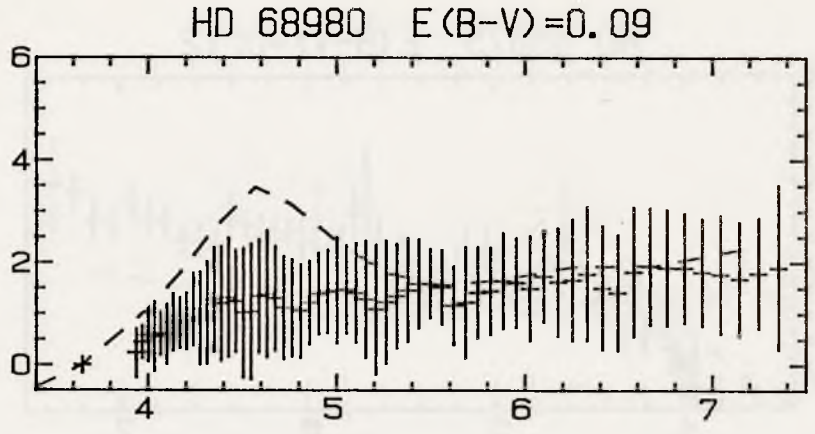
HD 68980 E(B-V)=0.09
6
4
2
0
4
5
6
7

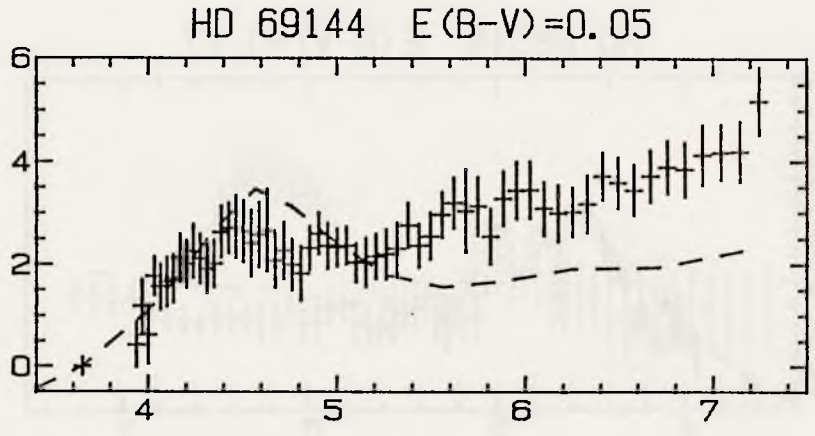
HD 69144 E(B-V)=0.05
6
4
2
0
4
5
6
7

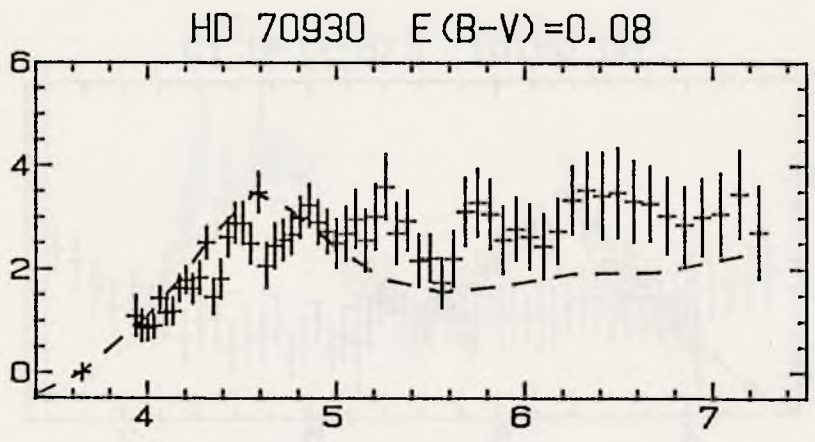
HD 70930 E(B-V)=0.08
6
4
2
0
4
5
6
7

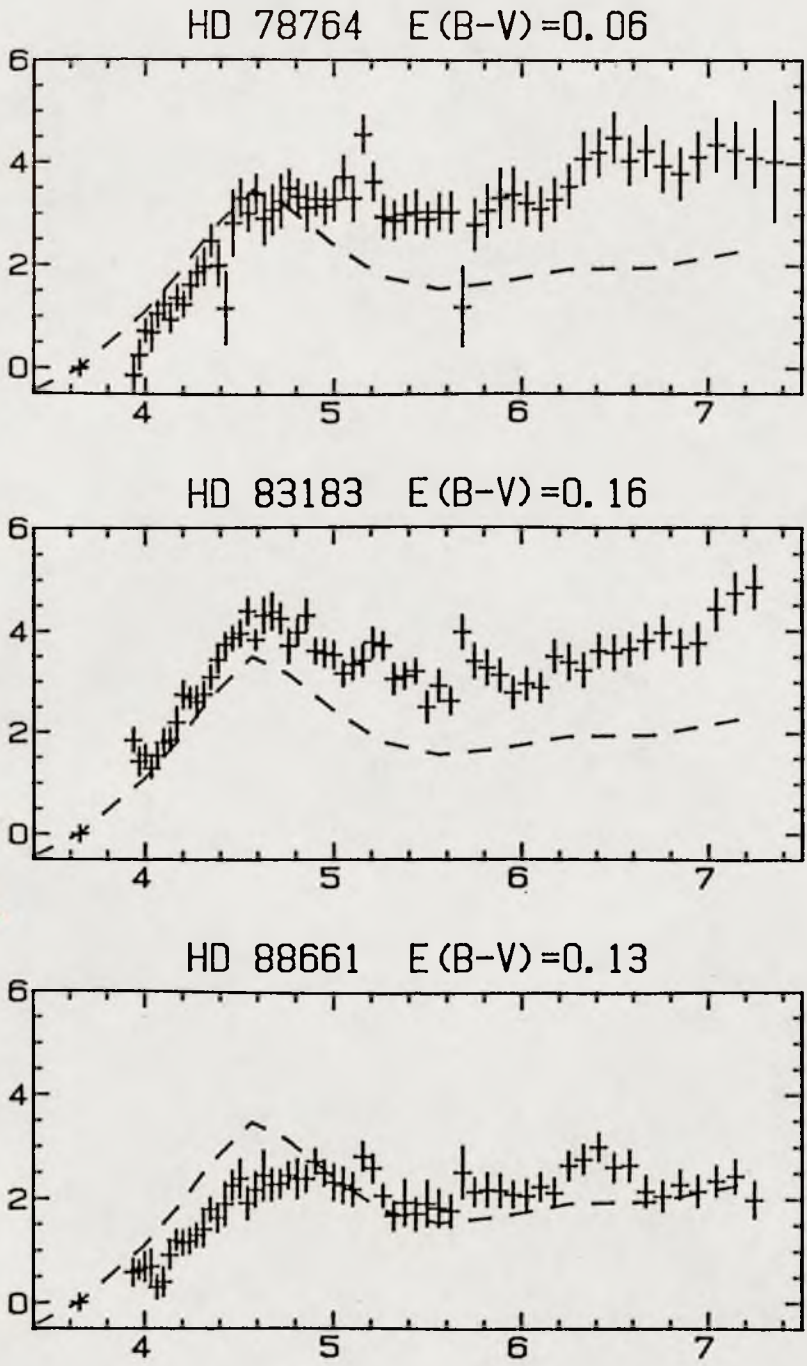
HD 78764 E(B-V)=0.06
HD 83183 E(B-V)=0.16
HD 88661 E(B-V)=0.13
0
2
4
6
4
5
6
7

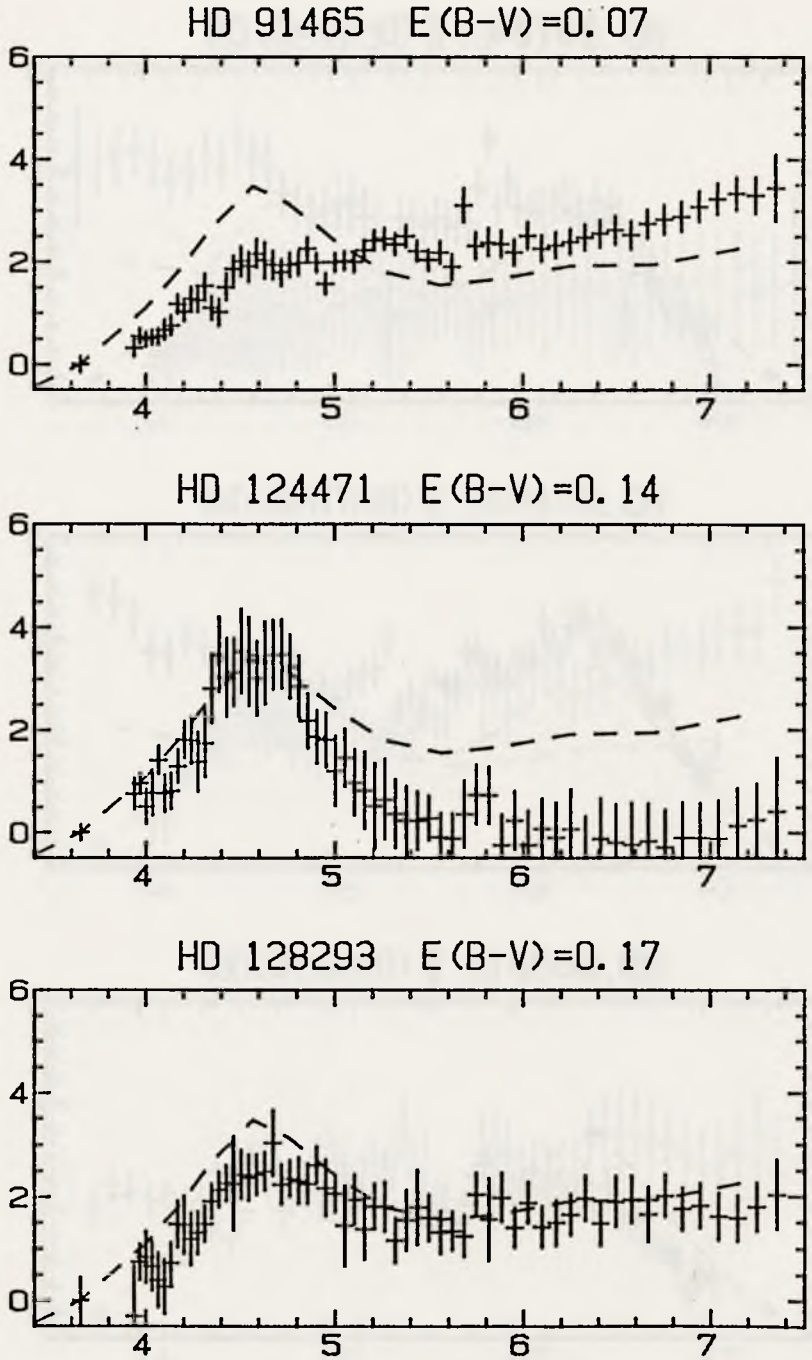
HD 91465 E(B-V)=0.07
HD 124471 E(B-V)=0.14
HD 128293 E(B-V)=0.17
6
4
2
0
4
5
6
7

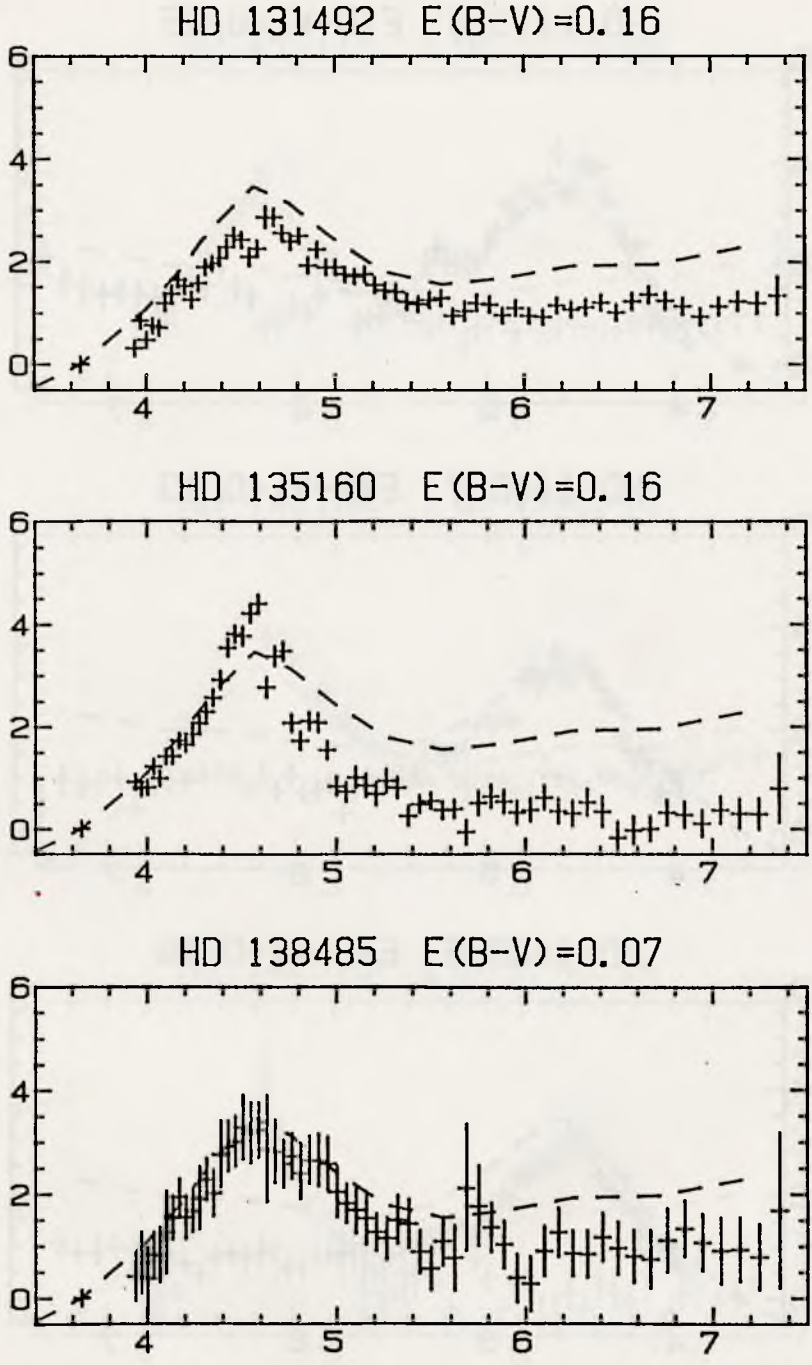
HD 131492 E(B-V)=0.16
HD 135160 E(B-V)=0.16
HD 138485 E(B-V)=0.07
0
2
4
6
4
5
6
7

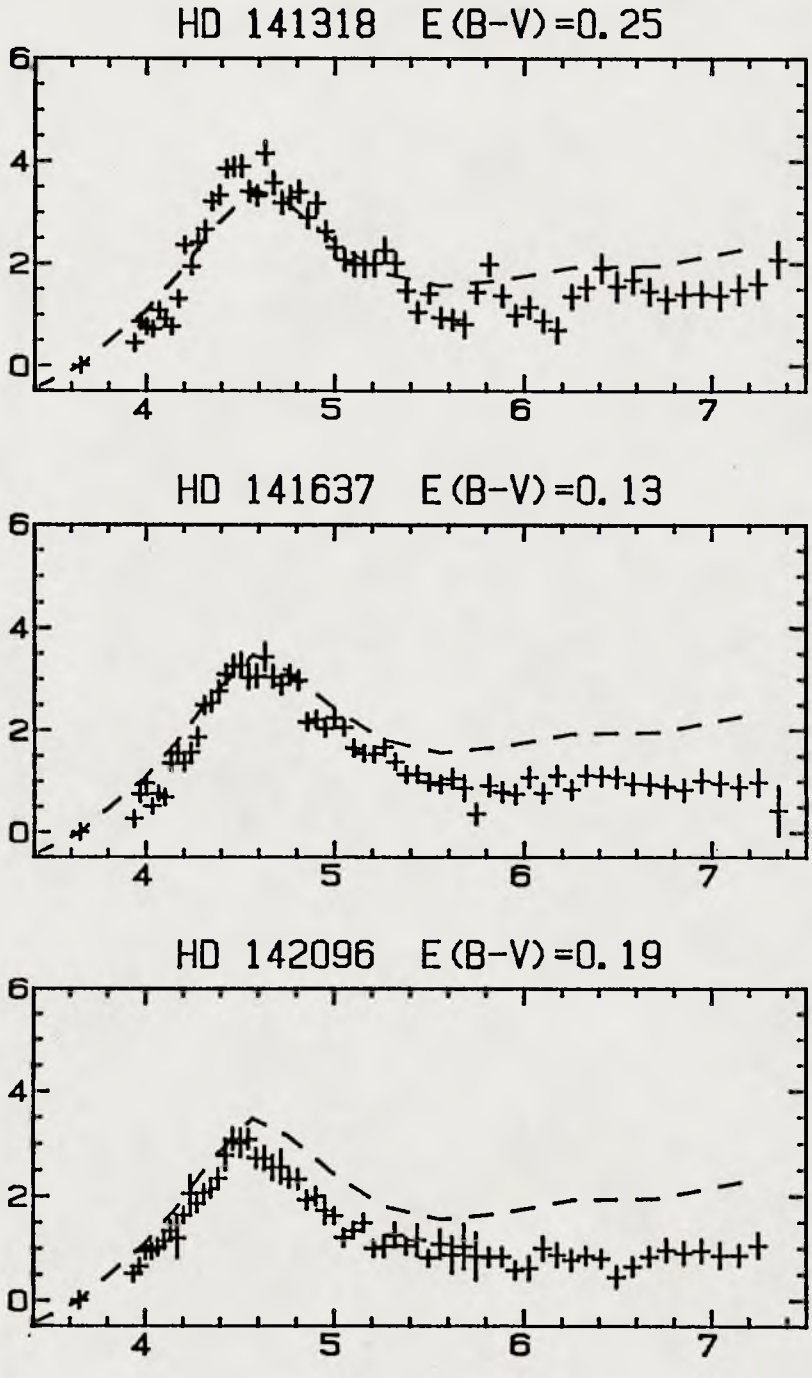
HD 141318 E(B-V)=0.25
HD 141637 E(B-V)=0.13
HD 142096 E(B-V)=0.19
0
2
4
6
4
5
6
7

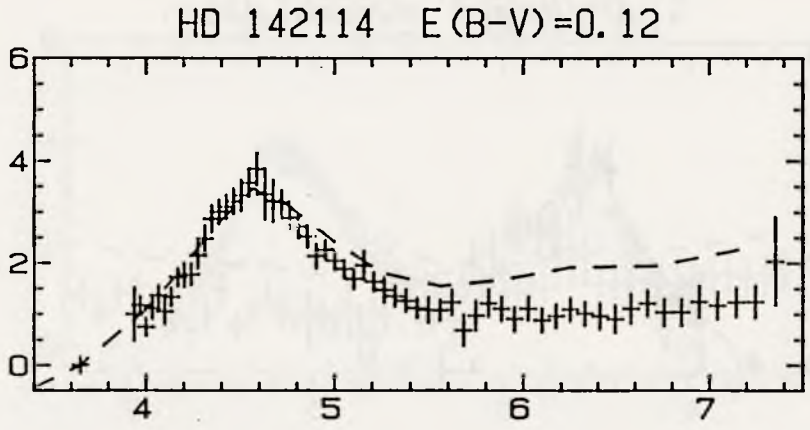
HD 142114 E(B-V)=0.12
6
4
2
0
4
5
6
7

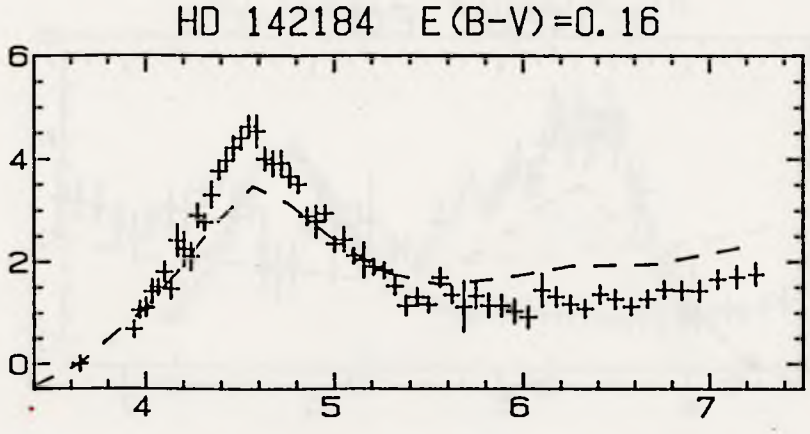
HD 142184 E(B-V)=0.16
6
4
2
0
4
5
6
7

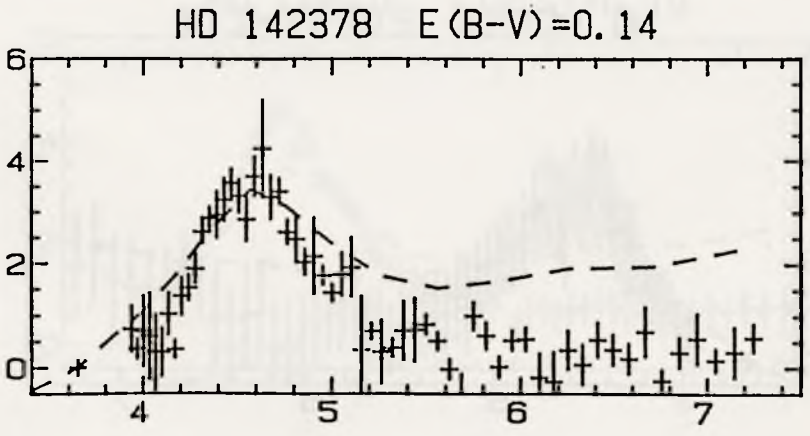
HD 142378 E(B-V)=0.14
6
4
2
0
4
5
6
7

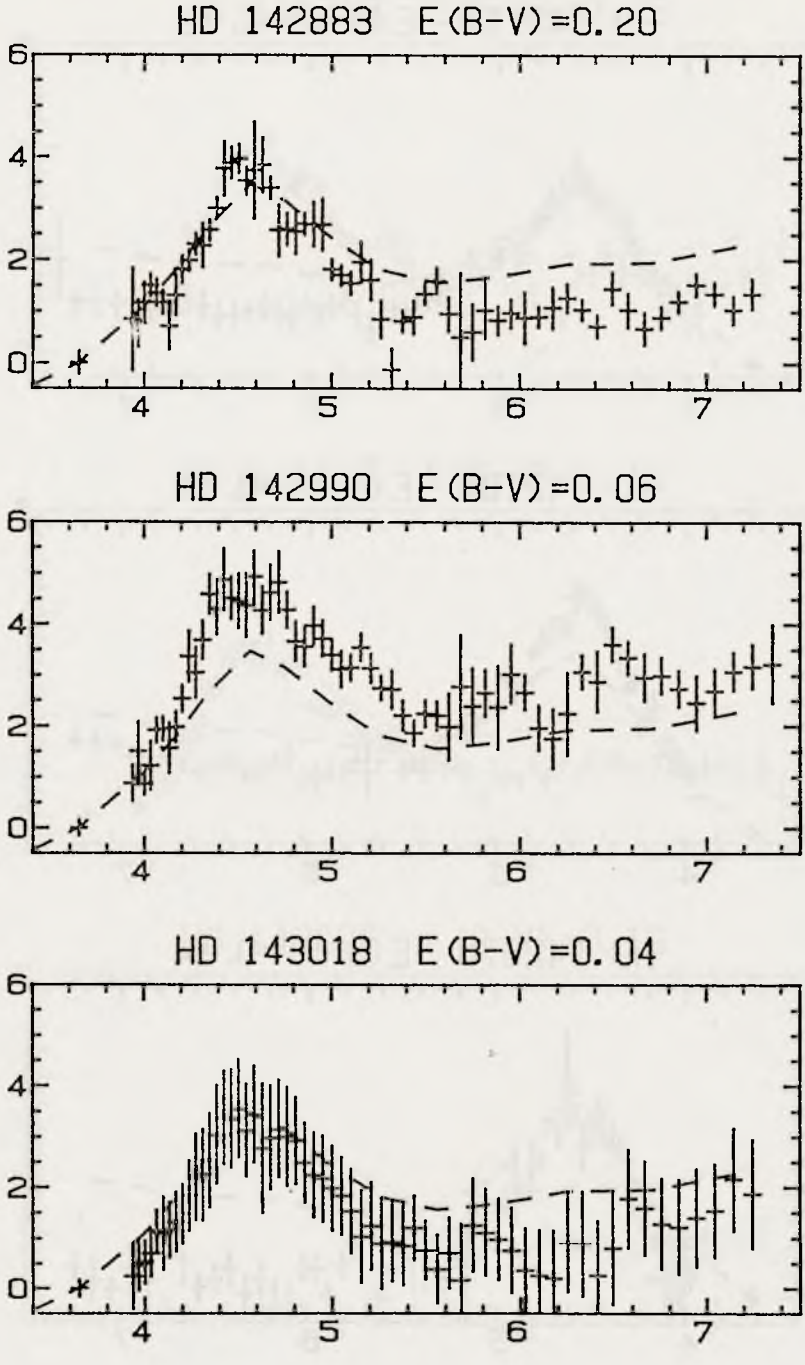
HD 142883 E(B-V)=0.20
HD 142990 E(B-V)=0.06
HD 143018 E(B-V)=0.04
0
2
4
6
4
5
6
7

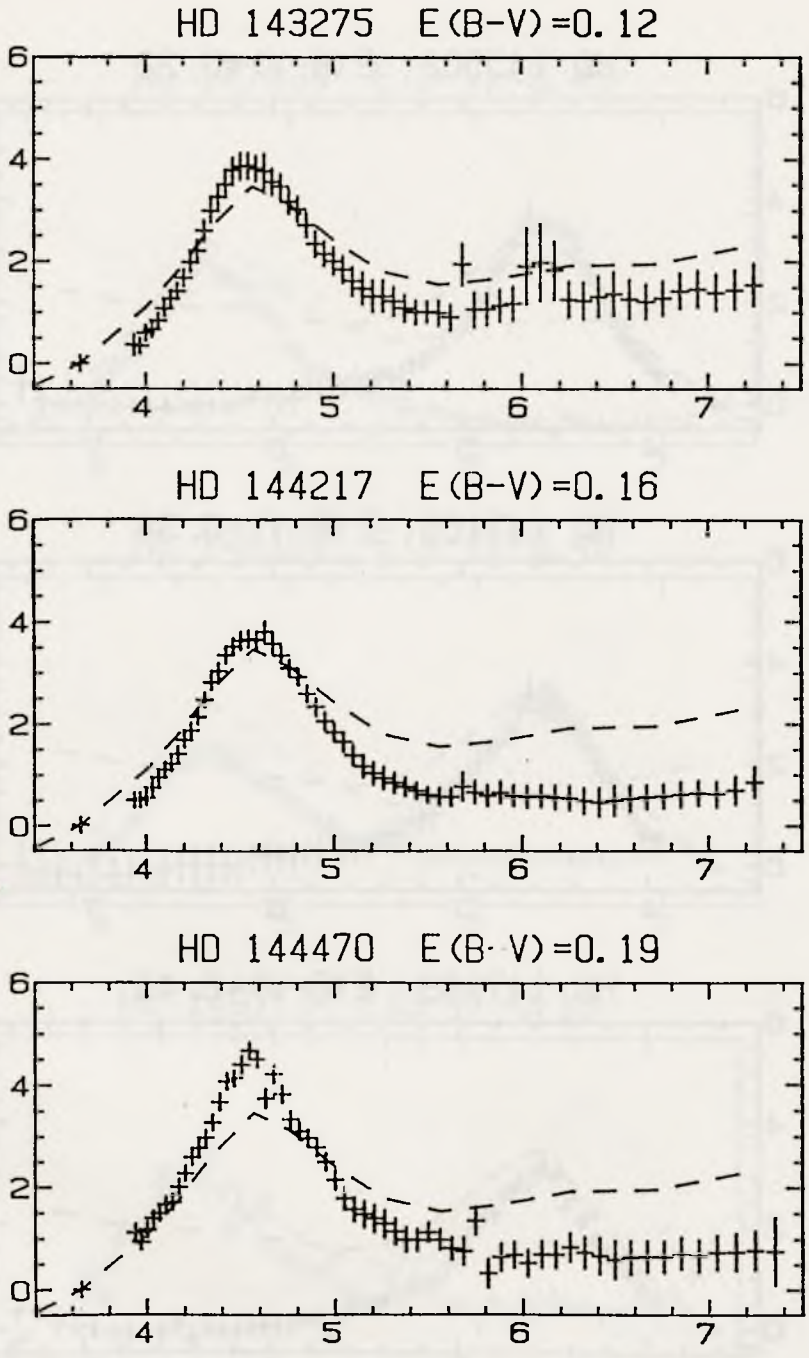
HD 143275 E(B-V)=0.12
HD 144217 E(B-V)=0.16
HD 144470 E(B-V)=0.19
0
2
4
6
4
5
6
7

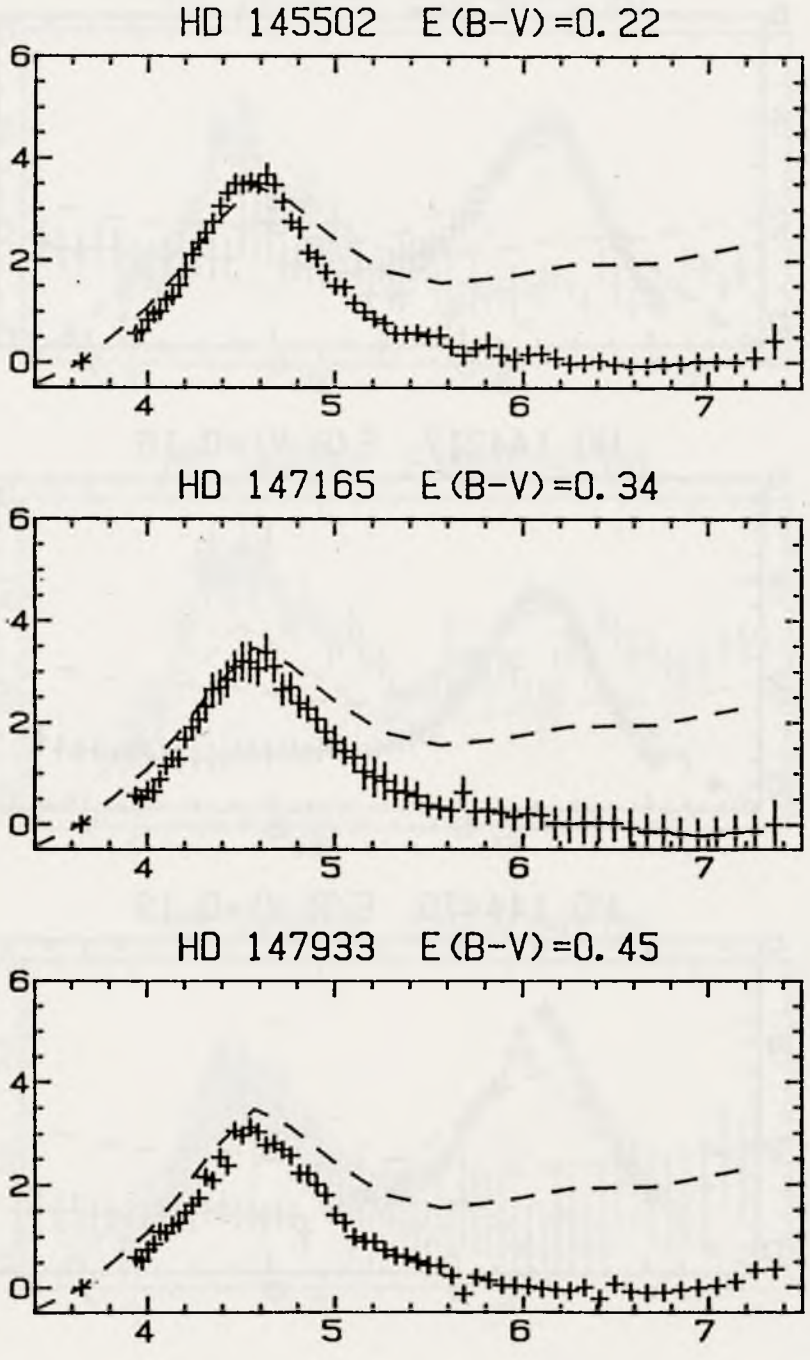
HD 145502 E(B-V)=0.22
HD 147165 E(B-V)=0.34
HD 147933 E(B-V)=0.45
6
4
2
0
4
5
6
7

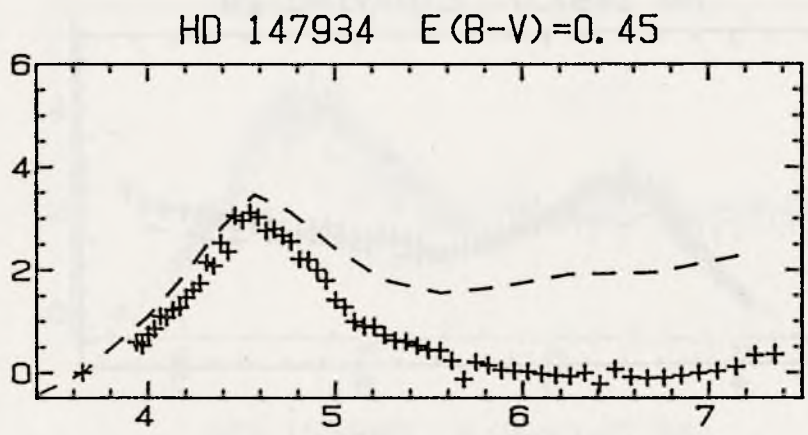
HD 147934 E(B-V)=0.45
6
4
2
0
4
5
6
7

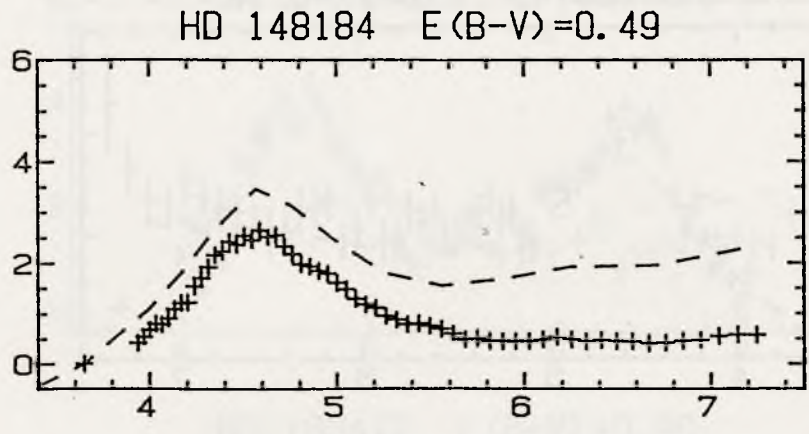
HD 148184 E(B-V)=0.49
6
4
2
0
4
5
6
7

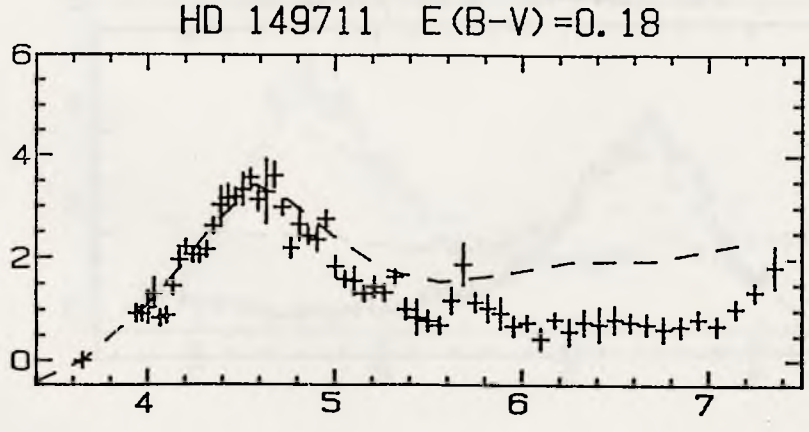
HD 149711 E(B-V)=0.18
6
4
2
0
4
5
6
7

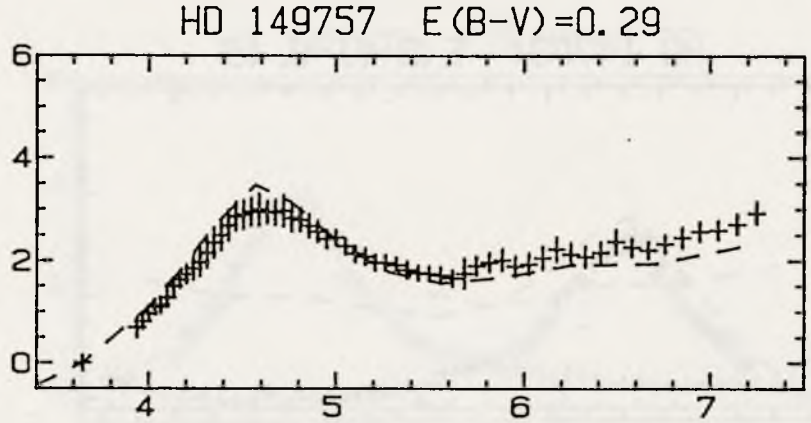
HD 149757 E(B-V)=0.29
6
4
2
0
4
5
6
7

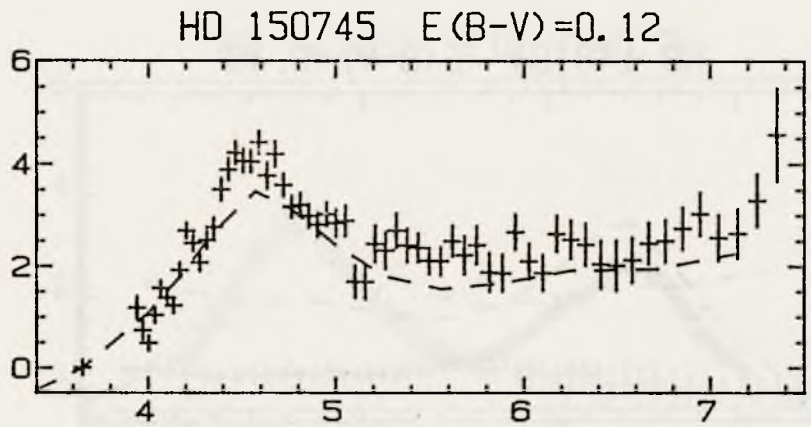
HD 150745 E(B-V)=0.12
6
4
2
0
4
5
6
7

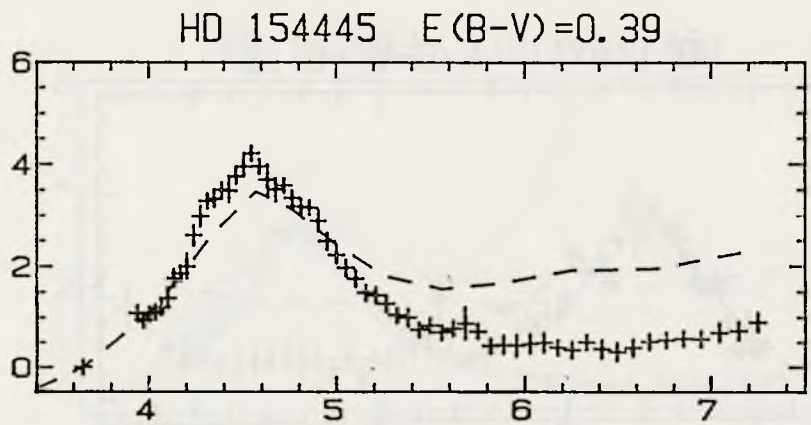
HD 154445 E(B-V)=0.39
6
4
2
0
4
5
6
7

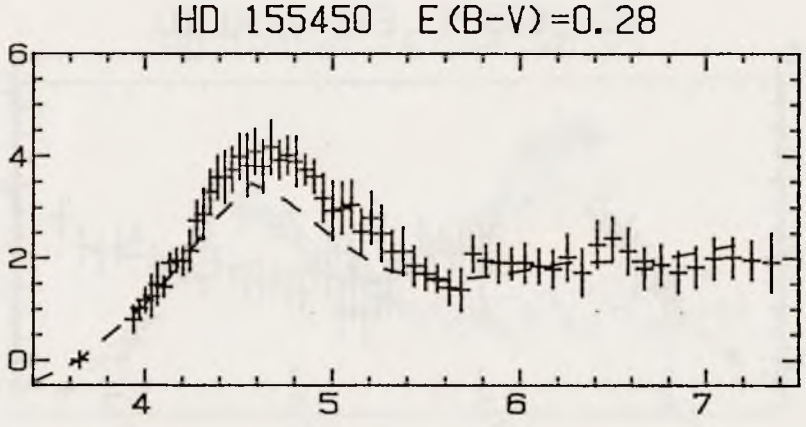
HD 155450 E(B-V)=0.28
6
4
2
0
4
5
6
7

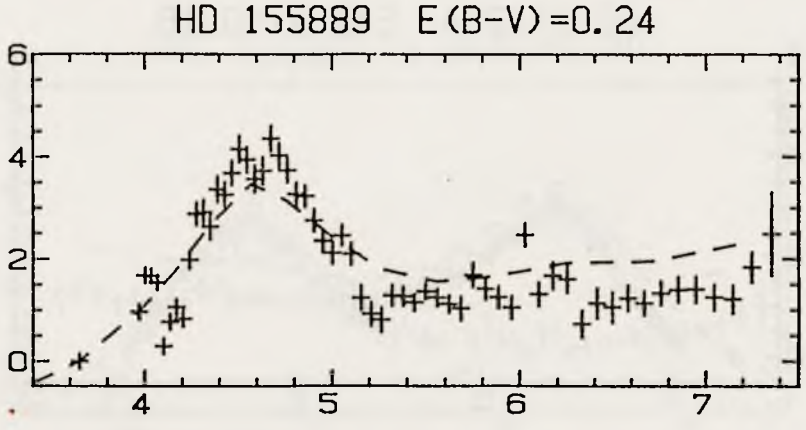
HD 155889 E(B-V)=0.24
6
4
2
0
4
5
6
7

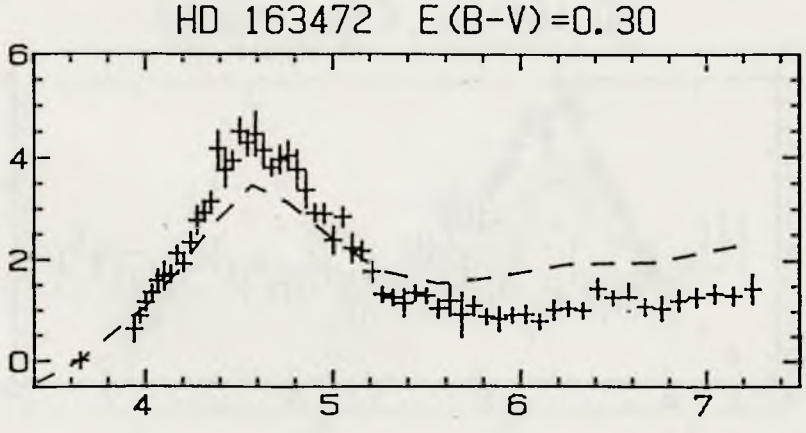
HD 163472 E(B-V)=0.30
6
4
2
0
4
5
6
7

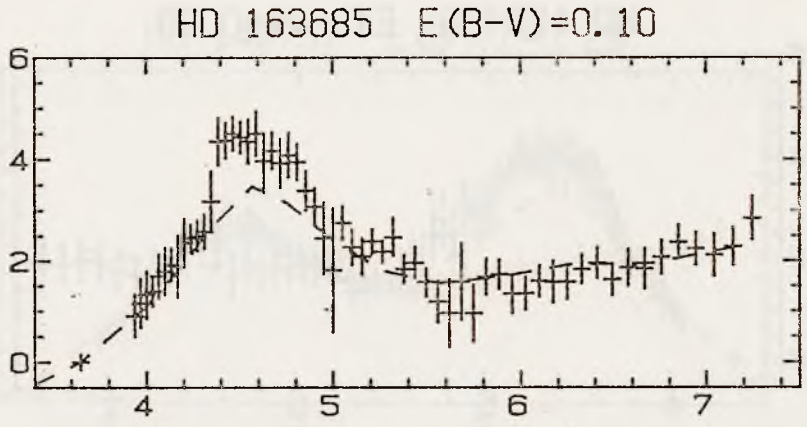
HD 163685 E(B-V)=0.10
6
4
2
0
4
5
6
7

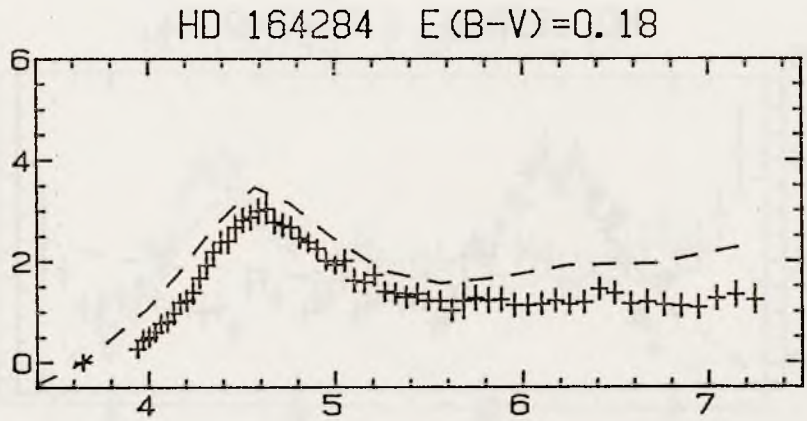
HD 164284 E(B-V)=0.18
6
4
2
0
4
5
6
7

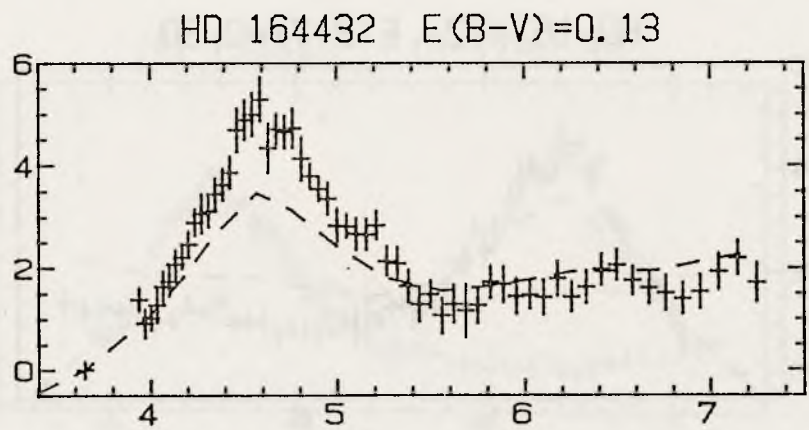
HD 164432 E(B-V)=0.13
6
4
2
0
4
5
6
7

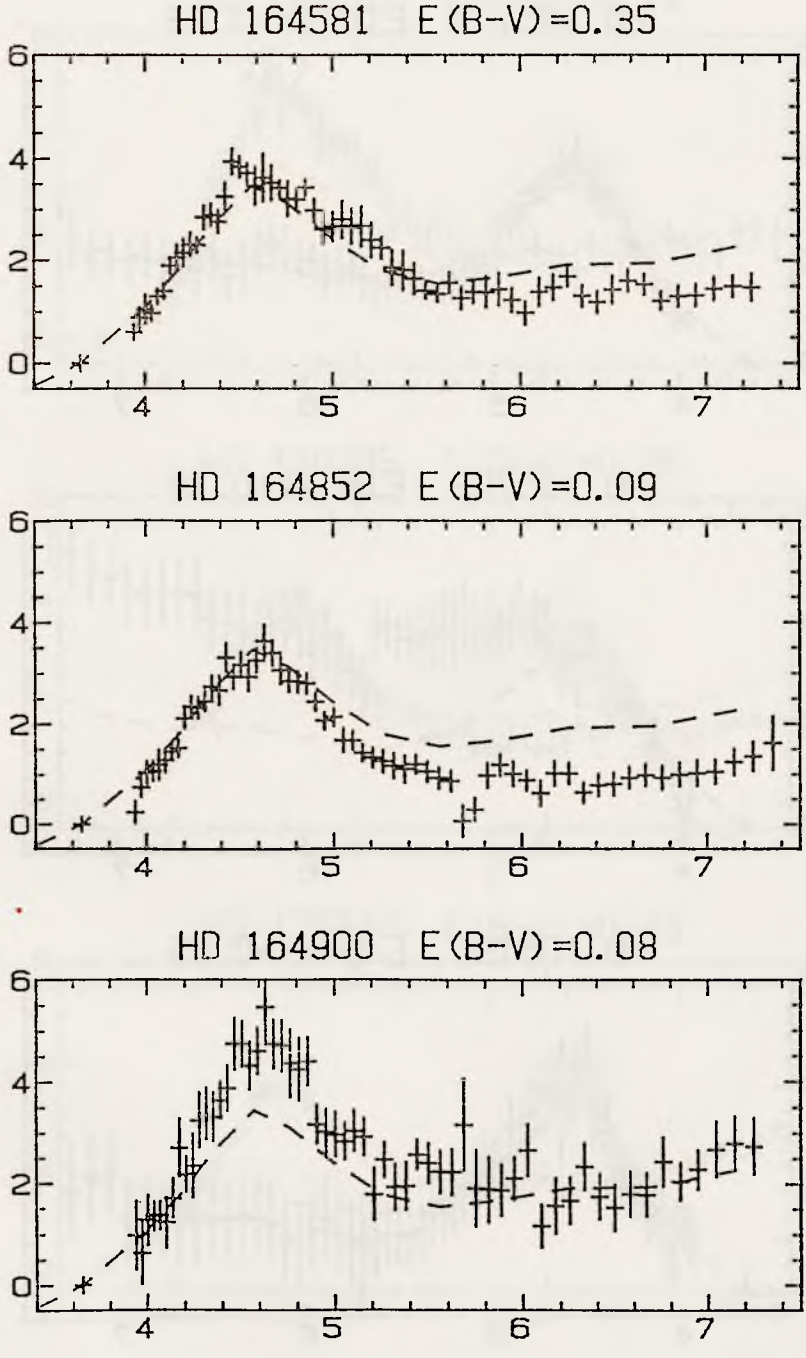
HD 164581 E(B-V)=0.35
HD 164852 E(B-V)=0.09
HD 164900 E(B-V)=0.08
0
2
4
6
4
5
6
7

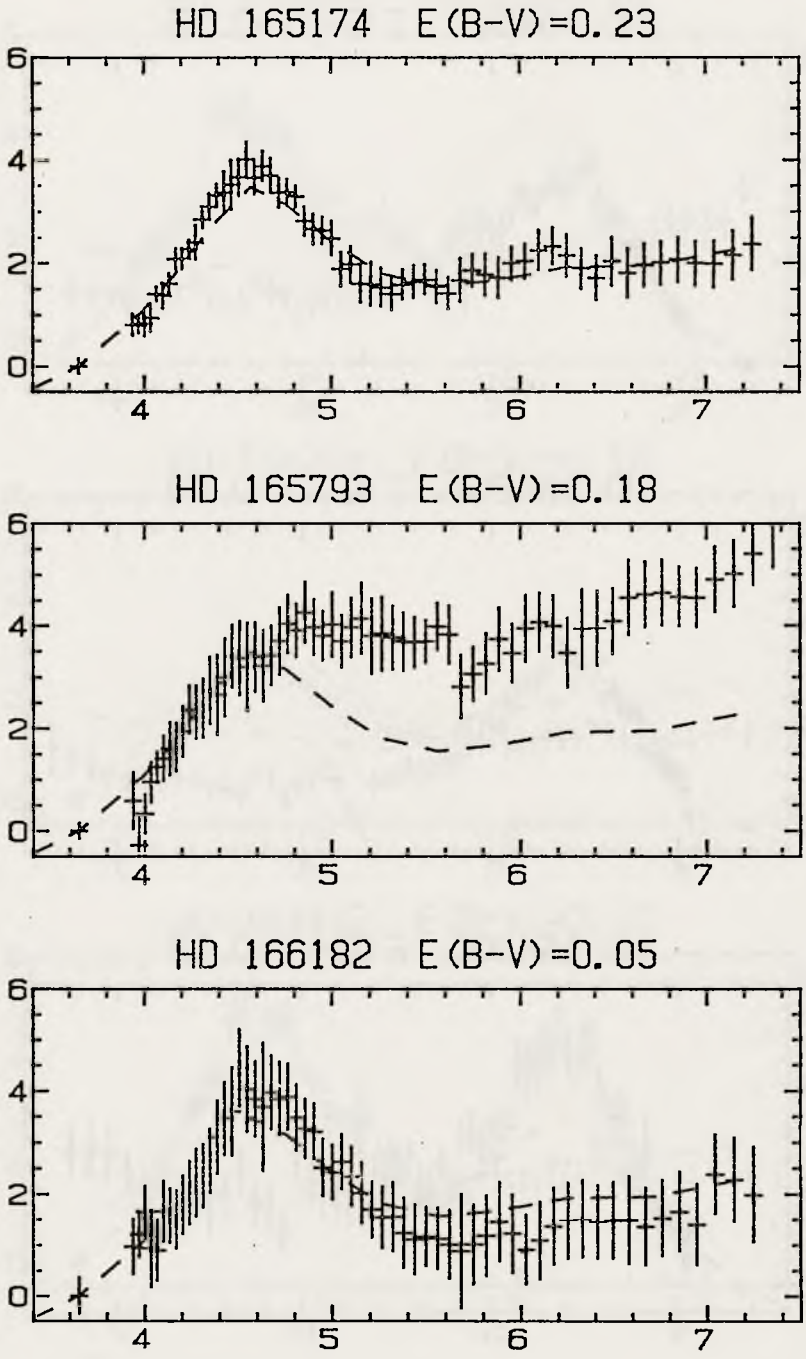
HD 165174 E(B-V)=0.23
HD 165793 E(B-V)=0.18
HD 166182 E(B-V)=0.05
0
2
4
6
4
5
6
7

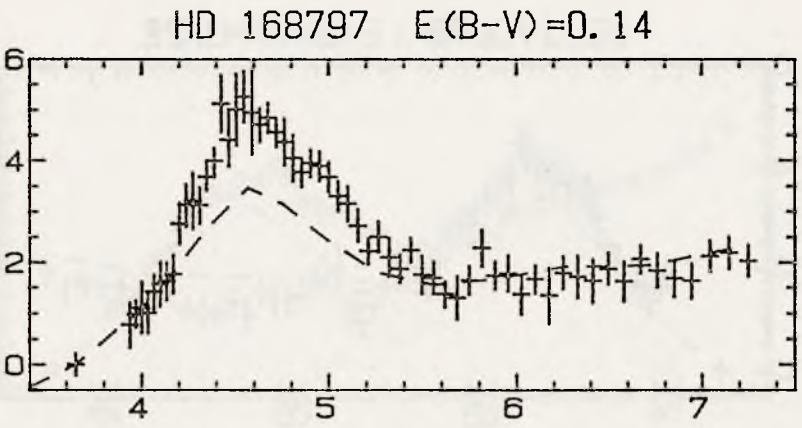
HD 168797 E(B-V)=0.14
6
4
2
0
4
5
6
7

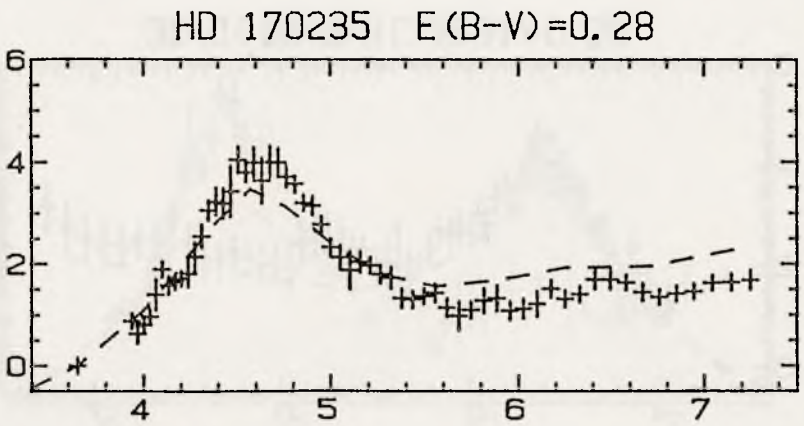
HD 170235 E(B-V)=0.28
6
4
2
0
4
5
6
7

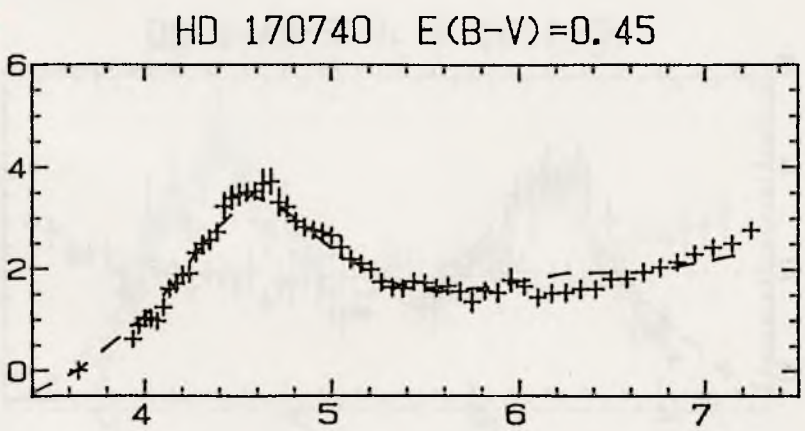
HD 170740 E(B-V)=0.45
6
4
2
0
4
5
6
7

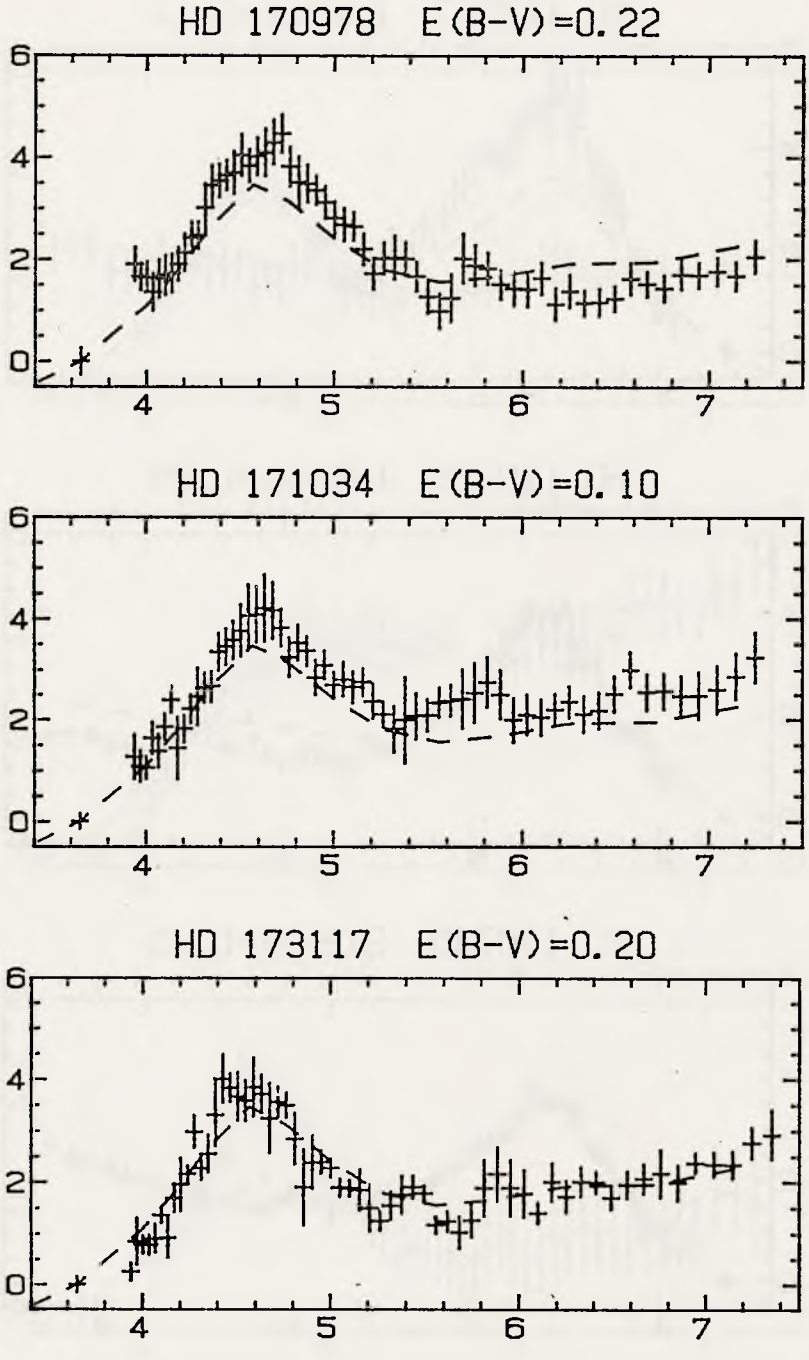
HD 170978 E(B-V)=0.22
HD 171034 E(B-V)=0.10
HD 173117 E(B-V)=0.20
0
2
4
6
4
5
6
7

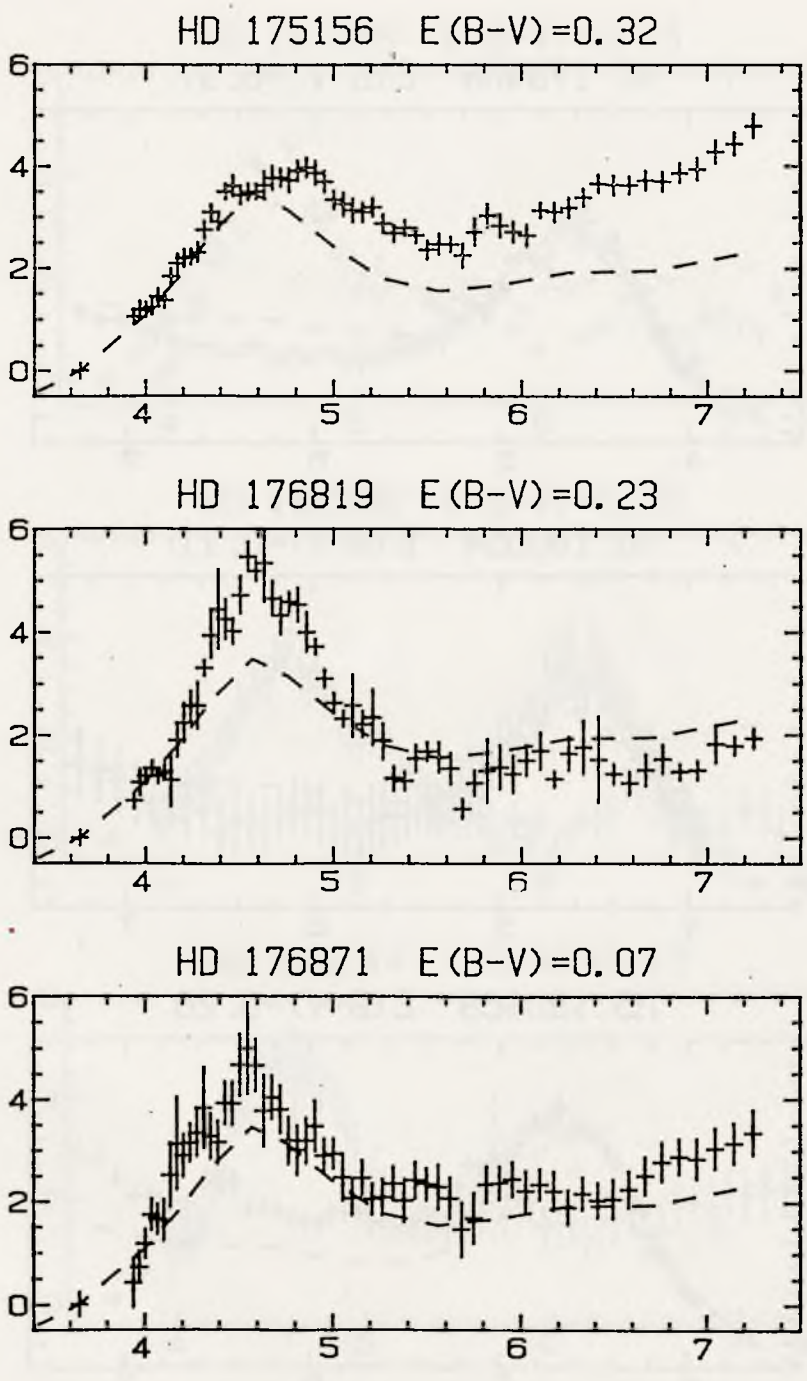
HD 175156 E(B-V)=0.32
HD 176819 E(B-V)=0.23
HD 176871 E(B-V)=0.07
0
2
4
6
4
5
6
7

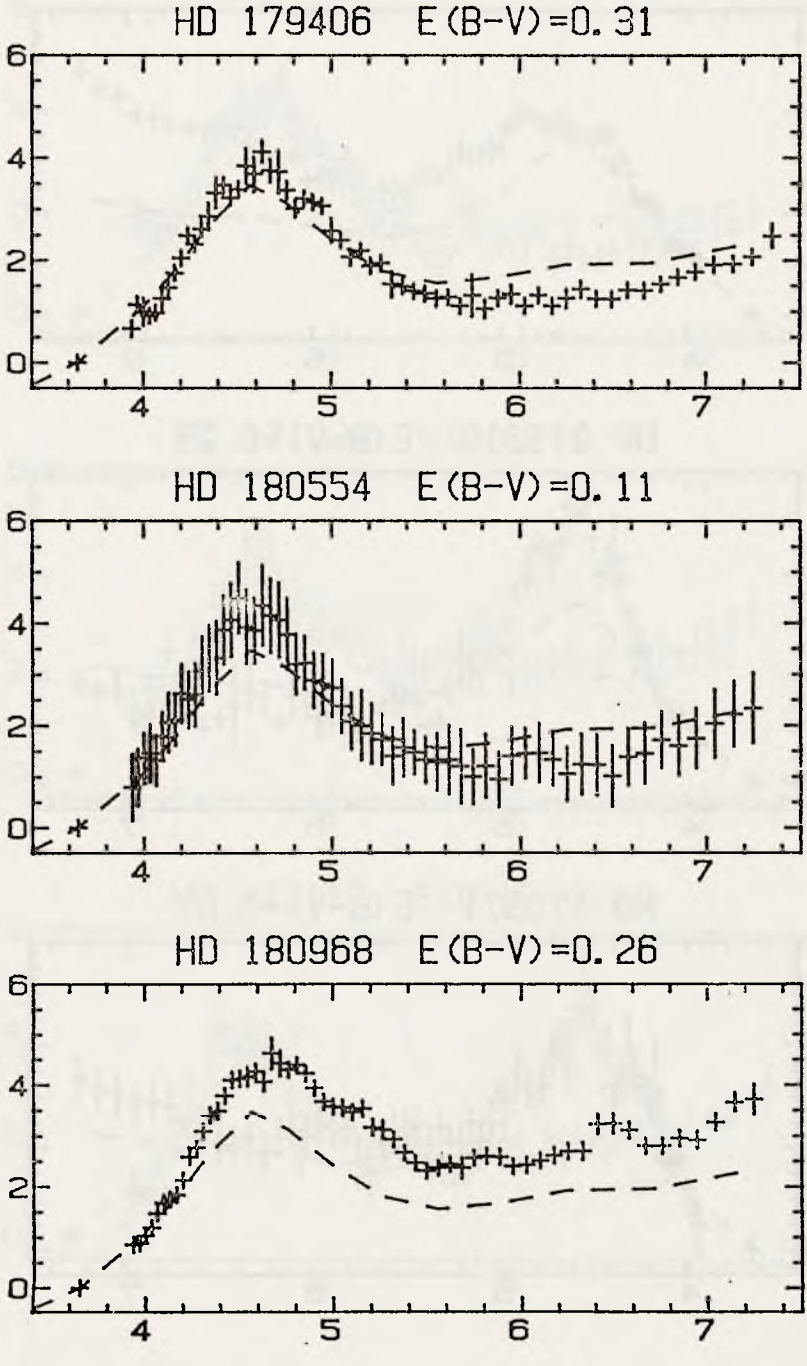
HD 179406 E(B-V)=0.31
HD 180554 E(B-V)=0.11
HD 180968 E(B-V)=0.26
0
2
4
6
4
5
6
7

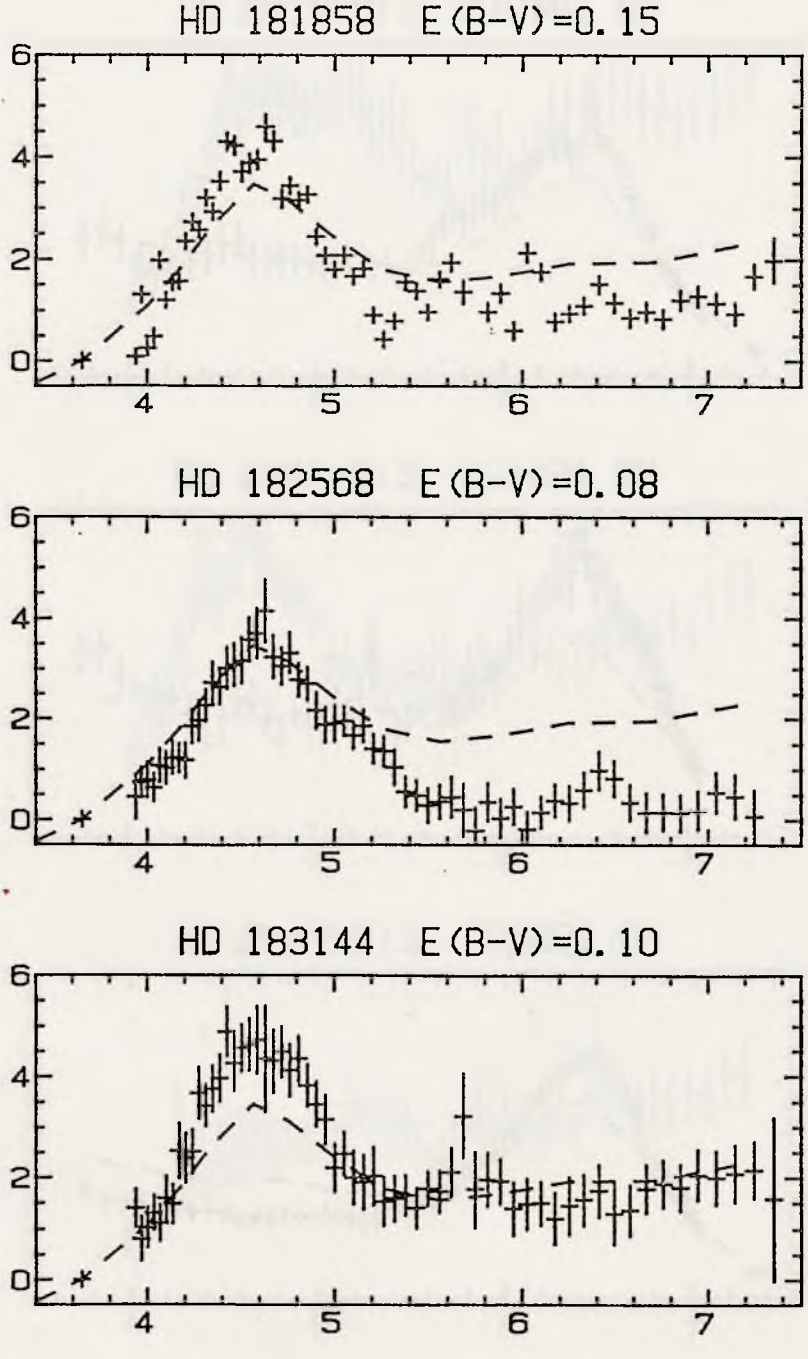
HD 181858 E(B-V)=0.15
HD 182568 E(B-V)=0.08
HD 183144 E(B-V)=0.10
0
2
4
6
4
5
6
7

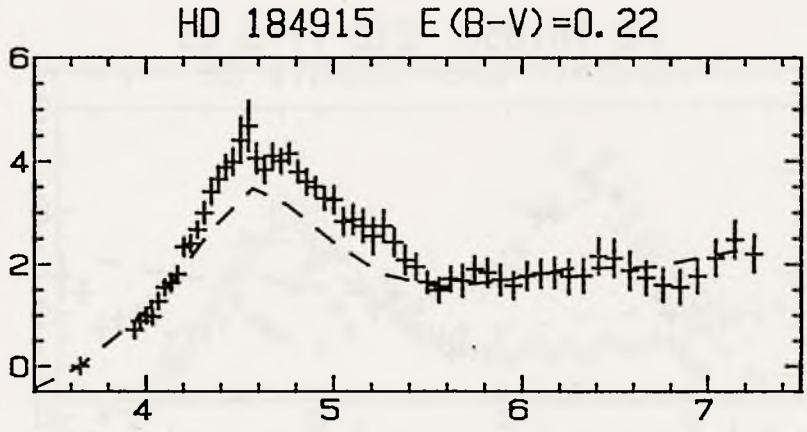
HD 184915 E(B-V)=0.22
6
4
2
0
4
5
6
7

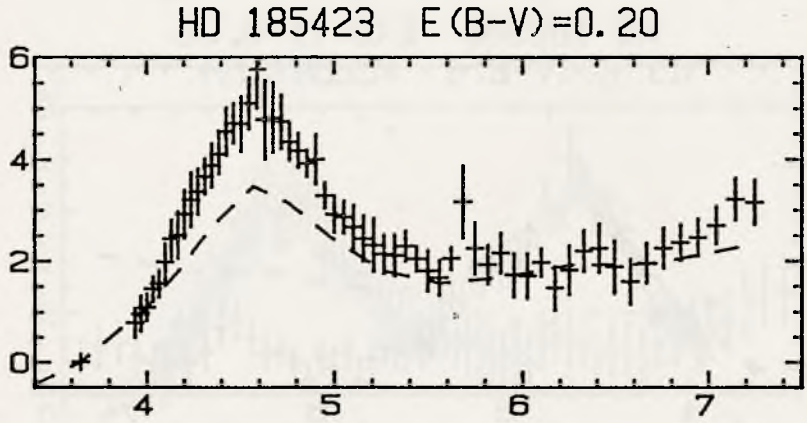
HD 185423 E(B-V)=0.20
6
4
2
0
4
5
6
7

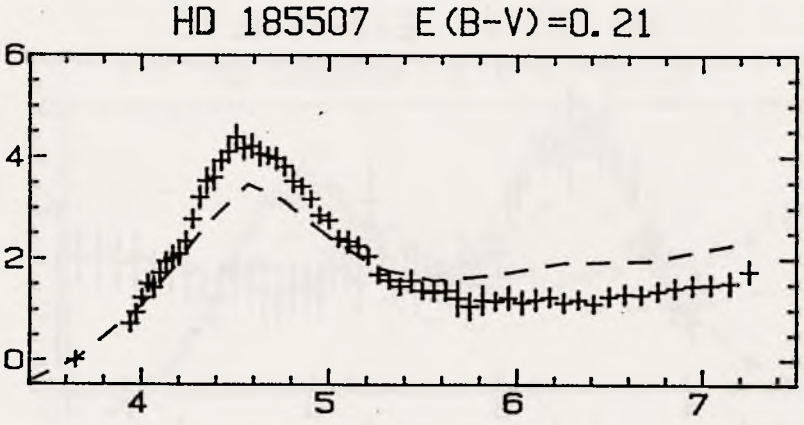
HD 185507 E(B-V)=0.21
6
4
2
0
4
5
6
7

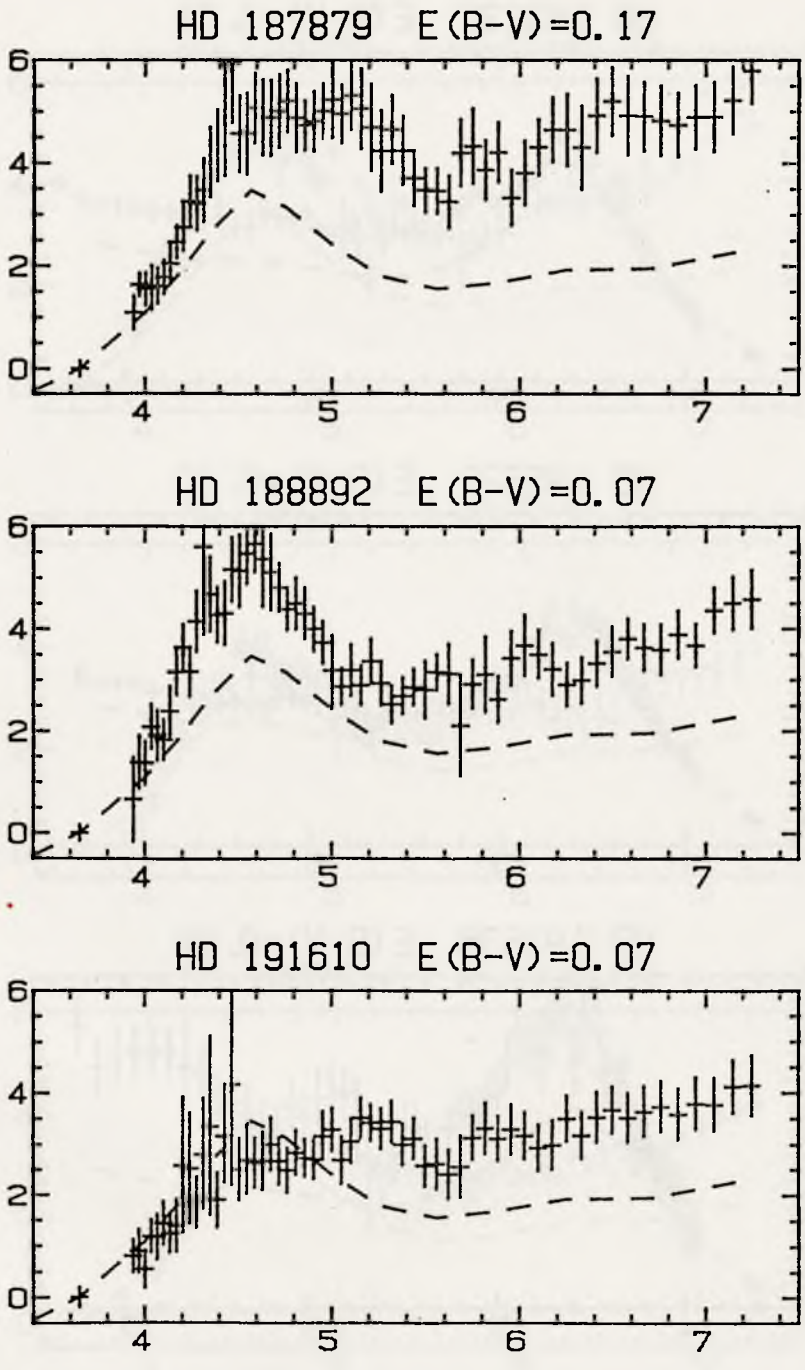
HD 187879 E(B-V)=0.17
HD 188892 E(B-V)=0.07
HD 191610 E(B-V)=0.07
0
2
4
6
4
5
6
7

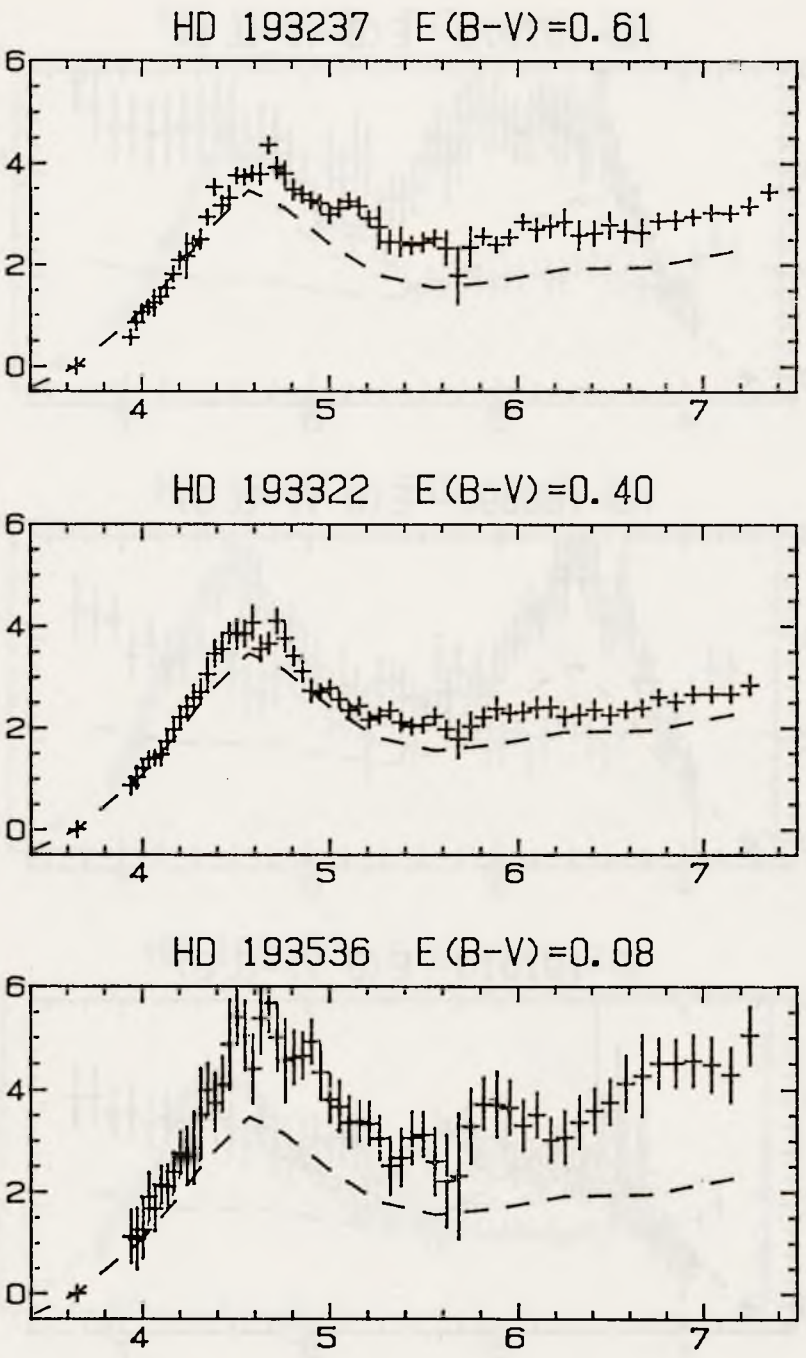
HD 193237 E(B-V)=0.61
HD 193322 E(B-V)=0.40
HD 193536 E(B-V)=0.08
0
2
4
6
4
5
6
7

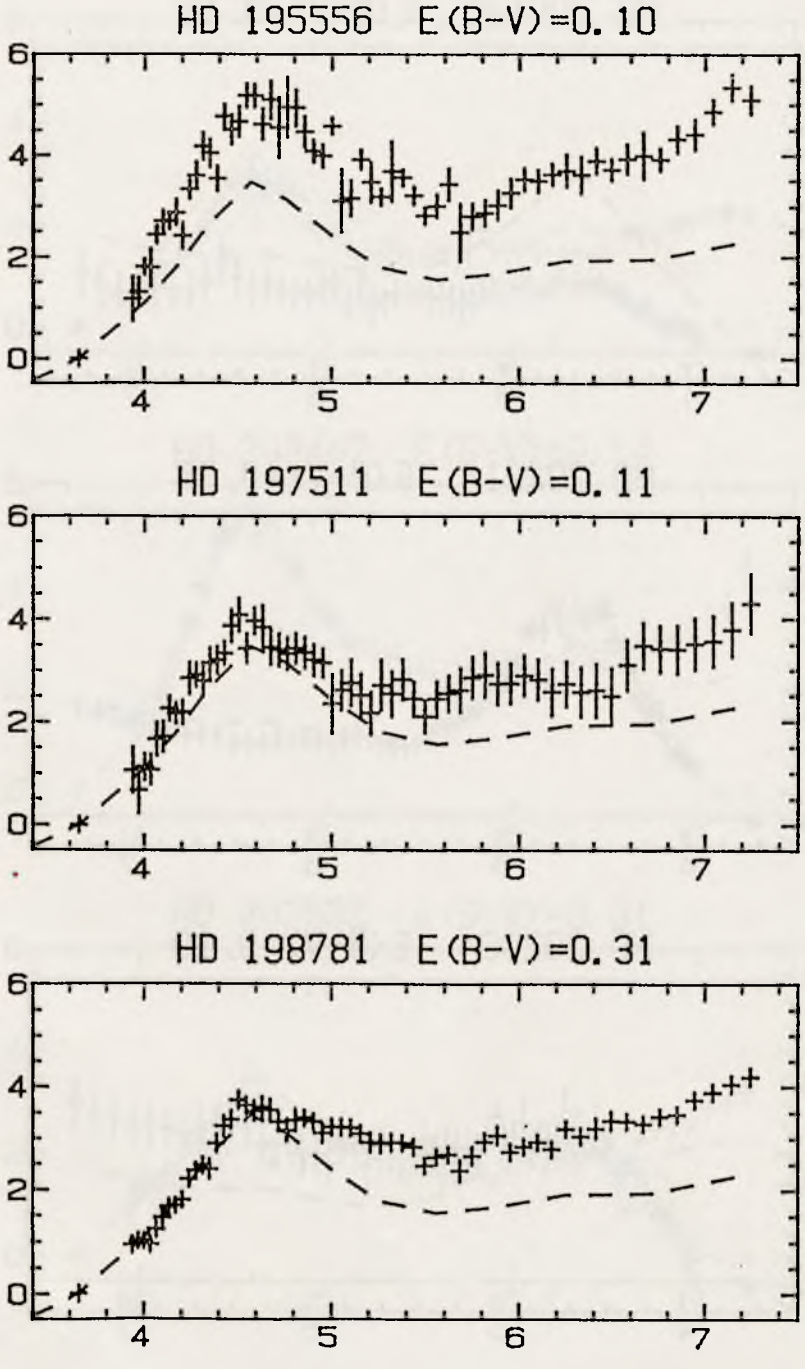
HD 195556 E(B-V)=0.10
HD 197511 E(B-V)=0.11
HD 198781 E(B-V)=0.31
0
2
4
6
4
5
6
7

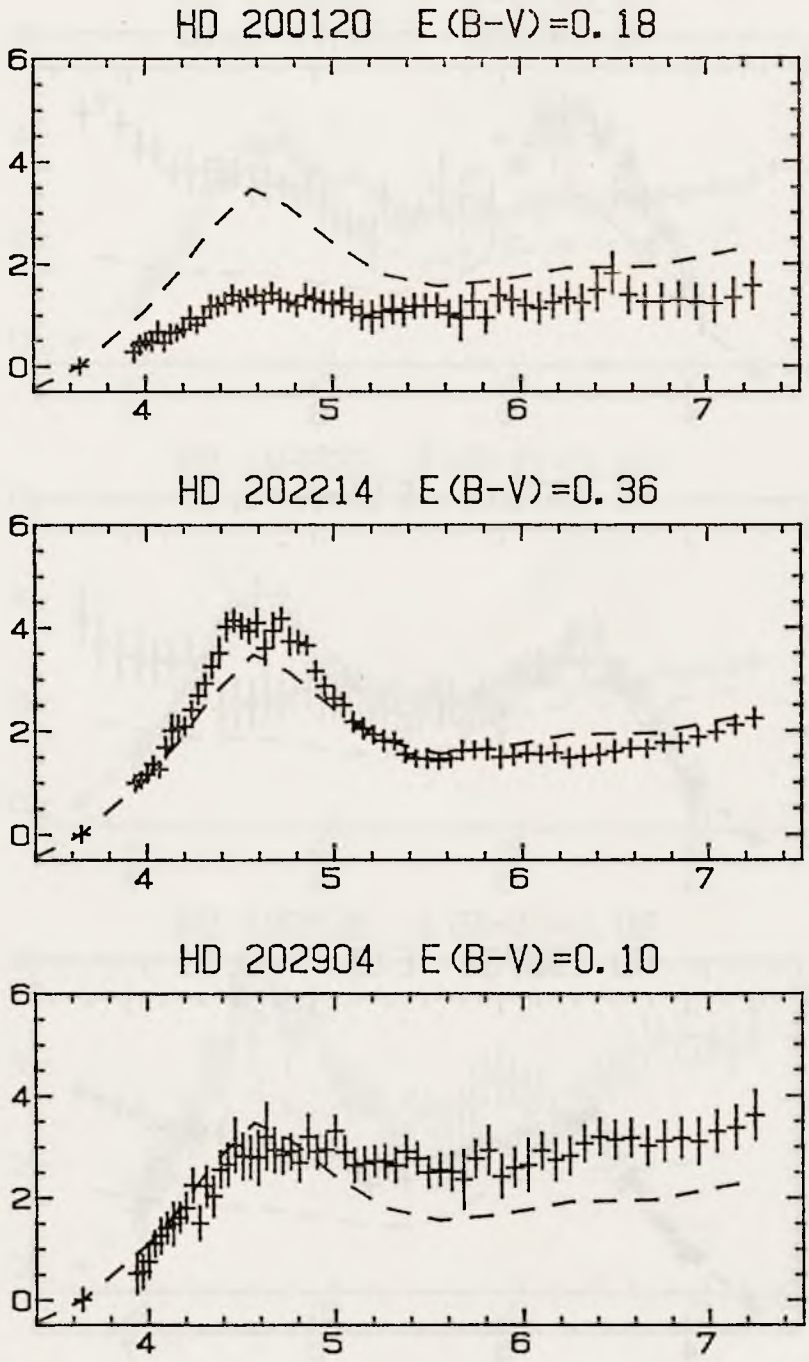
HD 200120 E(B-V)=0.18
HD 202214 E(B-V)=0.36
HD 202904 E(B-V)=0.10
0
2
4
6
4
5
6
7

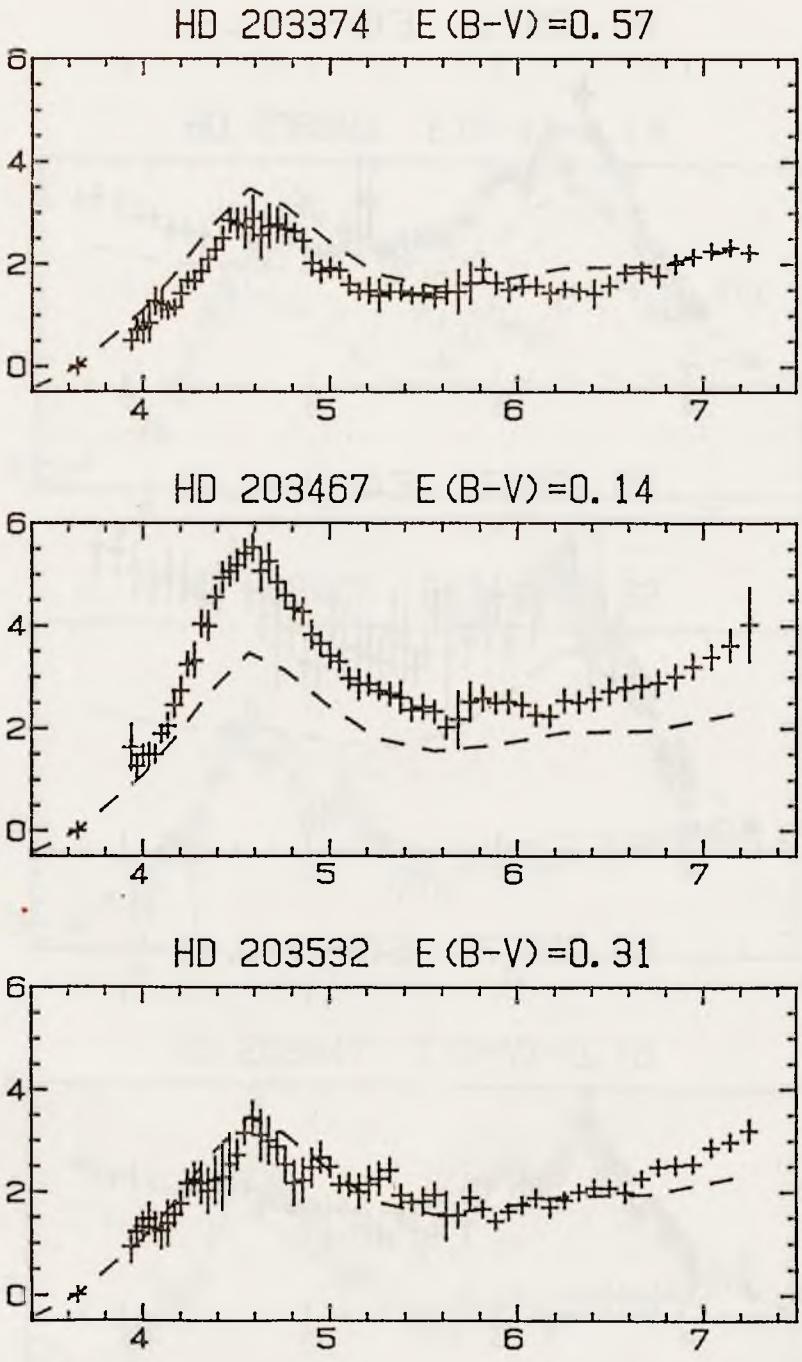
HD 203374 E(B-V)=0.57
HD 203467 E(B-V)=0.14
HD 203532 E(B-V)=0.31
0
2
4
6
4
5
6
7

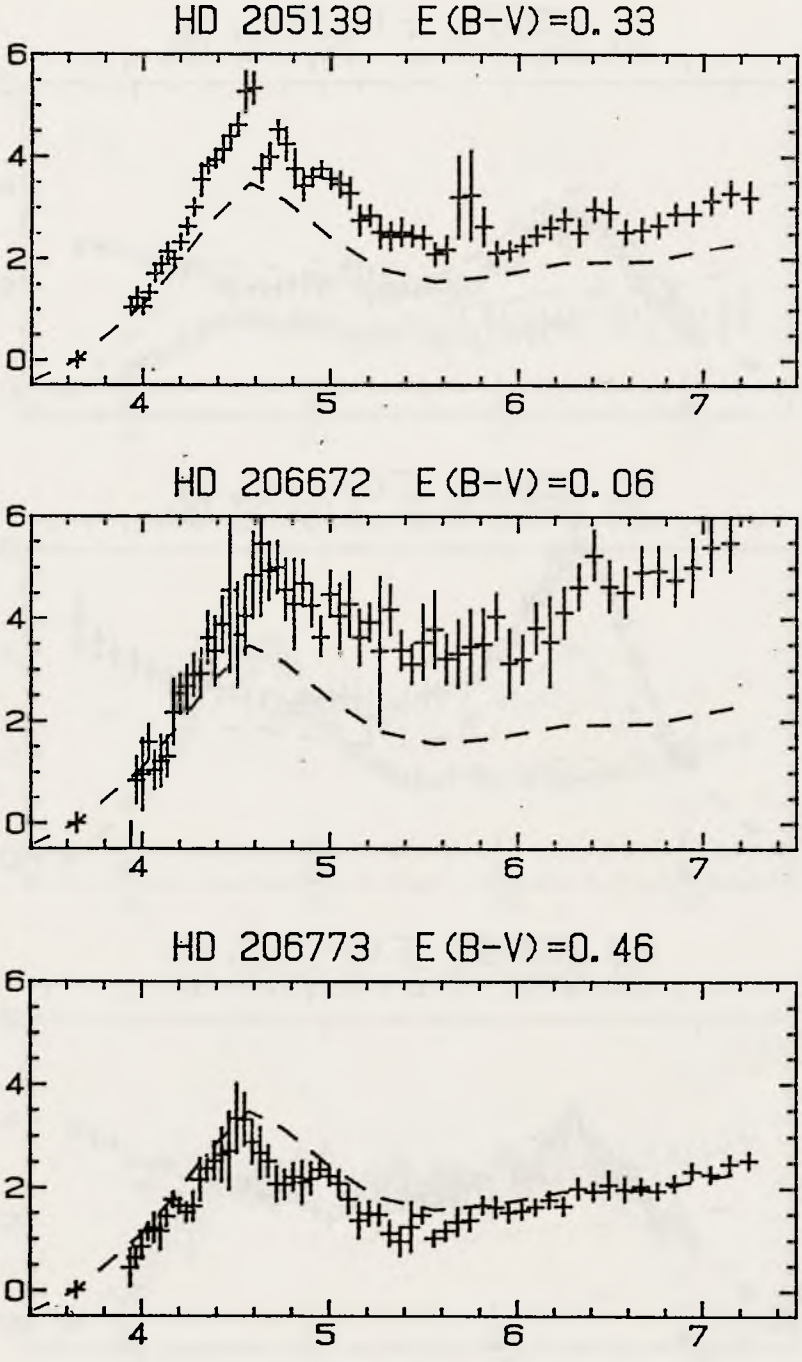
HD 205139 E(B-V)=0.33
HD 206672 E(B-V)=0.06
HD 206773 E(B-V)=0.46
0
2
4
6
4
5
6
7

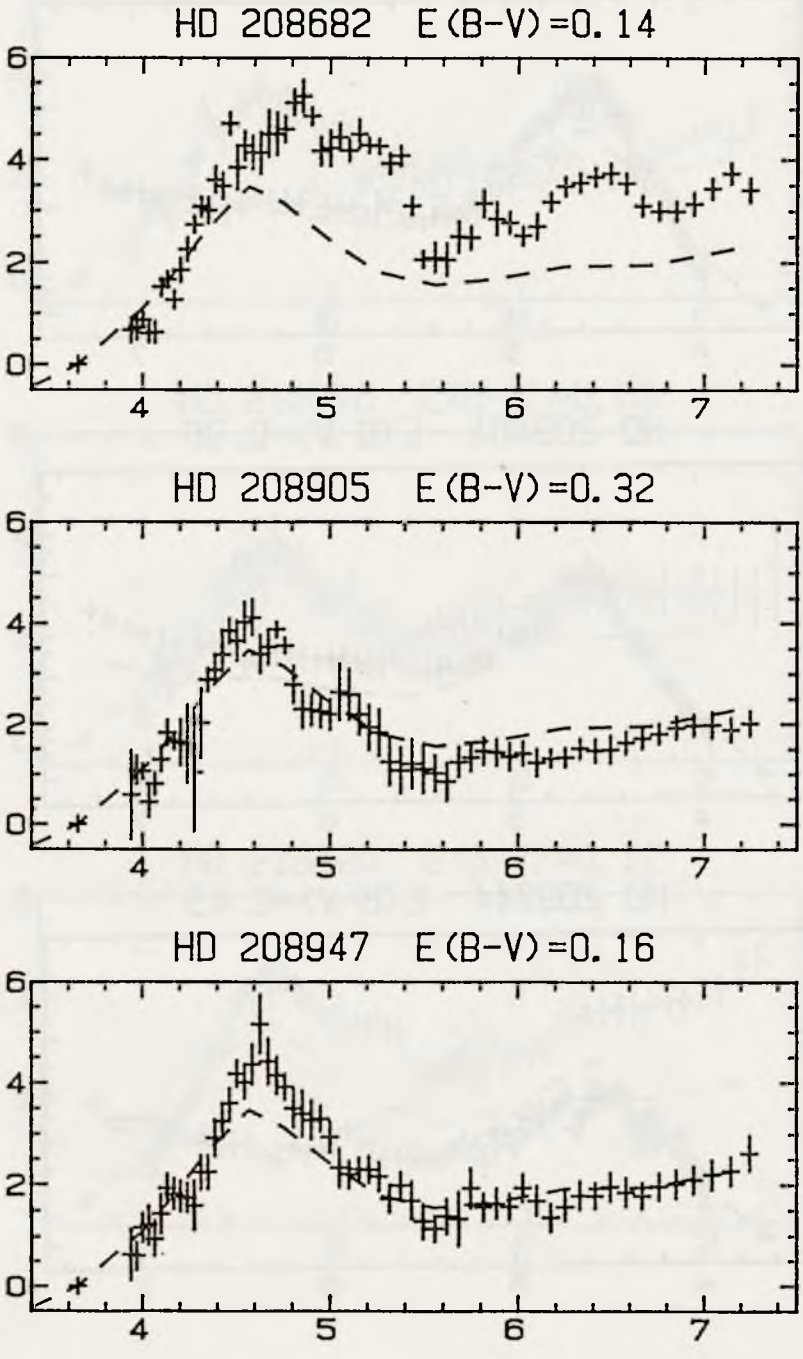
HD 208682 E(B-V)=0.14
HD 208905 E(B-V)=0.32
HD 208947 E(B-V)=0.16
0
2
4
6
4
5
6
7

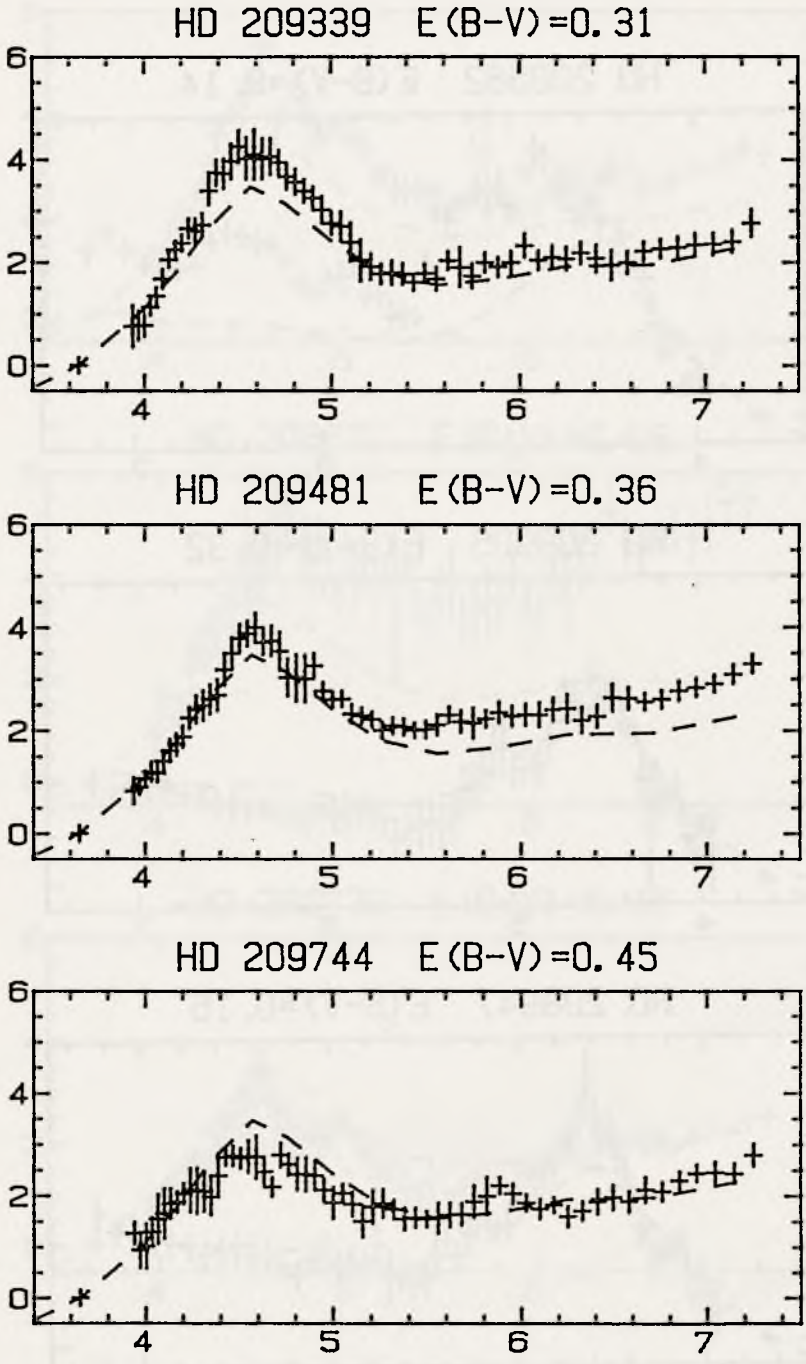
HD 209339 E(B-V)=0.31
HD 209481 E(B-V)=0.36
HD 209744 E(B-V)=0.45
0
2
4
6
4
5
6
7

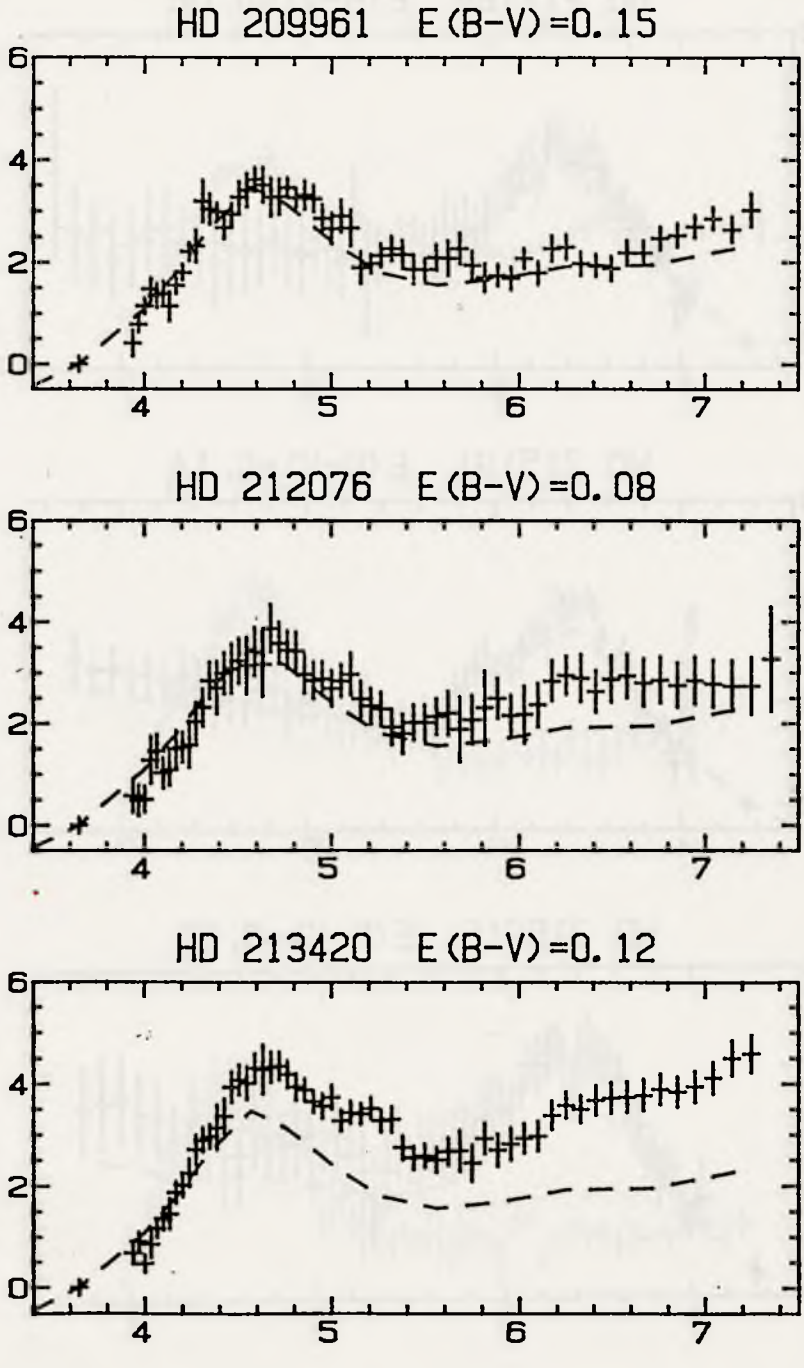
HD 209961 E(B-V)=0.15
HD 212076 E(B-V)=0.08
HD 213420 E(B-V)=0.12
0
2
4
6
4
5
6
7

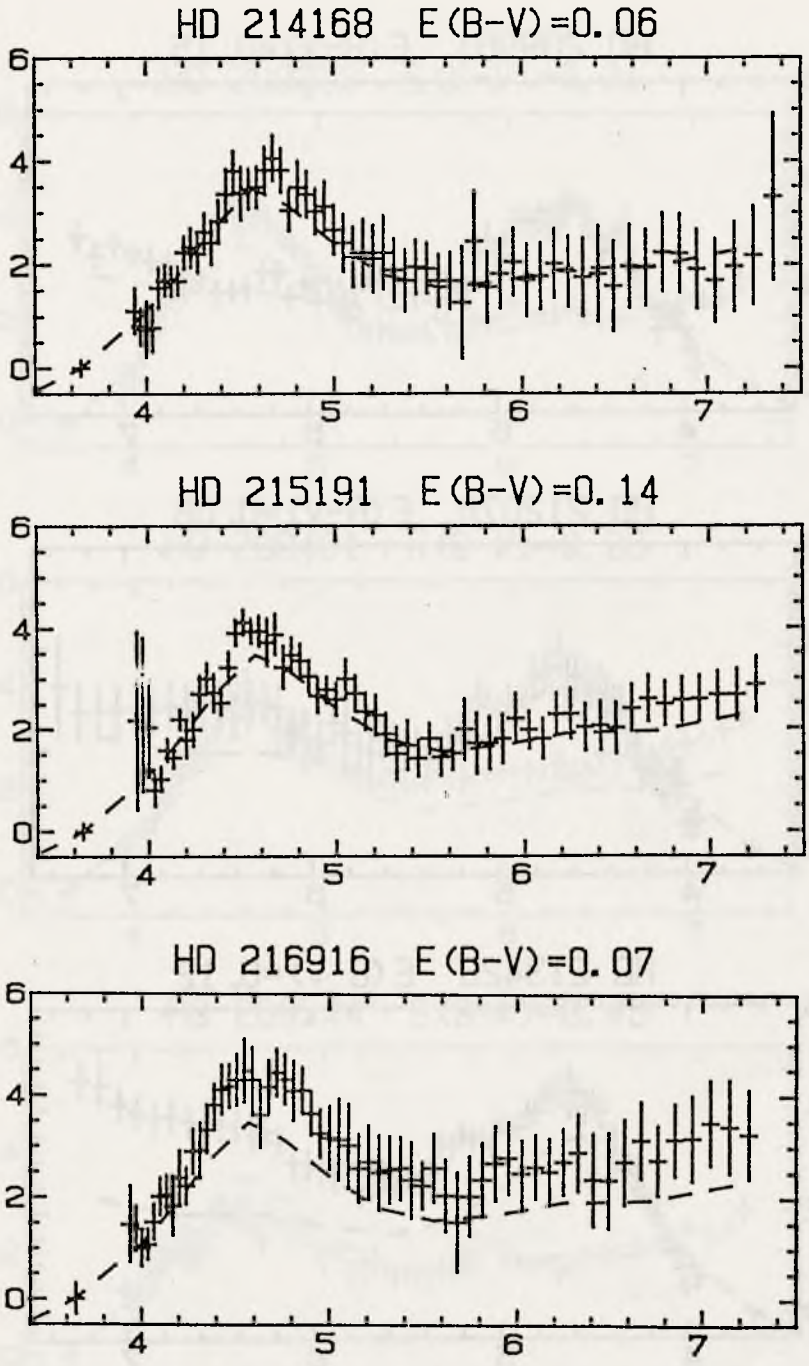
HD 214168 E(B-V)=0.06
HD 215191 E(B-V)=0.14
HD 216916 E(B-V)=0.07
0
2
4
6
4
5
6
7

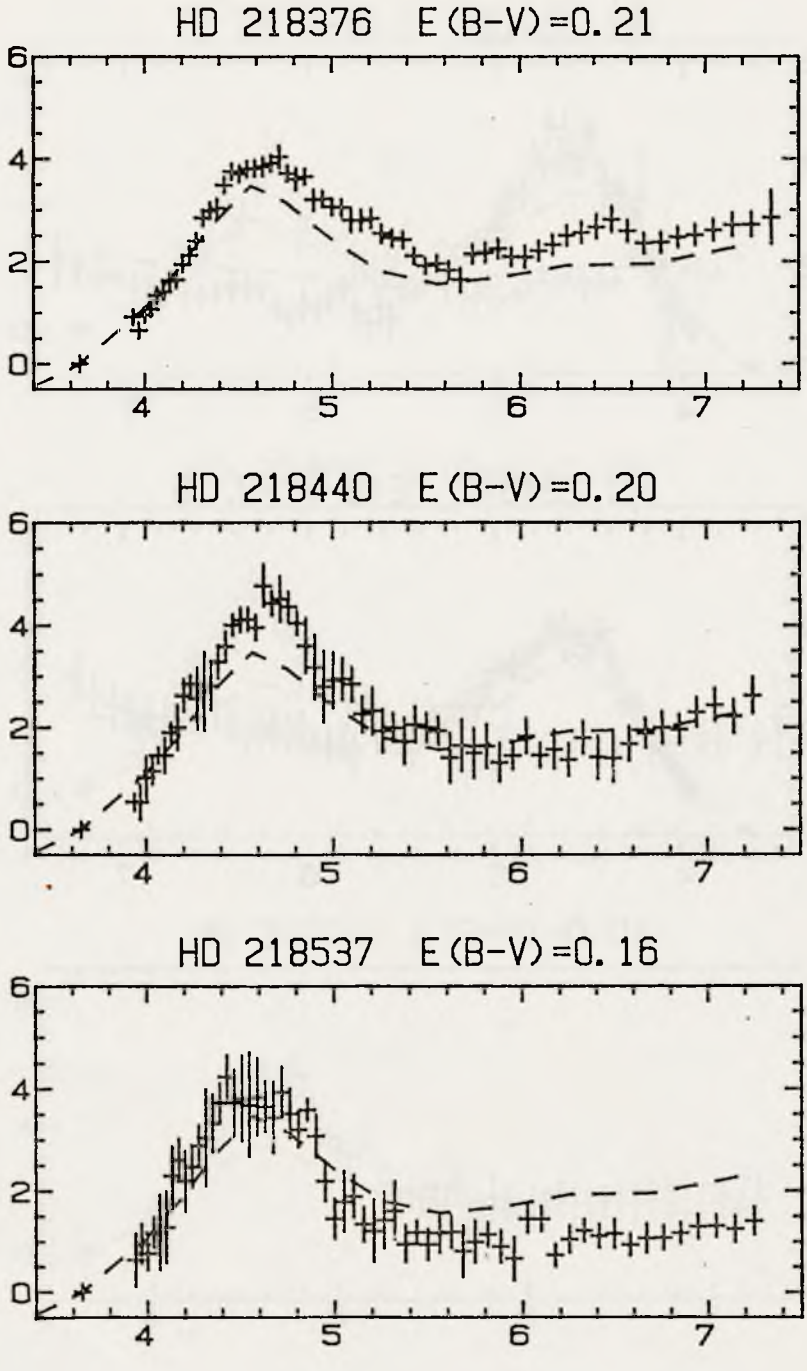
HD 218376 E(B-V)=0.21
HD 218440 E(B-V)=0.20
HD 218537 E(B-V)=0.16
0
2
4
6
4
5
6
7

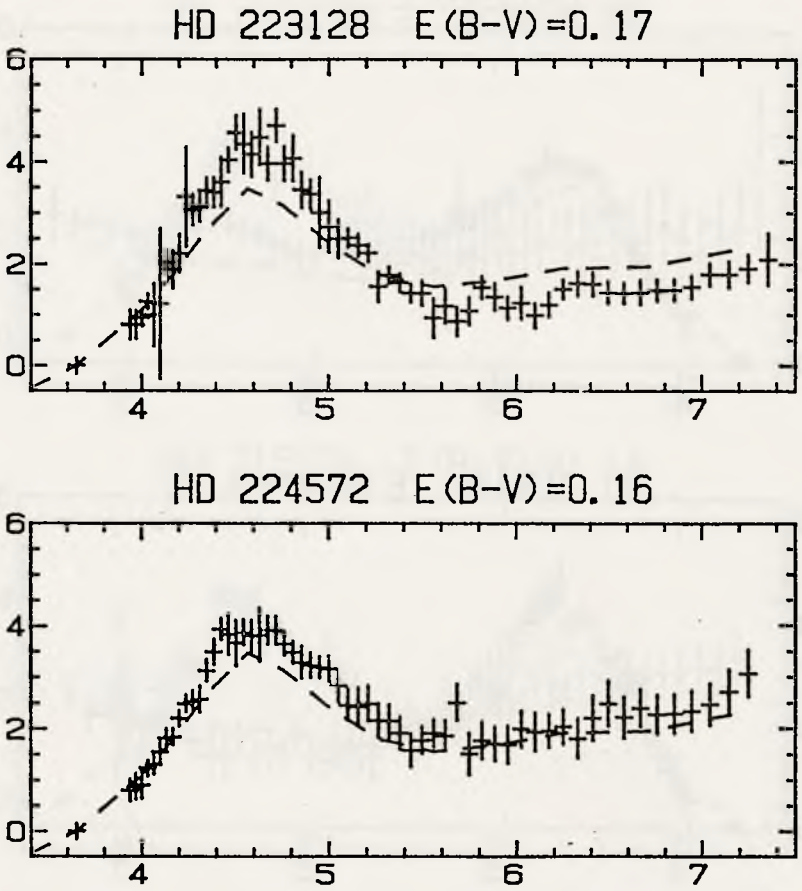
HD 223128 E(B-V)=0.17
6
4
2
0
4
5
6
7
HD 224572 E(B-V)=0.16
6
4
2
0
4
5
6
7

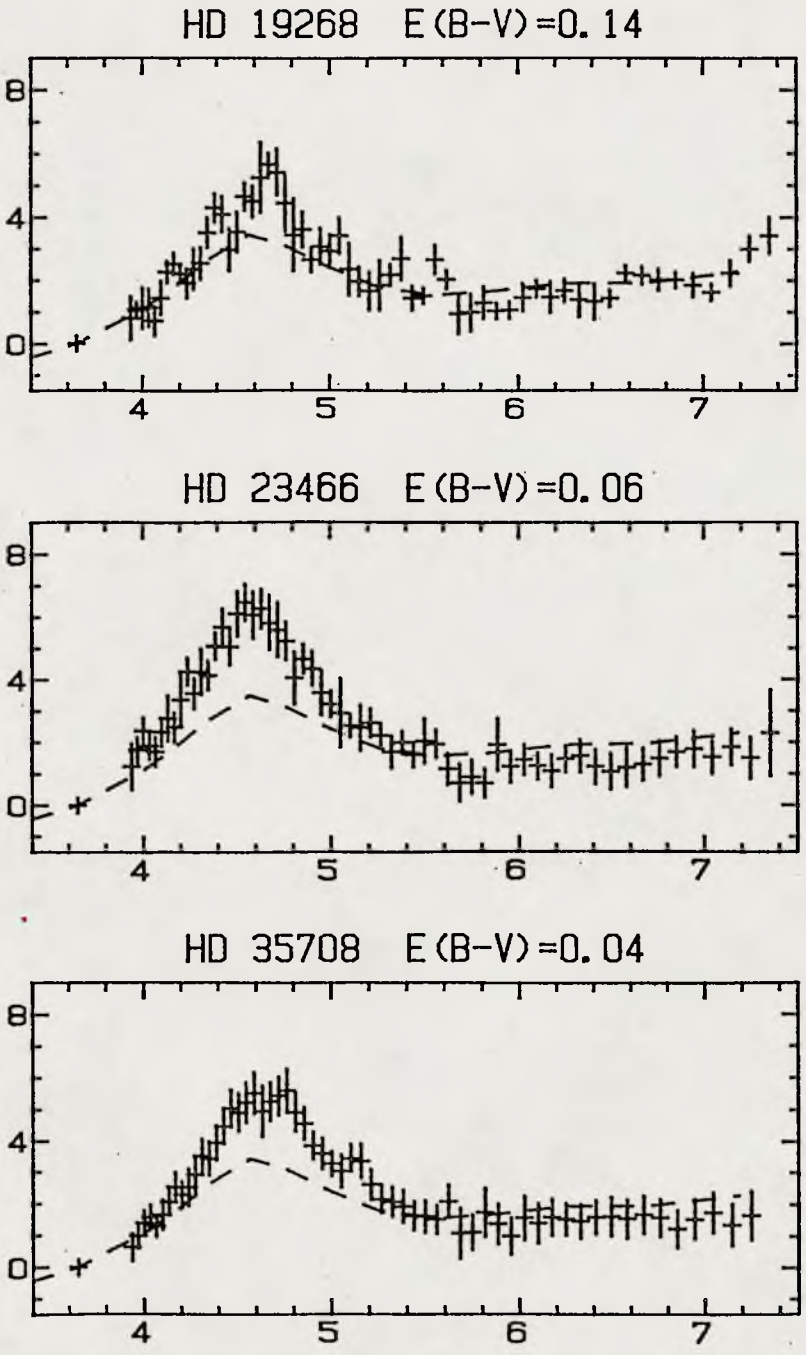
HD 19268 E(B-V)=0.14
HD 23466 E(B-V)=0.06
HD 35708 E(B-V)=0.04
8
4
0
4
5
6
7

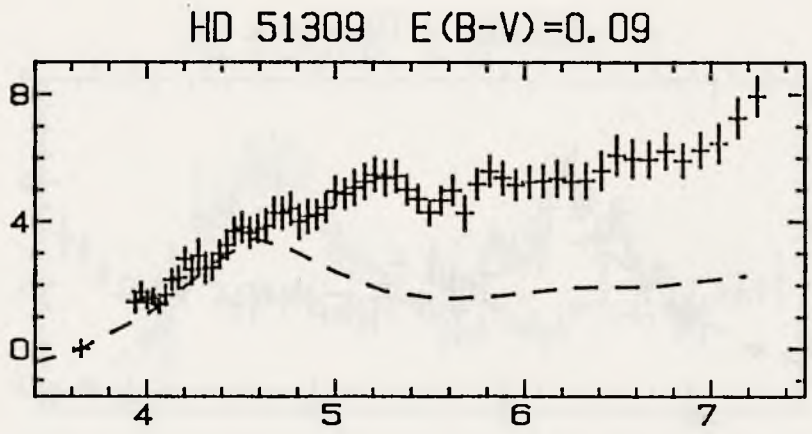
HD 51309 E(B-V)=0.09
8
4
0
4
5
6
7

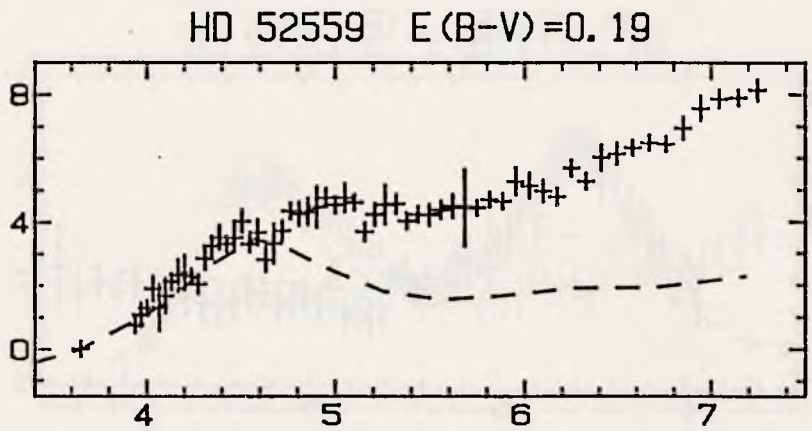
HD 52559 E(B-V)=0.19
8
4
0
4
5
6
7

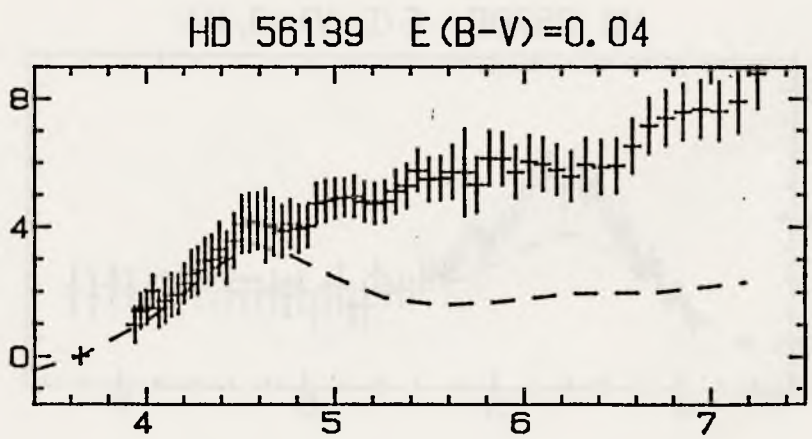
HD 56139 E(B-V)=0.04
8
4
0
4
5
6
7

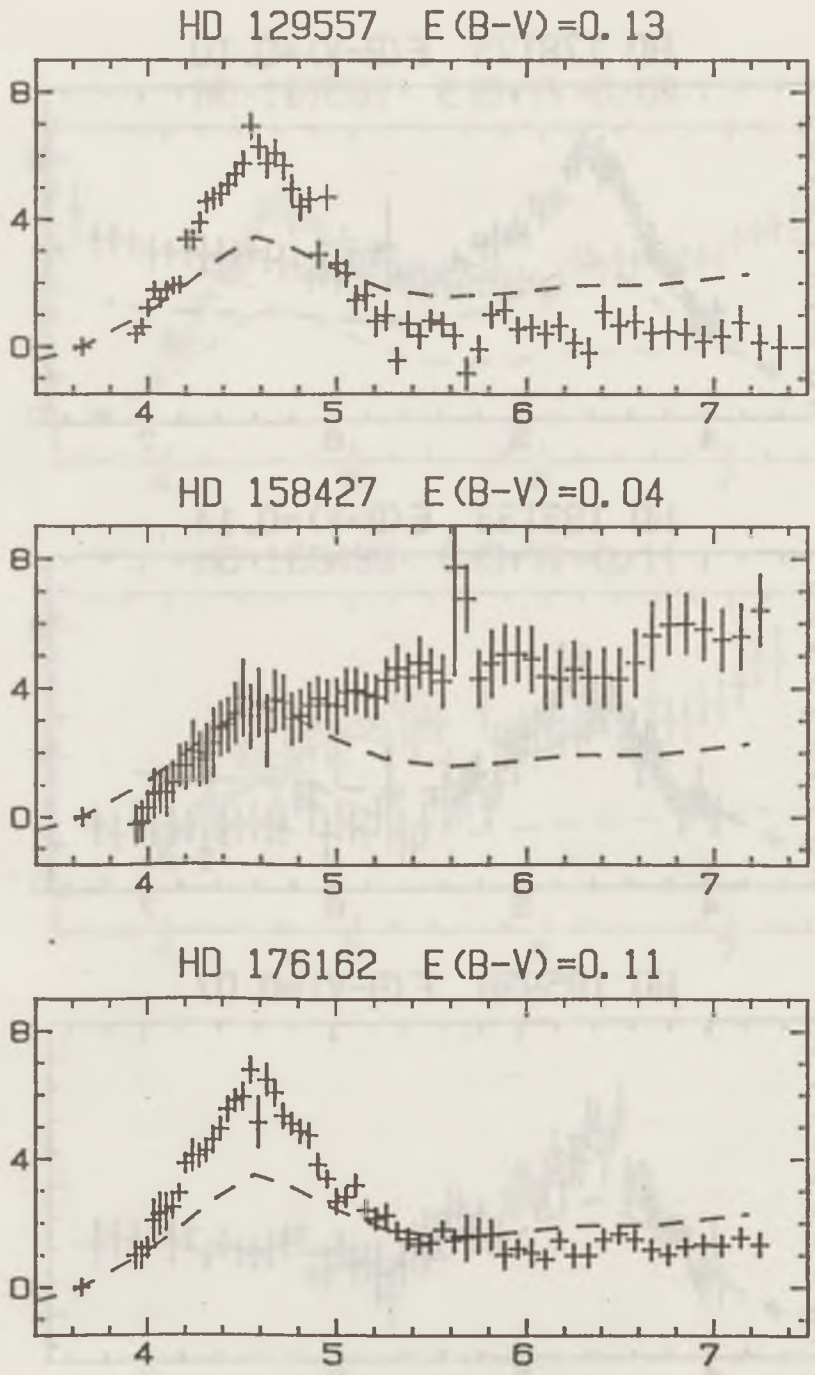
HD 129557 E(B-V)=0.13
HD 158427 E(B-V)=0.04
HD 176162 E(B-V)=0.11
8
4
0
4
5
6
7

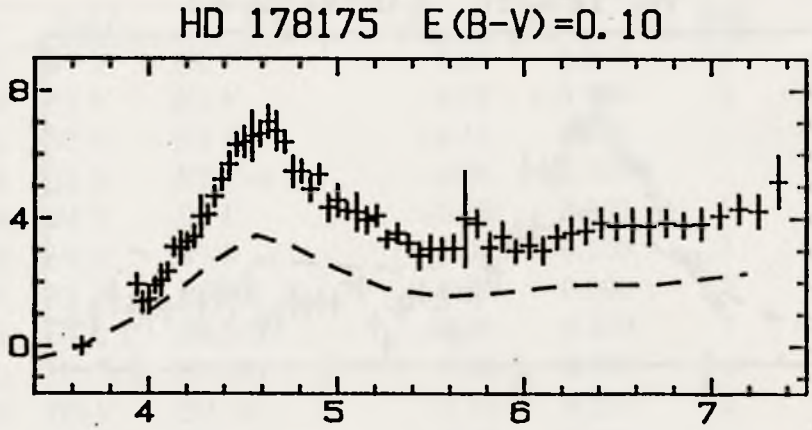
HD 178175 E(B-V)=0.10
8
4
0
4
5
6
7

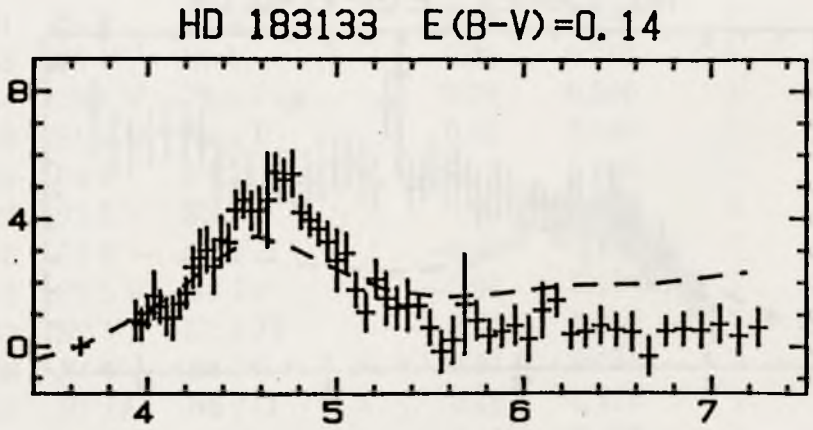
HD 183133 E(B-V)=0.14
8
4
0
4
5
6
7

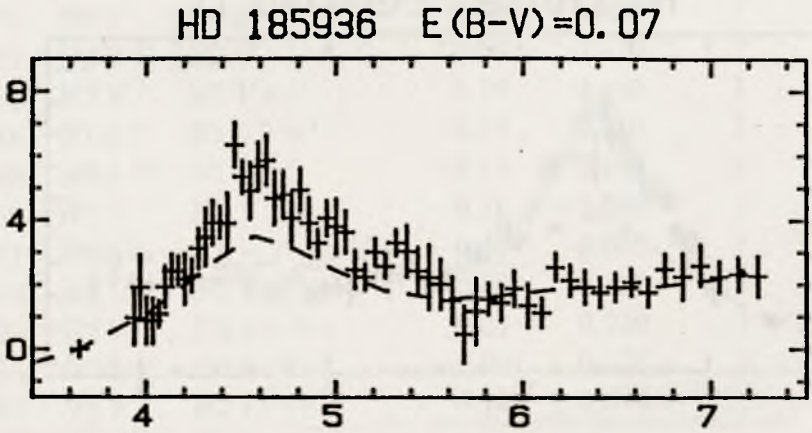
HD 185936 E(B-V)=0.07
8
4
0
4
5
6
7

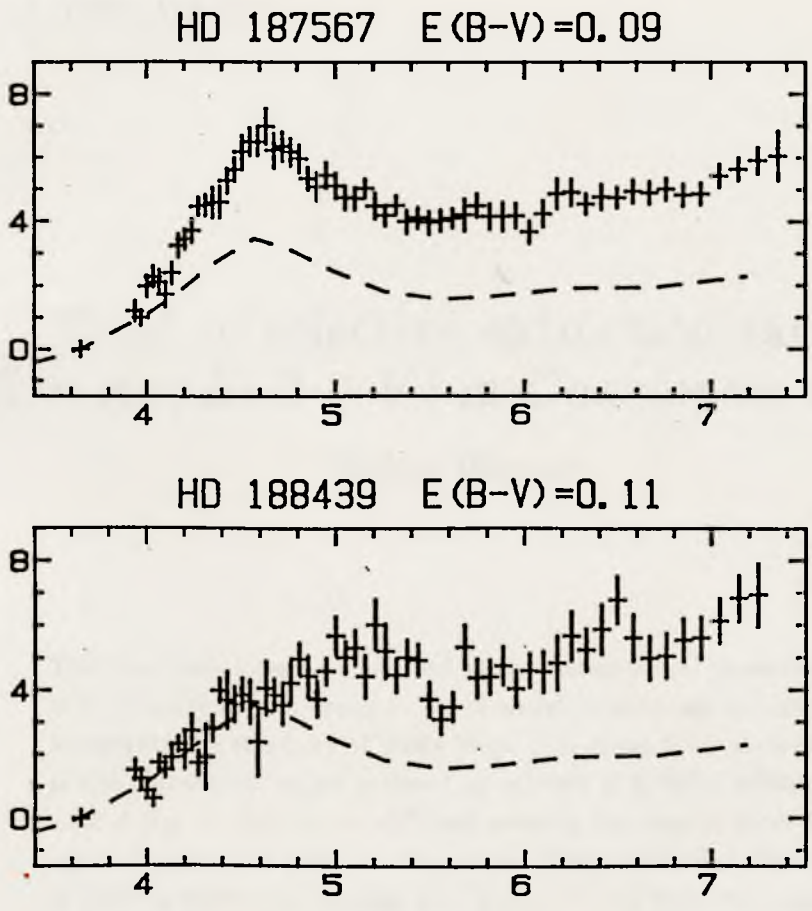
HD 187567 E(B-V)=0.09
8
4
0
4
5
6
7
HD 188439 E(B-V)=0.11
8
4
0
4
5
6
7